2020

Correlating the Physicochemical Properties of Magnesium Stearate with Tablet Dissolution and Lubrication

Julie L. Calahan

University of Kentucky, calahanjulie@gmail.com

Author ORCID Identifier:

🆔 https://orcid.org/0000-0001-8585-0407

Digital Object Identifier: https://doi.org/10.13023/etd.2020.385

Right click to open a feedback form in a new tab to let us know how this document benefits you.

CORRELATING THE PHYSICOCHEMICAL PROPERTIES OF MAGNESIUM
STEARATE WITH TABLET DISSOLUTION AND LUBRICATION

—————————————————————————

DISSERTATION

—————————————————————————

A dissertation submitted in partial fulfillment of the
requirements for the degree of Doctor of Philosophy in the
College of Pharmacy
at the University of Kentucky

By

Julie L. Calahan

Lexington, Kentucky

Co-Directors: Dr. Eric J. Munson, Professor of Pharmaceutical Sciences

and   Dr. Younsoo Bae,   Professor of Pharmaceutical Sciences

Lexington, Kentucky

ABSTRACT OF DISSERTATION

CORRELATING THE PHYSICOCHEMICAL PROPERTIES OF
MAGNESIUM STEARATE WITH TABLET DISSOLUTION AND LUBRICATION

Magnesium stearate (MgSt) is the most commonly used pharmaceutical excipient and is present in over half the tablet formulations on the market. In spite of its popularity as an effective lubricant, it has been repeatedly recognized that there is significant variability between MgSt samples, which can cause inconsistent lubrication between batches of MgSt. The hypothesis of this research is that the batch-to-batch variability in tablet lubrication and dissolution observed in tablet formulations containing different MgSt samples can be correlated with differences in MgSt physicochemical properties (fatty acid salt composition, crystal hydrate form, particle size and surface area). Developing correlations between MgSt properties has been challenging in part because there has not been a reliable method for determining crystal form. Recently, ^{13}C solid-state nuclear magnetic resonance (SSNMR) has been used to clearly identify the MgSt crystal forms.

^{13}C SSNMR is used extensively throughout this work to identify the crystal forms of samples of MgSt. Thermogravimetric analysis and dynamic scanning calorimetry were used as complimentary techniques to understand thermal behavior of the samples. MgSt is typically used in tablets at low levels (0.2-5%), leading to challenges with detection of MgSt in formulations. To enhance detection in SSNMR, samples of MgSt have been synthesized in the lab using ^{13}C-labeled stearic acid. Specific surface area (SSA) results were determined using N_2 and Kr adsorption with BET calculations, and samples were dried using nitrogen flow for various times. A discriminating dissolution method was developed to differentiate between MgSt samples with varying properties. Lubrication efficiency was performed using a Presster compaction simulator and tensile strength determination using diametrical compression.

Synthesis studies showed that the fatty acid composition and synthesis method affects the crystal form of MgSt produced, with higher stearic content preferring the dihydrate form. Temperature and humidity affect the form of MgSt and facilitate interconversion between forms. Drying MgSt was found to affect surface area results, with the dihydrate converting to the disordered form. Dissolution of indomethacin tablets containing various types of MgSt showed a strong dependence on particle size and surface area, with smaller particle size and higher SSA samples having slower dissolution rates. Fatty acid composition and hydrate form were investigated as secondary variables

influencing dissolution, with fatty acid showing no correlation with dissolution. Lubrication efficiency and tabletability studies showed an effect of crystal form, with monohydrate and dihydrate forms showing good lubrication efficiency compared to the disordered form, but also poorer tabletability.

In conclusion, the potential for variability in the crystal form of MgSt was found to be an important property of MgSt. There is variability in the form produced from synthesis, as well as interconversion between forms. Temperature, humidity and drying conditions are particularly important in controlling the crystal form of MgSt, as this can impact formulation stability and storage conditions. The primary variable affecting dissolution is particle size and surface area, but crystal form is a potential secondary variable. The physicochemical properties of MgSt, particularly crystal form and surface area, showed trends with lubrication and dissolution. This highlights the importance of choosing a MgSt material with the desired crystal form and surface area properties to match the lubrication and dissolution requirements for the formulation.

Julie L. Calahan

04/10/2020
Date

CORRELATING THE PHYSICOCHEMICAL PROPERTIES OF MAGNESIUM
STEARATE WITH TABLET DISSOLUTION AND LUBRICATION

By
Julie L. Calahan

Eric J. Munson
Co-Director of Dissertation

Younsoo Bae
Co-Director of Dissertation

David J. Feola
Director of Graduate Studies

04/10/2020

DEDICATION

To my Lord and Savior Jesus Christ, the strength of my life. I'm so grateful for your presence with me, and abundance provision for me throughout this PhD experience.

ACKNOWLEDGEMENTS

There are so many people that have contributed to my success in graduate school, and where this list contains only a brief mention of a few, much more could be said.

1 - First, I would like to thank my professor, Dr. Eric J. Munson for extending the invitation to study for my doctorate at the University of Kentucky, as well as for guidance and mentorship throughout my PhD experience. I deeply appreciate his understanding of how to train non-traditional PhD students like myself to think differently, both in terms of the research and in presentation.

2 – Thank you to my committee members Dr. Younsoo Bae, Dr. Barbara Knutson, Dr. Patrick Marsac, Dr. Joe Chappell who have pushed me to address some of my weaknesses and improve my skills in answering questions and presenting my work with confidence. A special thank you to Dr. Bradley Berron who served as the outside examiner for my defense.

3 – Thank you to Roger Zanon for the intensive coaching sessions during the last few months of preparation for my defense. Those discussions and visits were more significant than I can convey here and extremely important for my process of putting all the research together at the end.

4 – Next, I want to acknowledge all the students and postdocs in the Munson lab, the Marsac lab, as well as all the grad students at both UK and Purdue. Specifically, I want to thank Sean Delaney, Nico Setiawan, Kanika Sarpal, Ashley Lay-Fortenberry for welcoming me into the lab, as well as Matt Defrese, Freddy Arce, Travis Jarrells, Heather Campbell, Amin Abedini, Fahd, Taylor, Lauren and all the other UK COP grad students,

10 – I also want to thank all of my family, friends and colleagues who have supported my decision to pursue a PhD in my 40s, for all the many prayers and encouraging words along the way. It was wonderful to have so many join online to support me for the defense seminar. I couldn't have done this without their support in so many ways throughout my graduate experience.

TABLE OF CONTENTS

LIST OF TABLES

LIST OF FIGURES

CHAPTER 1.   INTRODUCTION TO MAGNESIUM STEARATE
            VARIABILITY

1.1   Previous Investigations into the Variability of Magnesium Stearate (MgSt)

    Magnesium stearate (MgSt) is the most commonly pharmaceutical excipient in
solid oral dosage forms and is used as a lubricant in over half of the tablet formulations
on the market.(1) Tablet prescriptions include a paper insert listing the active
pharmaceutical ingredient (i.e. the drug), along with dosing information and a list of the
inactive ingredients (known as excipients) used in the tablet formulation. Tablets are
often the preferred dosage form, as they are convenient to administer, have fewer
physical and chemical stability problems and can be manufactured in large quantities.
Still, the manufacturing process involves many steps to produce a tablet with the desired
characteristics. To make a tablet, the excipients are mixed together with the drug, making
a blend. Typically, MgSt is added as the last excipient at a level of only $0.5 - 2\%$ to the
powder blend prior to compaction with a tablet press. After the formulation powder is
compacted, the tablet must be removed (or ejected) from the tablet die. Lubricants, such
as MgSt, aid in the tablet ejection during the manufacturing process by reducing the
friction between the compacted tablet and the tablet press die. Without proper lubrication,
part of the tablet can adhere to the tablet die and punch faces of the tablet press, in what
has been called "picking and sticking." If the formulation is over-lubricated, such as by
mixing too long or adding too much MgSt, the tablet will not dissolve in the proper
amount of time. MgSt is a very effective powder lubricant and has been used in
pharmaceutical formulations for decades.(2)
    In spite of its popularity as an effective lubricant, it has been repeatedly
recognized that there is significant variability between MgSt samples which can cause
inconsistent lubrication between lots and batches of MgSt. Figure 1-1 is an illustration of
the balance between lubrication efficiency and dissolution which is necessary for good
tablet manufacturing. Typically, this balance is achieved by pharmaceutical formulators
by adjusting the mixing time in a trial-and-error process. Ideally, the mixing time would

be near the middle line, with high lubrication and minimal effect on dissolution. This process of adjusting the mixing time is acceptable as long as every MgSt sample behaves the same. However, many formulators have experienced lot-to-lot variability in the functional performance of different MgSt samples. For example, a new lot of MgSt mixed for the same amount of time may be under-lubricated, such that the line will shift to left, while another lot of MgSt may be over-lubricated, such that the line will shift to the right side of the figure. Either situation of under-lubrication or over-lubrication can yield unacceptable tablets, causing loss of time and money due to discarding the unacceptable tablet lots. In order to highlight the variability of MgSt impacting tablet lubrication, the current knowledge about magnesium stearate is reviewed in this chapter.
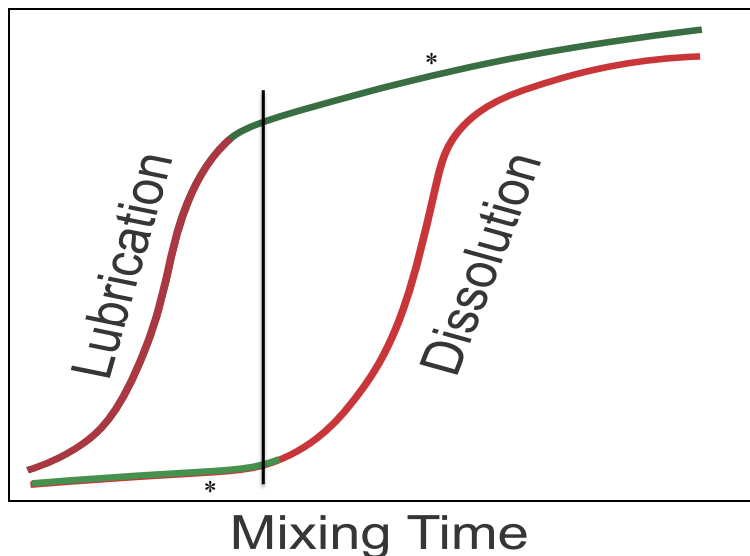
Figure 1-1. Impact of Lubrication – Dissolution as a function of mixing time. An ideal MgSt has high impact on lubrication and low impact on dissolution, as indicated by the asterisks in the green areas and the vertical line.

Magnesium stearate has been used in pharmaceutical formulations for decades. One of the early indications of MgSt variability came in 1970, when Hanssen et al. noted that different grades of MgSt affected compression properties (3) Soon after, Butcher et al. focused on how differences in packing and sieving affect lubrication (1972).(4) Then in 1984, Hoelzer published on "batch to batch variations of commercial magnesium stearate" focusing on surface area variations,(5) and Dansereau discussed how the variability in physicochemical properties of MgSt affects tablet lubrication, specifically

noting that excipients such as microcrystalline cellulose had decreased tablet tensile strength with increasing MgSt surface area.(6, 7) A little later in 1996, Barra and Somma investigated the physicochemical variability of MgSt with thirteen commercial samples and showed a range of results with minimal correlation.(8) Researchers from Mallinckrodt, a prominent supplier of magnesium stearate, have extensively studied and presented on the properties of MgSt and their effects on tablet lubrication, with a focus to describing the specific materials they manufacture with minimal lot-to-lot variability. Their conclusion is that the dihydrate form is a better lubricant than the more popular monohydrate form. (9) More recently, Kushner et al. have used quality by design (QbD) experiments to study excipient variation(10) and Haware et al. have used multivariate analysis (MVA) methods to identify significant variables affecting the lubricating properties of commercial MgSt.(11, 12) Most recently, Wang, Potts and Hoag also used principal component analysis (PCA) to investigate the variability of MgSt using analytical techniques such as near-IR spectroscopy, Raman spectroscopy and scanning electron microscopy (SEM).(13, 14) It is clear that the variability of MgSt still warrants significant study.

The hypothesis of this research is that the observed variability in lubrication efficiency and dissolution rate between batches of MgSt can be correlated with the physicochemical properties of MgSt samples, specifically fatty acid composition, crystal form, particle size and surface area. Several researchers (including reviews by Moody et al.,(2) Wang et al.,(15) Li et al.(16) and Kahner et al.(17) have identified chemical composition, particle size/surface area and crystal form as possible important variables impacting MgSt function,(7, 8) so these properties will serve as the starting point for the current investigation. The remainder of this chapter will focus on a review of the most prominent physicochemical properties of magnesium stearate (chemical composition, crystal form, particle size and surface area), followed by a discussion of how processing effects MgSt (focusing on mixing and disproportionation) and finally the effects of MgSt properties on function, in terms of lubrication and dissolution.

1.2   MgSt Physicochemical Properties

1.2.1   Fatty Acid Composition and Synthesis of MgSt

A wide range of chemical composition is allowed for magnesium stearate samples. The US Pharmacopeia is "a scientific, nonprofit organization that sets public standards for the identity, strength, quality and purity of medicines" and excipients.(18) The first US pharmacopeia was issued in 1820, with specific standards called monographs for a variety of drugs. Additionally, compounding standards are found in the USP and National Formulary (USP-NF) which includes monographs for many excipients, including magnesium stearate. The USP-NF monograph for MgSt allows for "variable proportions of magnesium stearate and magnesium palmitate"(19). To meet USP standards, the MgSt sample must be derived from at least 40% stearic acid, and at least 90% of the sample must come from a combination of stearic and palmitic acids. The remaining 10% of the sample may be derived from other fatty acids, such as myristic, pentadecanoic, margaric, arachidic and behenic acids. This leads to a Mg metal content between 4-5%, depending on the chain lengths of the fatty acids and their ratios. The content of stearic and palmitic acids in a MgSt sample can be determined using a boron trifluoride-methanol extraction method to convert the stearate and palmitate to their methyl esters and separate and identify them using GC-MS. (19-22) Although commercial MgSt samples have a range of chemical compositions, and USP has set broad guidelines for chemical composition requirements, several researchers have suggested that within these guidelines the fatty acid composition does not seem to affect lubrication. Interestingly, Rajala et al. found that two lots with similar chemical composition behaved very differently, possibly due to their hydration state differences.(23)

The synthesis preparation of MgSt has been described in the literature using two basic reaction methods. Equation 1-1 is the most basic reaction for MgSt synthesis, and was noted in Kahner's 2017 review as one of two methods to make MgSt.(17) The second reaction, shown in Equation 1-2, is a two-step reaction published by Miller and York in 1985, Ertel et al. 1987 and Rajala et al. in 1995. (23-25)

$$2 \text{ H-St} + \text{Mg(OH)}_2 \rightarrow \text{Mg-St}_2 + 2 \text{ H-OH} \qquad \text{Equation 1-1}$$

$$2 \text{ H-St} + 2 \text{ NaOH} \rightarrow 2 \text{ Na-St} + \text{MgCl}_2 \rightarrow \text{Mg-St}_2 + 2 \text{ NaCl} \qquad \text{Equation 1-2}$$
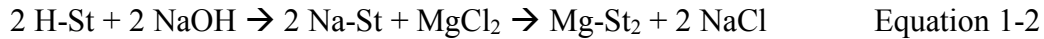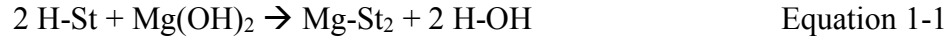
Parts of the reaction shown in Equation 1-2 has subsequently been patented by Mallinckrodt for manufacturing use with high ratios of stearate to prepare the dihydrate form of MgSt with a plate morphology. (26, 27) It is noted that other alternative salts may be substituted for NaOH and $MgCl_2$ in Equation 1-2. In particular, Wu at Mallinckrodt has also presented the same synthesis reaction substituting $MgSO_4*7H_2O$ for the $MgCl_2$.(28) As Mallinckrodt recognized, the most important effect of chemical composition appears to be its effect on the hydrate form produced during synthesis.(29) Marwaha and Rubenstein suggested that the alignment of fatty acid chains in a crystal is governed by the chain length in the crystal packing structure, which would affect the shearing potential of MgSt.(30)

Fatty acid composition has not yet been systematically investigated in relationship to dissolution and lubrication. To facilitate that study, the relationships between fatty acid composition and crystal form needs to be addressed. Also, the differences between the two synthesis methods for MgSt have not been defined in terms of their effects on the properties of MgSt produced. Chapter 4 addresses some of these questions around relationships between fatty acid composition and crystal form, in the context of MgSt synthesis. Of particular interest is the forms produced by the two known reaction methods, using varying fatty acid ratios.

1.2.2   Hydration State, Crystal Forms and Pseudopolymorphism

Magnesium stearate is currently known to exist in multiple pseudopolymorphic forms, but it has taken a few decades to reach this point. Back in 1977, Mueller et al. noticed that the amount of water in a MgSt sample was related to its lubrication properties, and that thermal drying can change its polymorphic properties. They suggested that drying changes the crystal structure from an orthorhombic or monoclinic crystal structure to hexagonal structure.(31) A few years later, Miller and York began

their investigation into physical characterization of MgSt powders by preparing and characterizing pure magnesium stearate and magnesium palmitate samples, without mixing fatty acids. They identified that both pure samples were associated with two molecules of water, and suggested that synthesis conditions such as pH played a role in hydration state.(25) Ertel and Carstensen also studied the physical properties of pure MgSt throughout the 1980s.(24, 32, 33) They determined that preparation conditions affect the hydration state and modifying the relative humidity (RH) can convert to a different hydration state. For example, heating at 105 °C led to water loss as well as crystal lattice collapse. In addition, they noted the importance of the long spacing of the crystal lattice structure, which is dependent on the hydration state.(18) Wada specifically looked at MgSt pseudopolymorphism and hydration using differential scanning calorimetry (DSC),(34) but it was not until 1997 that Sharpe et al. appears to be the first to identify the pseudopolymorphs as anhydrate, dihydrate and trihydrate (but without mention of a monohydrate form).(35) They proposed structures for the dihydrate and trihydrate phases based on the long crystal spacing from x-ray powder diffraction (XRPD) and deduce that the pseudopolymorphism is a result of "changes in the angle of inclination of the hydrocarbon chains relative to the plane of the Mg atom head groups, brought about by the water content in the lattice."(35) Bracconi et al. performed a thorough XRPD investigation of two commercial lots without single crystals in an attempt to fully elucidate the crystal structure.(36) Their subsequent differential scanning calorimetry (DSC) evaluation of the same two lots did not "fully clarify the relation between thermal and structural properties."(37) Although the single crystal structures of MgSt forms are still elusive, Delaney et al. showed that SSNMR can uniquely and reliably identify the different crystalline forms of MgSt. Five forms were identified as anhydrous, ordered monohydrate, dihydrate and trihydrate forms and an additional disordered monohydrate.(38) In terms of form conversions, Swaminathan and Kildsig published a schematic in 2001 showing conversions between the different hydrate forms,(39) which was updated to include the monohydrate form in a presentation by Wu et al. along with extensive evaluation of MgSt dihydrate properties from a commercial manufacturer's point of view.(28)

The ability to identify MgSt crystalline forms using ^{13}C SSNMR (Delaney et al.) is critical, as it not only allows for identification of the existing hydrate variability, but also provides a foundation for studying hydrate form interconversions, as well as the observation of MgSt forms in tablet formulations before and after processing.(38) Chapter 3 presents characterization data for MgSt, emphasizing the power of SSNMR to distinguish between crystal forms of MgSt and laying a foundation for the remainder of this research. Additionally, Chapters 5 and 6 take another step in furthering the understanding MgSt form conversions.

1.2.3   Particle Size and Surface Area

In addition to chemical composition variability and pseudopolymorphism variability, the particle size and surface area of MgSt have been investigated for their impact on MgSt performance variability.

In 1984, Frattini and Simioni reported a correlation between MgSt surface area and tablet ejection force. (40) Hoelzer also published on "batch to batch variations of commercial magnesium stearate" focusing on surface area variations.(5) Phadke et al. suggested that particle size analysis would be a potential way to evaluate batch-to-batch variation in MgSt, and also studied the degassing effects on MgSt, associated with surface area analysis, hypothesizing that lower surface area after degassing could be due to hydrate form conversion.(41, 42) In 1996, Barra and Somma tested 13 commercial samples which showed a range of results with minimal correlation, although chemical composition, particle size/ surface area and crystal form were all believed to be significant contributing variables affecting MgSt function.(8) A study of MgSt surface area by Andres et al. in 2001 recognized the need for an improved understanding of MgSt isotherm mechanisms and degassing effects,(43) followed by Koivisto et al. who noted in 2004 that although all hydrate forms converted to anhydrous at 105 °C, the hydrate surface area isotherms did not properly fit with BET theory, the standard method of surface area analysis. (44) Extensive investigation of the degassing of MgSt has recently

been undertaken by Lapham and Lapham, revealing dehydration and unreliable surface area results with degassing as low as 40 °C.(45, 46)

In the Lapham 2019 paper, the surface area and isotherms of four commercial samples were analyzed before and after degassing at temperatures ranging from 30 – 110 °C. The hydration state of the starting materials was determined from thermogravimetric analysis (TGA) weight loss and vacuum drying, with assumptions of anhydrous and hydrated forms based on weight loss temperatures. Looking closely at isotherms and low pressure hysteresis, the differences in adsorption/desorption isotherms for the samples were found to be related to the hydrated water in the starting form for each batch and a swelling effect causing adsorbate to be entrapped in the sample during the adsorption process.(45-47) The Lapham work stops short of relating the dehydration changes to MgSt crystal forms. This next step in understanding the dehydration of MgSt required a technique which can readily identify the crystal forms of MgSt. ^{13}C SSNMR enables this type of study and the form changes of MgSt with dehydration were clearly identified in Chapter 6.

1.3   Effects of Processing on MgSt

1.3.1   Mixing

In addition to the physicochemical properties of MgSt, processing conditions affect MgSt functional properties. The most important aspect of processing for MgSt is formulation mixing time. It is well-known that short mixing times for MgSt result in poor distribution of MgSt, but Ragnarsson et al. showed that this did not hurt lubrication efficiency in 1979.(49) However, longer mixing times with MgSt did affect tablet strength.(49) In 1993, Ong et al. compared surfactants mixed with MgSt in formulation blends and showed drug-excipient interactions taking place with extended mixing.(50) Chaudhuri discussed cohesion and mixture homogeneity with a description of the mixing model, finding that for free-flowing mixtures, higher mixing speed enhances mixing.(51) Virtanen showed that tablet crushing strength decreased with mixing time, and scale-up

conditions led to a greater decrease in tablet strength.(52) Then in 2010, Perrault et al. used gamma ray detection to investigate the blending mechanisms of mixing performance of MgSt and sodium laurel sulfate with a V-blender. The results indicated that shear mixing (blender rotational speed and fill volume) was more important than dispersive or convective mechanisms of blending.(53) Kushner followed with a mixing model for Turbula blenders using 1% MgSt.(54) Jojart analyzed the optimal mixing time and Turbula speed using energy dispersive x-ray fluorescence analysis.(55) Nakamura et al. determined ideal mixing time and MgSt amount based on the relationships between Carr's flowability index and practical angle of internal friction with tablet properties. It was found that powder flowability correlated with mixing time and tablet properties (but not with MgSt concentration).(56) A 2018 study by Horibe et al. used three different scales of V-type blenders to study mixing and lubrication with MgSt. Mixing time efficiency was determined to be related to the travel distance of the particles in the different blenders.(57)

In all of these studies, ranging from effects of colloidal silica and surfactants, mixing models, gamma ray detection of MgSt in tablets and flowability index, it was assumed that all MgSt lots will behave the same way. However, the previous three sections have shown significant variability in MgSt sample properties that can affect performance. A discussion of the effects of hydrate form on mixing would be a good addition to this discussion of the effects of processing on MgSt.

1.3.2   Chemical Reactions and Disproportionation

Another aspect of processing involves the effect of water to mediate chemical reactions between MgSt and the salt of an API, such as with disproportionation reactions. A disproportionation reaction is where a salt converts back to the free form, particularly for systems where the slurry pH of formulation needs to be greater than pH_{max} of the salt of a weak base.(58, 59) In 2009, Guerrieri and Taylor introduced disproportionation of salts in the solid state as an important topic in pharmaceutical science, identifying solubility and pH_{max} as important parameters for understanding disproportionation.(60)

Stephenson et al focused their efforts on understanding the importance of pH_{max}, pH microenvironment and Gibb's free energy, trying to determine what pH is too low to develop a salt. They concluded that active pharmaceutical ingredients (APIs) with low intrinsic solubility and low pK_a are likely to disproportionate and John et al. noted that carboxylate groups with pK_a above the pH_{max} of the salt are likely to disproportionate. (61) Hygroscopicity, alkalinity and stearate particle size were also found to impact the extent of disproportionation, as well as deliquescence of reaction products such as $MgCl_2$.(62-64)

With the basic theory of disproportionation established, the research turned to elucidating which materials promoted and hindered disproportionation. John et al. investigated several excipients for disproportionation likelihood. Formulations containing MgSt had a high water uptake above 31% RH and MgSt was the most likely to cause disproportionation because the disproportionation reaction yields the deliquescent $MgCl_2$ as a reaction product.(65) Merritt et al. performed quality by design (QbD) modeling for thirteen drugs in four formulations with XRPD and SSNMR analysis(66) while Wray et al. and Ewing et al. used NIR imaging and Raman mapping to study disproportionation during dissolution.(67, 68) Nie et al. studied the impact of polymers on disproportionation and investigated ways to stop or reduce disproportionation of Pioglitazone HCl (pHmax 2.8). In addition to using acidic pH modifiers such as maleic acid, crystalline solid dispersion with HPMC-AS was found to slow disproportionation of PIO HCl.(69) Further study by this group investigated the disproportionation of metallic stearates including MgSt, calcium stearate (CaSt) and sodium stearate (NaSt).(64) MgSt, CaSt and NaSt are stearate soaps with different counter ions, with NaSt being the most commonly used soap. It was suggested that sodium stearate (NaSt) may be an adequate lubricant to replace MgSt when disproportionation is a concern. Thakral studied the role of solubility and developed a flow chart to describe when to expect disproportionation based on the system conditions,(70) followed by a review of disproportionation from a material science perspective.(71) Koranne et al. investigated PIO-HCl mixtures with various excipients using synchrotron x-ray diffractometry to study disproportionation in tablets. It was found that MgSt showed greatest disproportionation followed by croscarmellose sodium. The reaction was mediated by water, initiated at the surface of

the tablets, and there was correlation between microenvironment pH acidity and disproportionation extent.(72) Patel et al. studied disproportionation using surface topography analysis and suggest that salt crystal structure plays a role in a drug's propensity to disproportionate.(73) Hirsh et al. are recently using ^{35}Cl SSNMR to quantify the disproportionation of Pioglitazone HCl in reaction with MgSt.(74)

The tendency to disproportionate is important to consider when formulating with MgSt and basic salts in the lower pK$_a$ range. However, there have been no studies so far investigating the effect of MgSt hydrate forms or other physicochemical properties on the extent of disproportionation. Additionally, SSNMR might easily be used to follow disproportionation reactions. It is also interesting to note that much of the disproportionation investigation comes out of industry, with Merck, Eli Lilly, BMS, Amgen and Pfizer all represented.

1.4 Effects of MgSt on Functional Properties

1.4.1 Effects of MgSt on Lubrication

Lubrication is the primary function of MgSt in pharmaceutical formulations. That is, a lubricant reduces friction by forming a film between two surfaces and is easily sheared.(2) MgSt has been used as a lubricant for many years and was recognized to reduce ejection force in 1979.(49) A review of lubrication was done by Moody et al. in 1981,(2) defining MgSt as a low shear strength laminar solid that adheres to the lubricated surface with the polar head, with the long hydrophobic fatty acid chains toward the opposing surfaces. MgSt is considered to be an effective lubricant due to its high melting point and good shear properties, as well as being able to reduce static charges in the formulation powder.(75) Shear strength has been measured using punch penetration,(76) but shear strength evaluations have not found correlations with lubricity.(77) One mechanism of action says that the lubricating film for MgSt is thought to be only one or two molecules thick.(2) It has also been shown by SEM that in granule lubrication, MgSt can fill the particle cavities and spaces between the lubricated

surfaces.(78) Johannson et al had previously showed that granular MgSt had better tablet properties than powdered MgSt when used at 2-5%. At low concentrations, powdered MgSt works better to prevent adhesion to punch faces.(79)

In 1988, Vromans et al. reported that MgSt did not always lubricate the same way. This was attributed to differences in particle size and surface area, flowability and mixing process.(80) Mixing time has often been implicated in MgSt lubrication performance.(81, 82) Many other studies have investigated the effects of different MgSt lots on lubrication properties. Marwaha et al. studied various % of St:Pa related to compression and ejection properties,(30) Ertel and Carstensen correlated MgSt fatty acid composition, moisture content and surface area with lubricant properties for three monohydrate commercial samples and three pure MgSt anhydrous, dihydrate and trihydrate samples.(33) Hussain looked at dissolution using different grades of MgSt.(83) Leinonen et al. noted that it was hard to make correlations because for most samples, too many properties varied at the same time, but they did find a correlation with particle size/surface area and lubricity.(84) Particle size and crystalline structure were found to impact the lubrication properties of MgSt in the thirteen commercial batches studied by Barra and Somma.(8) Six commercial samples and their physical properties were tested for lubrication efficiency using a texture analyzer in a study by Rao et al. again finding that particle size/surface area and crystal form impact lubrication.(85) Okoye, Hamad, Wu and Lugge also showed lubrication effects varied with hydrate form.(9, 86-88) A recent review by Kahner discusses the impact of hydration states on MgSt lubrication and demonstrates that more work is needed to understand the properties of the different forms and their effects on tablet performance.(17)

None of these studies was designed to isolate and control the range of physicochemical properties of a variety of MgSt samples. In order to further the understanding of MgSt properties on lubrication, the crystal form needs to be deconvoluted from the other properties. Chapter 9 begins to address this by looking at the effect of crystal form on lubrication properties.

1.4.2   Effects of MgSt on Dissolution

Dissolution is an important functional property for pharmaceutical formulations. It is known since before 1963 that MgSt causes slowed dissolution of API formulations(89) and that formulation mixing time and compression force, as well as the amount of MgSt in the formulations affect the dissolution rate.(90, 91) The mechanism of MgSt lubrication was investigated and the effect of MgSt on mixing time and compression force has been attributed to lamination and adhesion of MgSt to the other particles in the formulation, along with the flaking of MgSt causing an increase in surface area.(90, 92) Hussain et al. suggested that the extent of surface coverage of the hydrophobic film on the particles is the most important factor in affecting dissolution.(83) Patra et al. studied the effect of MgSt concentration and granule size on the dissolution rate of ciprofloxacin HCl and found that a hydrophobic lubricant like MgSt decreases the drug-solvent interface, causing slower dissolution due to decreased wettability and increased dissolution rate with smaller granules.(93) Possible interactions with MgSt have been explored for their effects on dissolution, including the addition of colloidal silica by Johansson et al.,(94) the interactions of surfactants with MgSt during mixing,(50) and the interaction of MgSt with HPMC-AS in ASDs and hydrogen bonding with itraconazole ASDs.(95, 96) The effects of acidic media was also investigated by Ariyasu et al. and indicates conversion of MgSt to stearic acid during dissolution.(97, 98) Additionally, other lubricants were explored as alternatives to MgSt, including calcium stearate,(98) glycerin fatty acid esters,(99, 100) Stear-o-Wet,(101) talc.(102) Hussain, York and Timmins compared the dissolution of paracetamol tablets with different grades of MgSt. No relationship between physical properties such as surface area and dissolution was found at the conditions used in their study.(83) In 2013, Okoye et al. observed differences in dissolution between naproxen and acetaminophen when comparing MgSt dihydrate, monohydrate and anhydrate forms.(87)

In general, it is known that MgSt particle size and surface area can affect dissolution of tablet formulations. However, the relationship of surface area with dissolution is not well-defined, possibly due to other factors also contributing to the

behavior of formulations containing MgSt. A definitive study of the influence of MgSt crystal forms on dissolution has not yet been published.

1.5   Conclusions and Next Steps

In conclusion, there has been significant research on many aspects of MgSt. However, there remains a lot to do. One of the primary knowledge gaps seen throughout the literature is a difficulty identifying crystal form. Without a technique to clearly identify the crystal forms, it is difficult to deconvolute the effects of form from the other physical properties, or to understand the relationships of the physical properties of MgSt with each other. It has also been challenging to monitor the forms of MgSt in a formulation, since MgSt is added to the formulation in a low amount. ^{13}C SSNMR addresses both of these issues by allowing straight-forward identification of MgSt crystal forms, paving the way for the study of MgSt forms in pharmaceutical formulations.

The theme of the present research is understanding the variability between different MgSt materials, as it relates to tablet function, with a focus on crystal forms. Investigations of the impact of MgSt physicochemical properties (chemical composition, hydrate crystal forms, particle size and surface area) on the functional properties of tablets in terms of dissolution and lubrication will be the subject of the following chapters.

Chapter 2 is a discussion of solid-state NMR (SSNMR) theory and methods employed during this research. Chapter 3 is an adaptation of a paper focusing on the characterization of MgSt. In this paper by Delaney et al., SSNMR is shown to clearly identify five different forms of MgSt, paving the way for easier study of MgSt hydration states and crystalline forms. Chapter 4 discusses the synthesis of MgSt, showing the trends in crystal form produced with differences in fatty acid composition and synthesis method conditions. Chapter 5 discusses form conversions between the different MgSt crystal forms and the conditions required to affect the form conversions, specifically the effects of temperature, relative humidity and rehydration. Chapter 6 takes a further step to understand the MgSt form conversions that may result from drying and dehydration, for

surface area analysis. Chapter 7 describes the method development process for a discriminating dissolution method for MgSt in tablet formulations, followed by Chapter 8 with an investigation into the effects of physicochemical properties (chemical composition, crystal forms, particle size and surface area) on dissolution of indomethacin tablet formulations. Chapter 9 is an investigation of the effects of MgSt hydrate form on the lubrication properties of ejection force, tensile strength, compactibility and compressibility. Chapter 10 has conclusions and next steps, followed by Appendices including tables of MgSt samples and their properties.

CHAPTER 2.   BACKGROUND ON SOLID-STATE NMR SPECTROSCOPY

SSNMR is one of the primary analysis techniques used in this work. For magnesium stearate (MgSt), ^{13}C SSNMR gives the clearest and most straight-forward distinction between crystal forms, compared to the other analytical techniques used to probe crystallinity. Using SSNMR to evaluate the crystal forms of MgSt, it was possible to separate and study the complicated and often convoluted properties of MgSt. Without SSNMR it has previously been impossible to accurately characterize the form of MgSt in tablets. Using ^{13}C labeled stearate and palmitate, MgSt and Mg palmitate were synthesized to enhance the ^{13}C level in the samples, enhancing the sensitivity by increasing the population of ^{13}C in the samples. Using this technique, tablets containing MgSt at a level of 1% in the formulation can be easily detected by SSNMR. This enabled the analysis of MgSt crystal form changes in tablets before and after processing. Another SSNMR experiment used in this research was ^{1}H T_1 relaxation values, which were found to show important correlations with fatty acid composition, water content and other properties of MgSt, as well as useful information relating to structural order. Overall, SSNMR proved to be a critical part of this research work with MgSt. However, since it is a technique that is much less widely understood compared to the other analytical techniques, such as diffraction scanning calorimetry (DSC), gas chromatography (GC), etc., it is important to describe the essential components of solid-state NMR as it relates to MgSt characterization.

This chapter will give an introduction to the basic theory of NMR, as well as basic SSNMR concepts as it applies to pharmaceutical industry, with special attention to techniques which are used in this dissertation research. For a more comprehensive study of SSNMR theory, the reader is directed to other sources.(103-106)

2.1   Basic NMR Theory

2.1.1   Nuclear Magnetic Resonance

Nuclear magnetic resonance is a technique that measures how nuclei in a magnetic field respond to an electronic pulse resonating at the same frequency. Specifically, nuclear magnetic dipole moments interact with the external magnetic field, providing chemical information on the sample. Nuclei contain protons and neutrons surrounded by electrons. In a strong magnetic field, B_0, the nuclei are moving charges, which creates a nuclear magnetic dipole moment, μ. All nuclei have a spin quantum number, I, which are quantized and can be 0, 1 or multiples of ½ (I = ½, 1, 3/2, 2, 5/2, etc.). There are 2I +1 possible spin states for a nucleus. Nuclei with spin quantum numbers greater than 0 possess nuclear spin angular momentum, P, and are considered NMR active. In this dissertation, only ^{1}H and ^{13}C will be discussed, which are both spin ½ nuclei.

The spin angular momentum, P, is proportional to the spin quantum number, I, and the nuclear magnetic dipole moment, μ, according to Equation 2-1.

$$\mu = \gamma\ P = \gamma\ I\ \hbar \qquad\qquad\qquad \text{Equation 2-1}$$

where h is Planck's constant and γ is the gyromagnetic ratio, specific to each type of nucleus. This means that nuclei having angular momentum with nuclear spin are like tiny bar magnets, precessing about the applied magnetic field at a frequency corresponding to the angular momentum of the nuclear spin. The rate of precession is called the Larmor frequency and is proportional to the external magnetic field, B_0, and the gyromagnetic ratio, γ. The gyromagnetic ratio is an indication of the magnitude of the interaction between nuclei, according to Equation 2-1:

$$P = B_0\ \gamma \qquad\qquad\qquad\qquad \text{Equation 2-2}$$

For a ^1H nucleus in a 7.05 T magnetic field, the Larmor frequency will be 300 MHz, while a ^{13}C nucleus in the same magnetic field will precess at 75 MHz.

In an external magnetic field, the spin states of spin ½ nuclei split into m = + ½ and m = – ½, and their magnetic moments are aligned with and against the magnetic field. The spins that are aligned with the magnetic field have lower energy and the spins aligned against B_0 have higher energy.
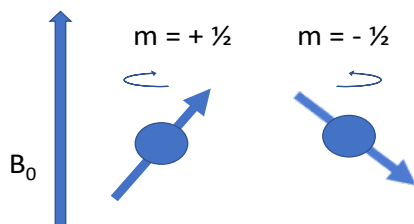
Figure 2-1. Model of precessing nuclear spins in a magnetic field, B_0, for a spin ½ nuclei with m = + ½ and m = - ½.

There is a slight population difference between lower energy and higher energy states, which is governed by the Boltzmann distribution (see Figure 2-2):

$$\Delta N_0 = Ne^{\Delta E/kT}$$ Equation 2-3

where N is the number of nuclei present, ΔE is the energy between the two spin states, k is the Boltzmann constant and T is temperature. The slight excess of spins in the lower energy state allows for nuclear magnetic resonance to occur when a nucleus can change its spin state by absorbing energy equal to:

$$\Delta E = h\nu = \gamma \hbar B_0$$ Equation 2-4

where ν is the resonance frequency, or Larmor frequency. Applying a pulse at the resonance frequency, ν, excites the spins to absorb energy. The energy is also related to γ and B_0. A stronger external magnetic field, B_0, increases the population difference of nuclei in the two spins states and increases the sensitivity of the NMR signal. The population difference between NMR states is very small, on the order of 10^{-6} compared

with other spectroscopic techniques such as IR with population difference on the order of 10^8. As a result, NMR is a relatively insensitive technique requiring high magnetic fields as a primary way to enhance sensitivity.
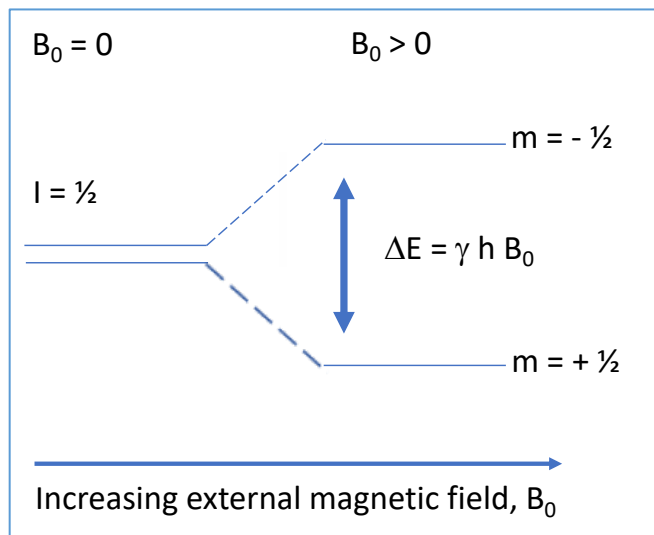
Figure 2-2. Diagram illustrating the splitting of nuclear spin states in a magnetic field. There will be a slight population difference between the states, according to the Boltzmann distribution of spins.

In an NMR experiment, a sample is placed inside a coil in a static external magnetic field. A radiofrequency pulse at the Larmor frequency is applied to the coil, perturbing the precessing spins and creating an alternating current in the coil surrounding the sample. The 90 ° radiofrequency pulse is applied at the resonance frequency and interacts with the nuclear spins, pushing the nuclear spin from rotating around the z-axis to rotate around the x-axis. This excites the nuclei to absorb energy, ΔE, and a signal is recorded as the sample returns to equilibrium. The resonating signal rings out with all the frequencies in the sample. The decaying resonance signal is collected as a free induction decay (FID) in the time domain, which is then amplified and processed through Fourier transform into an NMR spectrum in the frequency domain.(107, 108)

NMR is an inherently quantitative technique with the signal, S and magnetization, M_0, directly proportional to the number of nuclei in the sample, N:

$$S \sim M_0 = N(\gamma \hbar)^2 B_0 /4kT \qquad\qquad \text{Equation 2-5}$$

where N is the number of nuclei in the sample, k is the Boltzmann constant and T is temperature.

The relative amounts of two ingredients in a sample can be determined by comparing the ratios of the peak signals. Equation 2-5 illustrates that sensitivity is enhanced with higher external magnetic field and lower temperatures. The proportionality to N means that using isotopically-labeled material can have a significant effect on sensitivity. Throughout this dissertation, ^{13}C labeled magnesium stearate is used to enhance the sensitivity of the carbonyl peak of MgSt when it is used low levels in tablets. Additionally, signal-to-noise is proportional to the square of the number of scans, so increasing the signal by a factor of two requires four times the number of scans.

2.1.2   Chemical Shift

The most common use of NMR is to determine the chemical structure of a molecule based on the resonance frequency of the nuclei. The resonance frequency is usually plotted as the difference from a reference standard in parts per million (ppm). The chemical shift was first observed by Arnold et al. in the 1950s when distinct ^{1}H resonances were observed for ethanol, following the discovery of nuclear magnetic shielding(109). Nuclear magnetic shielding refers to the effect of electrons moving around the nucleus. When the negatively charged electrons circulate around the nucleus, a magnetic field is induced which changes the local magnetic field of the nucleus. The same type of nuclei experiencing a slightly different electronic environment can have different resonance frequencies, since magnetic field around the nucleus is affected by both the external magnetic field, B_0, and the local magnetic field from the orbiting electrons around each individual nucleus. The local magnetic field lowers the total magnetic field experienced by the nucleus, lowering their Larmor frequencies, and this effect is called shielding. Small differences in local magnetic field between different nuclei in a molecule result in slightly different magnetic shielding, referred to as chemical

shift. Differences in electronegativity of different functional groups in a molecule affect the magnetic shielding and determine the chemical shift. In this way, the chemical shifts of peaks in the NMR spectrum are dependent on the electronic environments of the nuclei in the sample. The electronic environment can be affected by the electronegativity of the attached atoms/functional groups, the molecular conformation of the molecule (or crystal packing in solids), and the ionization state of the molecule and interactions between molecules (such as hydrogen bonding). As noted before, chemical shifts are the peak positions of the nuclei in the sample, reported in parts per million (ppm) with respect to a reference peak. The frequency of the nuclei in Hz with respect to the external magnetic field in MHz gives the value in ppm. ^{13}C chemical shifts typically range from $0 - 200$ ppm, while ^{1}H chemical shifts typically range from $0 - 10$ ppm.

Lower ppm chemical shift values in the NMR spectrum indicate stronger shielding, so methyl and aliphatic carbons have lower chemical shifts. In a ^{13}C NMR spectrum, aliphatic carbons generally have a chemical shift of $10 - 40$ ppm, alcohols are $50 - 70$ ppm and aromatics are typically found in the range 110-150 ppm. Carboxyl and carbonyl carbons experience greater deshielding due to the electronegativity of the attached oxygen atoms and are usually in the $160 - 200$ ppm chemical shift range.

2.2   Solid-State NMR Spectroscopy

Solid-state nuclear magnetic resonance (SSNMR) spectroscopy is an important analytical tool in pharmaceutical science. It is non-destructive, selective and quantitative and can be used to aid understanding of the structure and molecular dynamics of a solid material, particularly as it relates to identifying polymorphic forms. Solid-state NMR is unique in being able to provide information on structure (chemical identification), order (crystalline form) and dynamics (through relaxation properties). However, there are a few important differences between solution and solid-state NMR.(110)

The chemical shift is orientation dependent, causing an important difference between solution NMR and solid-state NMR. In solution, molecules are able to move freely, resulting in sharp peaks with high resolution. In contrast, solids are rigid with

fixed orientation with respect to the magnetic field, leading to chemical shift anisotropy (CSA). CSA means that there is a distribution of chemical shifts, resulting in broad peaks and poor resolution in the solid state.

Several techniques are commonly used in solid-state NMR to alleviate the effects of CSA and line broadening, which will be discussed here: magic angle spinning (MAS), high powered dipolar decoupling (DD), cross polarization (CP) and total spinning sideband suppression (TOSS).

2.2.1 Magic Angle Spinning (MAS) and Total Sideband Suppression (TOSS)

One of the causes of CSA in the solid state is the rigid structure of solid materials that do not move freely in space compared to molecules in solution. The observed chemical shift is described by Equation 2-6:

$$\sigma_{obs} = \sigma_{iso} + \sigma_{aniso} (3 \cos^2 \theta - 1)$$
Equation 2-6

where σ_{obs} is the observed chemical shift, σ_{iso} is the isotropic component of the chemical shift and σ_{aniso} is the anisotropic component of the chemical shift. Magic angle spinning is a technique where the sample is placed in the magnetic field at an angle of 54.7°. The magnetic pole of the proton nucleus sits at an angle of 54.7°.(110, 111) The nucleus cannot line up straight with the B_0 field and instead precesses around the B_0 axis. When the sample is spun at this angle, it spends equal amounts of time oriented at the x, y and z axes and most of the anisotropy averages to zero. Mathematically, the anisotropic contribution to σ_{obs} in Equation 3 goes to zero when $\theta = 54.7°$. Samples are typically spun at rates between 2 kHz and 100 kHz, depending on the rotor size and capability of the sample probes holding the sample. When the spinning rate is changed, the width of the spinning sidebands changes, but the position of the isotropic chemical shift, σ_{iso}, does not move with variable spin speeds. The spinning rate used for the experiments discussed in this dissertation is 4kHz.

When samples are spun at a spinning rate faster than the width of the anisotropic chemical shift, the anisotropic contribution is zero and a single peak is observed for the chemical shift. If the sample spinning is slower than this, a residual anisotropic peak intensity can manifest, called spinning sidebands. Spinning sidebands are observed on both sides of a peak at a distance equal to the spinning speed. These spinning sidebands can be mathematically removed using a pulse sequence called TOtal Suppression of Spinning Sidebands (TOSS). Using MAS and TOSS together produces a spectrum with only the isotropic chemical shifts present.(112)

2.2.2   High-power Decoupling

High-power decoupling is another technique to minimize the effects of peak broadening in the solid-state NMR spectrum. Dipolar decoupling is when two or more nuclei interact through space, with the magnetic moment of one nucleus interacting with the magnetic moment of another neighboring nucleus. Again, the fast molecular motion of molecules in solution averages out to zero, but the effect of dipolar decoupling is pronounced in solids with rigid molecular structure. Dipolar decoupling can be homonuclear (i.e. between $^1H - {}^1H$ or $^{13}C - {}^{13}C$) or heteronuclear (i.e. $^1H - {}^{13}C$). The interactions are very strong, causing large line broadening in the solid state, so SSNMR primarily focuses on ^{13}C analysis. The chance of $^{13}C - {}^{13}C$ coupling is small due to the low relative abundance of ^{13}C, but the dipolar decoupling effect of $^1H - {}^{13}C$ is significant. The dipolar coupling effect is strongest for $CH > CH_2 > CH_3$ and less for quaternary carbons. In solution, the effects are averaged to zero, but anisotropy is seen in solids due to the fixed orientation dependence.

High power ^1H decoupling sequences such as Spinal 64 or two-pulse phase modulated (TPPM) sequences can be used to minimize this effect, giving narrower peaks and better resolution. In the decoupling phase of such an experiment, the magnetic moments are prevented from interacting by pulsing such that the nuclei are flipped back and forth between the up and down states very fast in order to average the dipolar

interaction to zero. The experiments in this work are performed using a Spinal 64 high power decoupling sequence.

2.2.3   Cross Polarization

Low sensitivity of the ^{13}C nuclei is addressed in NMR by the cross-polarization technique. Cross-polarization (CP) is used to improve the sensitivity of SSNMR for low-abundance nuclei such as ^{13}C, which has only 1.1% natural abundance. During CP, the magnetization of a high abundance nucleus (i.e. ^{1}H, 99.9% natural abundance) is transferred to a low abundance nucleus (i.e. ^{13}C, 1.1% natural abundance). The increase in magnetization transfer from ^{1}H to ^{13}C is proportional to the gyromagnetic ratios and results in a gain in sensitivity of four for ^{1}H to ^{13}C.(113) A 90 ° pulse is applied at the proton resonance frequency, causing the magnetization to align in the xy plane. Then the phase of the pulse is rotated by 90 ° to lock the spins in the xy plane. At the same time, a pulse is applied to the resonance frequency of the ^{13}C spin, for a specified "contact time". When the pulse times and power levels are chosen according to the Hartmann-Hahn matching equation (see below), cross polarization is achieved. That is, the spins precess at the same frequency, allowing them to interact for the specified contact time. During CP, magnetization is transferred from the high abundance nuclei (^{1}H) to the low abundance nuclei (^{13}C), thereby increasing the sensitivity of the low abundance nuclei being detected. The Hartmann-Hahn matching condition is given as:

$$\gamma_H \, B_H = \gamma_C \, B_C \hspace{3cm} \text{Equation 2-7}$$

where γH is the gyromagnetic ratio of the ^{1}H nucleus, γC is the gyromagnetic ratio of the ^{13}C nucleus, and B_H and B_C are the magnetic strength applied to the ^{1}H and ^{13}C nuclei, respectively.

Using CP, the magnetization transfer rates are not the same for every nucleus in the sample. This means that CP is not quantitative without special considerations, which will be discussed in section D. This property also means that CP can be used for spectral

editing purposes, such as when a sample contains a solvent that is not chemically bound to the molecule of interest. CP can filter out the more mobile parts of the sample by varying the contact time. Using shorter contact times (i.e. 50 µs instead of 2 ms), CP will not transfer the magnetization of the more mobile carbons in the sample, such as unbound solvent and some CH_3 peaks that relax fast. Using these techniques, the cross polarization can be exploited to understand the sample in greater detail.

2.3   Relaxation

SSNMR is a versatile technique which not only gives chemical structure information, but also information about the dynamics of a sample.(114) This information on sample dynamics (i.e. sample mobility) can be probed through relaxation experiments, three of which are discussed here. Relaxation is a term used to describe the process in NMR where the nuclear spins in a sample return to equilibrium after an NMR pulse. This usually happens through spin-lattice relaxation (T_1), spin-lattice relaxation in the rotating frame ($T_{1,rho}$) and spin-spin relaxation (T_2).

Spin-lattice relaxation (T_1), also called longitudinal relaxation, occurs when the spins relax after a 90 ° pulse. In other words, the nuclear spins that were excited to a higher spin state during the pulse lose their energy and the population difference of the nuclear spin states returns to what it was before the pulse. The magnetization of the T_1 relaxation is described by Equation 2-8:

$$\Delta N = \Delta N_0 \left(1 - e^{-\tau/T1}\right)$$ Equation 2-8

where ΔN is the population difference, ΔN_0 is the population difference at thermal equilibrium, and t is the recycle delay time. Note that ΔN is proportional to the magnetization of the spins. The relaxation decay is an exponential process where the T_1 value can be measured using a saturation recovery experiment or inversion recovery experiment. In a saturation recovery experiment, the spins are allowed to return to equilibrium after a pulse. The time, τ, is varied and the time to return to 63% of

equilibrium is taken as the T_1 value. In order to acquire quantitative data, the spins must fully relax between scans. This requires five times the T_1 time. For non-quantitative analysis, the highest signal with the best signal-to-noise comes from using a recycle delay of approximately 1.2 times the T_1 value.

^{1}H T_1 relaxation happens through a process of spin diffusion. In spin diffusion, the magnetization of a nuclear spin is transferred to a neighboring spin through dipolar coupling. When one spin changes from $+ \frac{1}{2}$ to $- \frac{1}{2}$, it prompts the next one to change, and next and the next, until it reaches the end of the domain or edge of the particle. As a result of this spin diffusion, all the spins in a homogeneous sample have the same ^{1}H T_1 time. Spin diffusion also allows for the measurement of domain sizes, and is related to particle size, in solid samples. ^{1}H T_1 values are used for the experiments shown here and were acquired using CP. For magnesium stearate samples, the ^{1}H T_1 value is related to the crystal hydration state, as well as disorder and crystal defects originating from processing conditions.

Additionally, the ^{1}H T_1 values are typically much shorter than ^{13}C T_1 values, allowing for more scans in a shorter period of time, due to shorter relaxation time between scans. This greatly decreases the amount of time required for a ^{13}C SSNMR experiment. The T_1 relaxation experiment will be discussed in the next section.
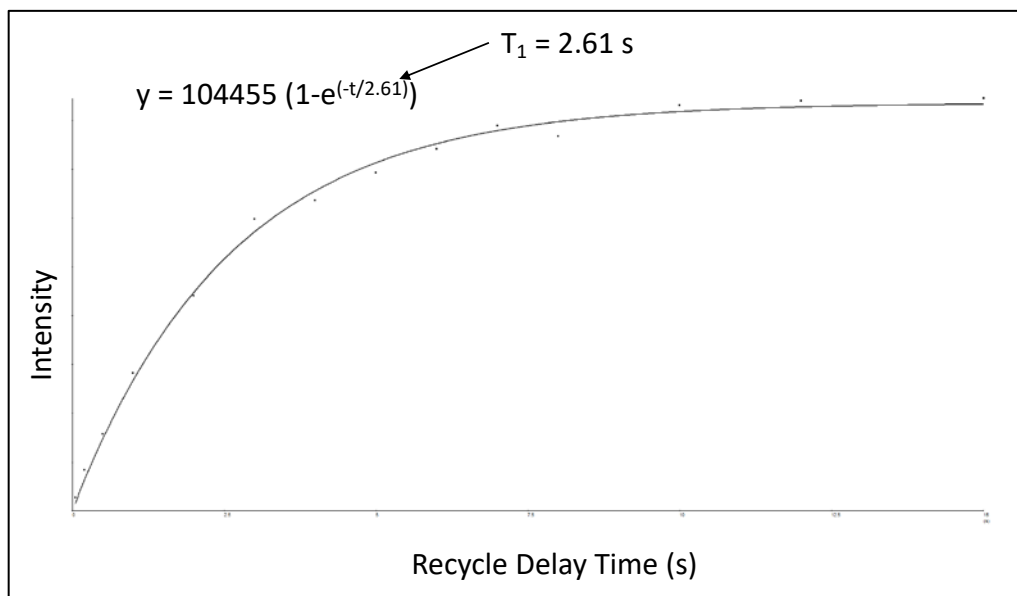
Figure 2-3. T_1 Relaxation Experiment. The magnetization intensity is plotted as a function of recycle delay time. The data is fitted to an exponential curve to determine the T_1 value.

Spin-spin relaxation (T_2), also called transverse relaxation, describes the relaxation after the 90° pulse, when the magnetization fans out in the x-y plane. The magnetization is losing coherence in the x-y plane and T_2 is the time it takes to return back to equilibrium. It occurs prior to T_1 relaxation and if the T_1 is set shorter than the T_2, then the T_1 is affected by the T_2 loss in coherence. The FID is dependent on the T_2 and a longer T_2 relaxation rings out longer in the FID, which is the order of milliseconds in solids. T_2 is proportional to the line width (line width ~ $1/T_2$), being much longer in solution than in solids.

$T_{1,rho}$ is the relaxation in the rotating frame (i.e. when the magnetization is spin-locked in the yz plane). It can give information on dynamics in a system and is often used along with T_1 to evaluate miscibility of mixed samples such as amorphous solid dispersions. T_2 and $T_{1,rho}$ values are both shorter than the T_1 relaxation, but effects of $T_{1,rho}$ on magnetization transfer can be seen when the CP contact time is varied. Offerdahl et al. describes quantitation of neotame using ^{13}C SSNMR CP experiments where the CP contact time is varied. The magnetization of variable contact time experiments decays according to the $T_{1,rho}$ relaxation. Extrapolating back to contact time of zero corrects for

the variability in CP magnetization transfer between different nuclei. This allows for quantitation of different forms in a solid sample, specifically using the CP variable contact time method for quantitation of the various forms of MgSt in tablet formulations.

2.4   Pharmaceutical Applications of SSNMR

There are several reviews discussing solid-state NMR applications to pharmaceutical science.(114-119) Using SSNMR, there is a sensitivity trade-off between sample size, sidebands from the MAS spinning rate and magnet size. Larger samples provide more molecules to increase the signal based on the number of nuclei in the sample between spin states. Spinning sidebands can be eliminated by spinning fast, but spinning at ultrafast spin rates can be physically challenging. Consider that 4 kHz is 250,000rpm, which is slow for SSNMR but 100X faster than a car engine. Smaller rotors can spin faster, but smaller samples have a lower number of nuclei, and therefore produce less signal. Large magnets can increase sensitivity, but cost is often prohibitive. Overall, in the current state of the field, 400 - 600 MHz magnets seem to be the sweet spot to balance between MAS rates and sample size.

In a pharmaceutical setting, the most useful nuclei to study with solid-state NMR are ^{13}C, ^{1}H, ^{19}F, ^{15}N, ^{31}P and ^{23}Na. Table 2-1 shows some basic SSNMR data for these nuclei, including natural abundance and relative sensitivity, which are very important for choosing a nucleus that will give sufficient signal for useful analysis. The practical notes indicate nuclei-specific considerations. Proton (^{1}H) is highly abundant and highly sensitive, allowing for single pulse experiments, but the resolution of peaks in the solid state is often very poor, requiring fast spinning to eliminate dipolar coupling. Carbon (^{13}C) is the most common nuclei used, but it has low abundance and low sensitivity, and several accommodations are needed to get useful data, including magic angle spinning (MAS), cross polarization (CP), dipolar decoupling (DD) and total sideband suppression (TOSS). Nitrogen (^{15}N) has lower abundance and sensitivity than carbon, but can supply information about ionization and pK_a information if accommodations such as CP, MAS, DD are used. Fluorine (^{19}F), with high abundance and high sensitivity, has been gaining

28

popularity in pharmaceutical settings in recent years, since fluorine is becoming more commonly incorporated into drug molecules. It can be ran using single pulse or DD experiments and is often ideal for quantification studies. Phosphorus (^{31}P) has high abundance and low sensitivity, requiring only CP to obtain good signal. Sodium (^{23}Na) has high abundance and is useful for studying Na salts, but has a quadrupolar spin which results in line broadening. Many other nuclei can be studied using SSNMR, but these nuclei are the most relevant to drug development and have NMR properties that facilitate their common use in pharmaceutical industry.(120)

Table 2-1. NMR Information for Selected NMR-active Nuclei

Nuclei	% Natural Abundance	Relative Sensitivity	Gyromagnetic Ratio (MHz/Tesla)	Frequency at 7.05 T	Practical notes*
^{1}H	99.99	1	42.58	300	Fast spinning Single pulse
^{13}C	1.13	0.016	10.71	75.4	Most common CP/MAS/DD/ TOSS
^{15}N	0.37	0.001	-4.32	30.4	Ionization, pK$_a$ CP/MAS/DD
^{19}F	100	0.83	40.05	282.3	Quantitation Single pulse or HPdec
^{31}P	100	0.0663	17.24	121.4	High abund, Low sens CP
^{23}Na	100	0.0927	11.26	79.4	Quadrupolar spin 3/2

*Note that all nuclei require magic angle spinning (MAS)

CHAPTER 3.   CHARACTERIZATION OF THE CRYSTAL FORMS OF MAGNESIUM STEARATE USING DIFFERENTIAL SCANNING CALORIMETRY, THERMOGRAVIMETRIC ANALYSIS, X-RAY POWDER DIFFRACTION AND SOLID-STATE NMR SPECTROSCOPY

3.1   Author and Journal Information

Julie L. Calahan[1], Sean P. Delaney[1,2], Matthew J. Nethercott[1,3], Christopher J. Mays[1], Nickolas T. Winquist[1], Donia Arthur[1], Manish Sethi[1], Daniel S. Pardue[1] and Eric J. Munson[1,4]*

[1]Department of Pharmaceutical Sciences, University of Kentucky, Lexington, KY 40536, USA

[2] United States Pharmacopeia, Rockville, MD

[3] Kansas Analytical Services, LLC., Ft. Collins, CO 80526

[4] Purdue University, West Lafayette, IN

*Corresponding author: Address: Purdue University, Robert E. Heine Pharmacy Bldg Rm 124D, 575 Stadium Mall Drive, West Lafayette, IN 47907-2091, Phone: (765) 494-1450, munsone@purdue.edu

3.2   Abstract

Magnesium stearate (MgSt) is the most popular pharmaceutical excipient used in tablet formulations. MgSt is the fatty acid salt of stearic acid and often is a mixture of fatty acid salts, such as palmitic acid. Additionally, there are several reported crystal forms. It is used as a powder lubricant in tablet formulations, typically added at a level of 0.5 – 2% and is typically mixed into the formulation as the last step, with a controlled mixing time. Inadequate lubrication results from too low an amount of MgSt or too short a mixing time, too much MgSt or excessive mixing time often results in slower dissolution rates. Switching between MgSt samples with variability in the properties of MgSt can cause variable performance of samples with the same mixing time, so it is important to understand the variable properties of MgSt. Several advanced analytical techniques were used to characterize the properties of commercial MgSt and synthesized MgSt samples. Solid-state NMR (SSNMR) was able to uniquely identify several crystal forms of MgSt. Several additional techniques also showed correlations with MgSt crystal form, including thermogravimetric analysis (TGA), differential scanning calorimetry (DSC) and scanning electron microscopy (SEM).

3.3   Introduction

Magnesium stearate (MgSt) is the most popular pharmaceutical excipient used in tablet formulations. It is included as an excipient in over half of the tablet formulations on the market, and is an effective solid lubricant, reducing the friction between the formulation powder and manufacturing equipment during the tableting process. (23, 121, 122) Chemically, MgSt is the fatty acid salt of stearic acid and often is a mixture of fatty acid salts, such as palmitic acid. The chemical structure of magnesium stearate is given in Figure 3-1. It is a di-salt of Mg, with Mg^{2+} ionically bonded with the carboxyl ends of two stearic acid (C18) fatty acid chains.
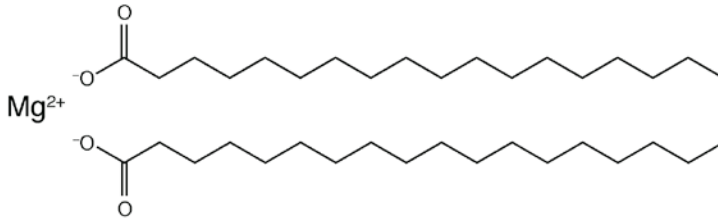
Figure 3-1. Chemical structures of magnesium stearate, the magnesium di-salt of stearic acid, with chemical formula of $Mg(C_{18}H_{35}O_2)_2$.

MgSt has been used as a solid lubricant in pharmaceutical tablet formulations since its introduction in 1970 by Hansen et al.,[11] typically added at a level of $0.5 - 2\%$ and is mixed into the formulation as the last step, with a controlled mixing time. Inadequate lubrication and tableting issues such as picking and sticking results from too low an amount of MgSt or too short a mixing time, (123-126) while too much MgSt or excessive mixing time often results in slower dissolution rates and potential bioavailability problems.(126-128) The proposed mechanism for MgSt is that it provides a hydrophobic coating on the surface of the drug and other excipients in the formulation, acting to reduce friction and lubricate on the one hand, and simultaneously inhibit dissolution on the other.(129)

Although MgSt is very popular and investigated extensively,(33, 130) the complex nature of the crystal forms and hydration state of MgSt is still not well understood.(7) There are at least five different crystal forms of MgSt: an anhydrous form, a disordered form and three hydrate forms: monohydrate, dihydrate and trihydrate form. Delaney et al. have suggested that the disordered form is a monohydrate, ordered on the fatty acid end of the molecules, rather than the carbonyl end. Some MgSt samples, including many commercial samples, exist as mixtures of two or more forms. Distinguishing between crystal forms to identifying and/or quantifying these crystal form mixtures can be challenging using many traditional analytical techniques. For instance, results from XRPD are often complicated by the variability in chemical composition between MgSt samples. Other techniques provide results which are not specific. As an

32

example, TGA analysis provides information about dehydration temperatures and total water content, but not about where the water is located in the crystal lattice.

In addition to the variety of crystal forms that may exist in a MgSt sample, the chemical composition can also vary. As noted earlier, the salt of the fatty acid (e.g. stearate) is present in MgSt, but the fatty acid may also be described using the acid form (e.g. stearic acid) and the two notations are used interchangeably in this work. Traditionally, MgSt is found as a natural product in both plants and animals, but pharmaceutical use is restricted to plant-based MgSt. (43) According to United States Pharmacopeia (USP) monograph for MgSt, at least 40% of MgSt must be derived from stearic acid (C18) and > 90% must come from a combination of stearic and palmitic acids. This allows for the remaining 10% to come from other fatty acids with varying chain lengths, including myristic, margaric, arachidic, etc.(19) Any crystal form can exist in any fatty acid combination and the chemical composition was found to vary with commercial suppliers. MgSt forms crystals in lipid bilayers with MgSt with the long fatty acid chains aligned together and the hydrophilic carboxylic acid groups aligned with the magnesium ions on the other end. (34, 131) The different hydrates are thought to incorporate water molecules into the crystal lattice between and around the magnesium ions.(36)

Many investigations have attempted to understand the effects of MgSt on tablet properties, (132-135) York and coworkers were among the first to thoroughly investigate MgSt properties. Their early work focused on characterization of the synthesized dihydrate form of MgSt, as well as the pure stearate and pure palmitate materials. (136, 137) Later studies focused on tableting properties, finding that commercial MgSt samples affected the dissolution more than the pure stearate samples.(83, 138-140)

Back in 1977, Mueller et al. noticed that the amount of water in a MgSt sample was related to its lubrication properties and that thermal drying can change its polymorphic properties. Their work investigating the pseudopolymorphism and crystal structure of MgSt(141) led to an interest in the hydration state and polymorphism of MgSt by many groups.(23, 24, 30, 33, 36, 131, 136) The most detailed study by Brittain and coworkers used DSC, PXRD and microscopy to analyze three forms of MgSt: the anhydrate, dihydrate, and trihydrate forms of pure magnesium stearate and magnesium

palmitate.(35) Their analytical and thermal investigation suggested that the dihydrate water of hydration is bound more tightly than the trihydrate water of hydration.

In a 2005 paper, Bansal and coworkers thoroughly characterized six different MgSt lots by DSC, TGA, XRPD, particle size, morphology, specific surface area, optical microscopy and Fourier-transform infrared spectroscopy.(85) The lubrication performance of their six samples suggested that the interplay of particle-level characteristics (particle size, larger specific surface area, and plate-like crystal habit) were more important than molecular level characteristics in terms of lubrication potential. This interplay of characteristics highlights possible causes of lubrication issues when using MgSt.

This chapter focuses on the variability that exists in MgSt samples using advanced analytical techniques to characterize MgSt materials from both commercial and lab-synthesized sources. In addition, this work incorporates ^{13}C solid-state NMR (SSNMR) spectroscopy(142) of MgSt, a non-destructive and quantitative technique that can provide detailed information about not only structure and form quantification, but also miscibility, and mobility through ^{1}H T_1 relaxation values. The results show that ^{13}C SSNMR can uniquely identify the distinct crystalline forms of MgSt, and these forms correlate well with other analytical techniques such as DSC, TGA, and PXRD.

3.4   Materials and Methods

3.4.1   Materials

Eight magnesium stearate samples were obtained from six different commercial sources: Alfa Aesar (lots H03W054 and C01Y019), MP Biomedicals (lot 75281), Chem-Impex International (lot 6301123019902), Acros Organics (lots A0288107 and A0235781), Sigma Aldrich (lot STBC0861V), and Fisher Scientific (lot 740042). The samples will be identified by their source and lot, as needed.

3.4.2 Synthesis of MgSt

The dihydrate form of MgSt was synthesized by dispersing a combination of stearic, palmitic, and other fatty acids (~0.1 mole) in 600 mL of Milli-Q water previously heated to 90 °C. Ammonium hydroxide solution (14.8 N) was added drop wise until the solution reached a pH of 9, generating a fatty acid soap with the stearic/palmitic acids. MgSt was precipitated out of solution by the addition of a stoichiometric excess of $MgCl_2$ * $6H_2O$. Finally, the magnesium stearate was isolated by vacuum filtration and was washed with acetone and water for 24 hour periods.(24, 30) Although ammonium hydroxide was used for this work, sodium hydroxide could also have been used to change the pH.(24, 131) Utilizing sodium hydroxide for the reaction results in a sodium soap being formed which is then replaced by the magnesium ions with the addition of the $MgCl_2$.

A second method for synthesizing magnesium stearate, specifically magnesium stearate monohydrate, has been developed. In this synthesis, ~0.1 mole of a combination of stearic, palmitic, and other fatty acids was placed into a beaker with a stir bar and was heated in an oil bath to ~90 °C. Once the fatty acids are melted, ~650mg of $Mg(OH)_2$ (Sigma Aldrich) was added to the melt followed shortly by 10mL of Milli-Q water to precipitate the magnesium stearate. The final product was washed with water for 24 hours and allowed to air dry (placing sample in a vacuum oven at 25 °C can also be done to hasten the drying process).

The anhydrous form of MgSt was made by placing the dihydrate form in an oven overnight at 105 °C, while the trihydrate form of MgSt was made by placing the anhydrous form in a container with a relative humidity of 75% or greater (although other studies have determined that 50% RH will also produce the trihydrate).(131) The disordered monohydrate form can be made by placing a monohydrate sample in the oven at 105 °C for two or more hours.

3.4.3 Solid-state NMR Spectroscopy

SSNMR spectra were acquired at ambient conditions using a Tecmag Redstone spectrometer (Tecmag, Inc., Houston, TX) operating at 100.57 MHz for ^{13}C (9.4 T static magnetic field). Samples were packed into 7 mm zirconia rotors and sealed with Teflon or Kel-F end caps (Revolution NMR, LLC, Fort Collins, CO). Experiments were performed using a 7 mm double resonance MAS probe (Varian, Palo Alto, CA). All ^{13}C spectra were acquired under MAS(143) at 4 kHz, using ramped-CP(144), TOSS(145), and SPINAL64 decoupling(146) with ^{1}H decoupling field about 66 kHz. A 1.5 ms contact time was used in all experiments. 3-methylglutaric acid (MGA) was used for optimizing spectrometer and as an external standard, with the methyl peak referenced to 18.84 ppm(147). Spectra were acquired with a 3 – 5 second pulse delay (~1.5 - 2 times the measured T_1 value).

^{1}H T_1 relaxation values were measured using a saturation-recovery experiment through ^{13}C observation. In the Fourier-transformed spectra, the peak of interest was integrated and plotted against recovery delay times and the values were fitted to the following equation:

$$M = M_0 \times \left(1 - e^{-\frac{\tau}{T_1}}\right) \qquad \text{Equation 3-1}$$

where M is the integrated signal intensity and τ is the recovery delay time. M_0 is an amplitude parameter obtained from the fit and T_1 is the obtained spin-lattice relaxation time.

3.4.4 Thermal Analysis

DSC thermograms were acquired using a Q2000 differential scanning calorimeter equipped with an RCS90 refrigerated cooling system (TA Instruments, Newcastle, DE). Nitrogen was used as the purge gas at a flow rate of 50 mL/min. Temperature and

enthalpy were calibrated using indium. Samples (~2-5mg) were placed in TZero aluminum pans and sealed with TZero aluminum hermetic lids with one pinhole (TA Instruments, New Castle, DE). Samples were heated at 10 °C/min from room temperature to 200 °C. Data were processed using Universal Analysis software (TA Instruments, Newcastle, DE).

A Q50 thermogravimetric analysis system (TA Instruments, Newcastle, DE) was used for investigation of the water content, i.e. hydration state, of the magnesium stearate samples. Nitrogen was used as the purge gas at a flow rate of 40 mL/min for the balance and 60 mL/min for the samples. Temperature was calibrated using a nickel standard and a magnetic bar for the Curie Point Temperature. Weight was calibrated using standard weights (200mg and 1g). Approximately 10mg of sample was placed on a platinum pan and heated at 10 °C/min from room temperature to 200 °C. The total weight loss from room temperature to ~125 °C was analyzed for water content.

3.4.5   X-ray Powder Diffraction

Differences in the hydrate form of magnesium stearate samples were also investigated using a powder X-ray diffractometer (MiniFlex 600, Rigaku Corporation, Japan) with Cu Kα radiation operating at 40 kV and 15mA. Samples were scanned from a 2θ of 2-45° at the rate of 2°/min and a step size of 0.02°.

3.4.6   Scanning Electron Microscopy

Scanning electron microscopy (SEM, Hitachi S-4300) was used for visual aid and particle size approximations in the investigation of the commercial samples. The SEM used a cold-cathode field emission filament type and has SE/BSE/EBSD detectors attached. The image resolution was secondary electron (1.5 nm). Various images were taken between 500x and 10000x zoom, although only the 1000x images are shown herein.

3.5   Results and Discussion

3.5.1   Synthesized MgSt Samples

Thermal data (DSC thermograms and TGA gravimetric weight loss) for the five forms of MgSt are shown in Figure 3-2. The TGA weight loss for the monohydrate form indicates ~ 3.0% water, with ~ 6% for the dihydrate and ~ 9% for the trihydrate. The observed weight loss amounts are consistent with the expected stoichiometric weight loss of ~ 3% weight loss per water molecule associated with the MgSt, with slight variations depending on fatty acid composition. The weight loss temperature range for the monohydrate, dihydrate and trihydrate are 100 - 125 °C, 80 - 110 °C and 60 - 80 °C, respectively. The dehydration difference between the hydrates suggests a difference in thermal stability between the mono-, di- and tri- hydrate forms. The disordered form shows a similar amount of total water loss as the monohydrate (~3%), but the weight loss event is much broader than for the hydrates. The monohydrate water loss is measured from around ~100 °C to 125 °C and the disordered weight loss is measured from 25 °C to 125 °C, since it begins losing water at a much lower temperature compared to the monohydrate. This can be an indication of surface bound water for the disordered form, rather than hydrated water bound in the crystal lattice.

The DSC thermograms show thermal transitions for the mono-, di-, and trihydrate forms, where the trihydrate has a dehydration onset around 60 °C, the dihydrate around 80 °C and the monohydrate has the highest transition with dehydration onset around 90 °C. Both the trihydrate and the dihydrate have a secondary transition with a peak around 120 °C, potentially indicating that there is a second thermal event occurring for these samples. It is possible that this is a conversion to monohydrate and the onset is obscured by the first transition. The disordered form and the anhydrate form have low temperature thermal events, occurring around 55-70 °C. The early transition for the disordered form appears to be a glass transition, with a subsequent melting onset matching the anhydrate melting onset around 130 °C. This is supported by the observation that the disordered

38

form converts to the anhydrous form upon extended heating above 100 °C. The low temperature transitions in both the disordered and anhydrous samples are consistent with the idea that a disordered structure around the fatty acid head group does not retain the water as effectively as the ordered crystalline forms.
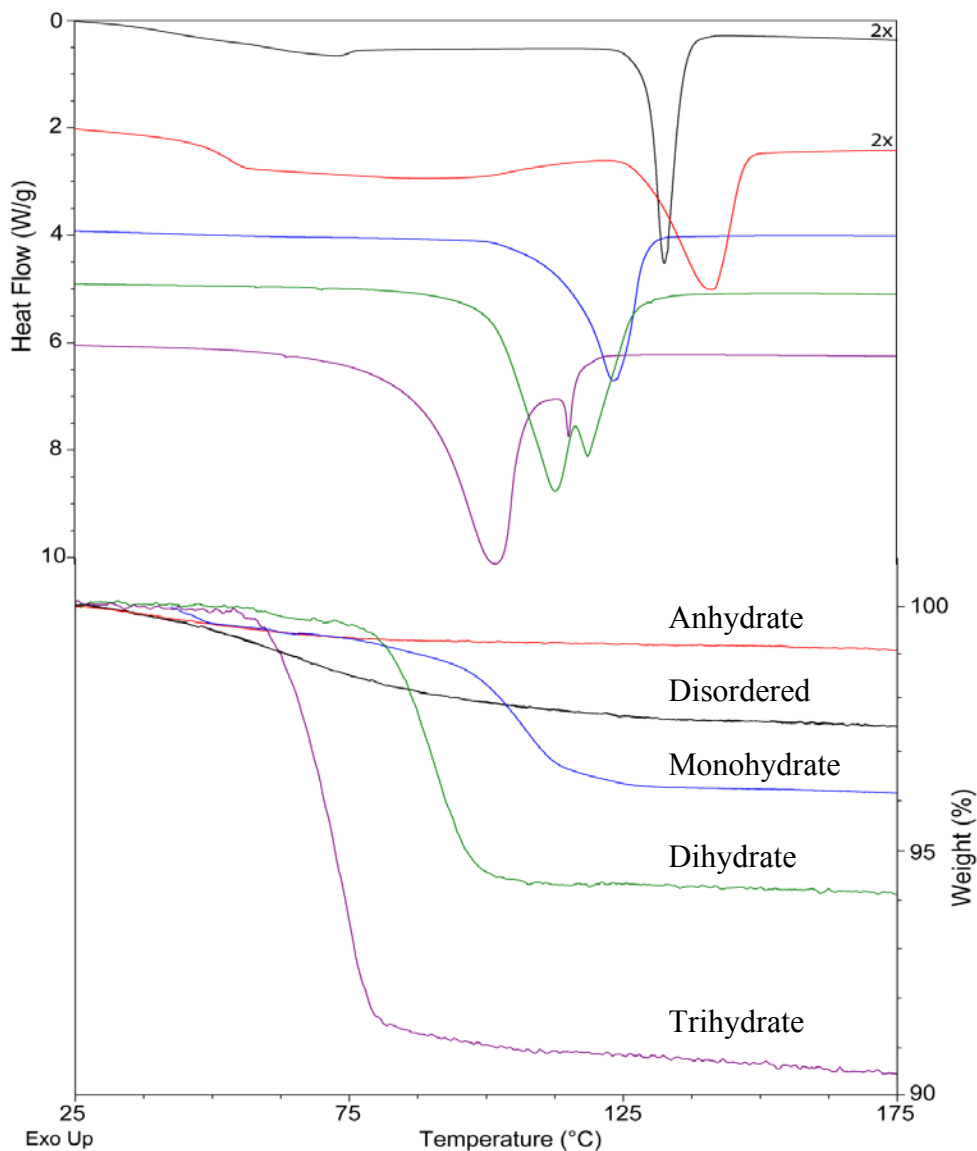
Figure 3-2. Differential Scanning Calorimetry (DSC) thermograms and Thermogravimetric Analysis (TGA) gravimetric weight loss plots for the five different forms of MgSt. DSC thermograms from top to bottom: Disordered, Anhydrate, Monohydrate, Dihydrate, and Trihydrate. TGA plots from top to bottom (at 175° C): Anhydrate, Disordered, Monohydrate, Dihydrate and Trihydrate. Figure used with permission.

Figure 3-3 shows the X-ray powder diffraction (XRPD) patterns of the five forms of MgSt. In general, the peaks for the monohydrate, dihydrate and trihydrate forms are slightly sharper than the peaks for the disordered and anhydrous forms. The disordered and anhydrous forms do not show a broad amorphous halo, but each has several poorly crystalline peaks, consistent with a partially ordered crystal structure. It appears that the XRPD analysis of the crystal structure of these materials may be complicated due to the differences in ordered and disordered structures in the carbonyl and the aliphatic regions of the fatty acid chains, respectively. Diffraction peaks in the $10 - 30$ degrees 2θ region show clear differences in the diffraction patterns for the mono-, di- and tri- hydrate forms, allowing for identification of the different pure hydrate forms. However, other studies have shown that the peak positions can change depending upon fatty acid composition.(85, 131) Additionally, many MgSt samples are mixtures of forms. These variations in fatty acid composition and/or crystal forms make it very challenging to rely on XRPD to identify the form of MgSt.
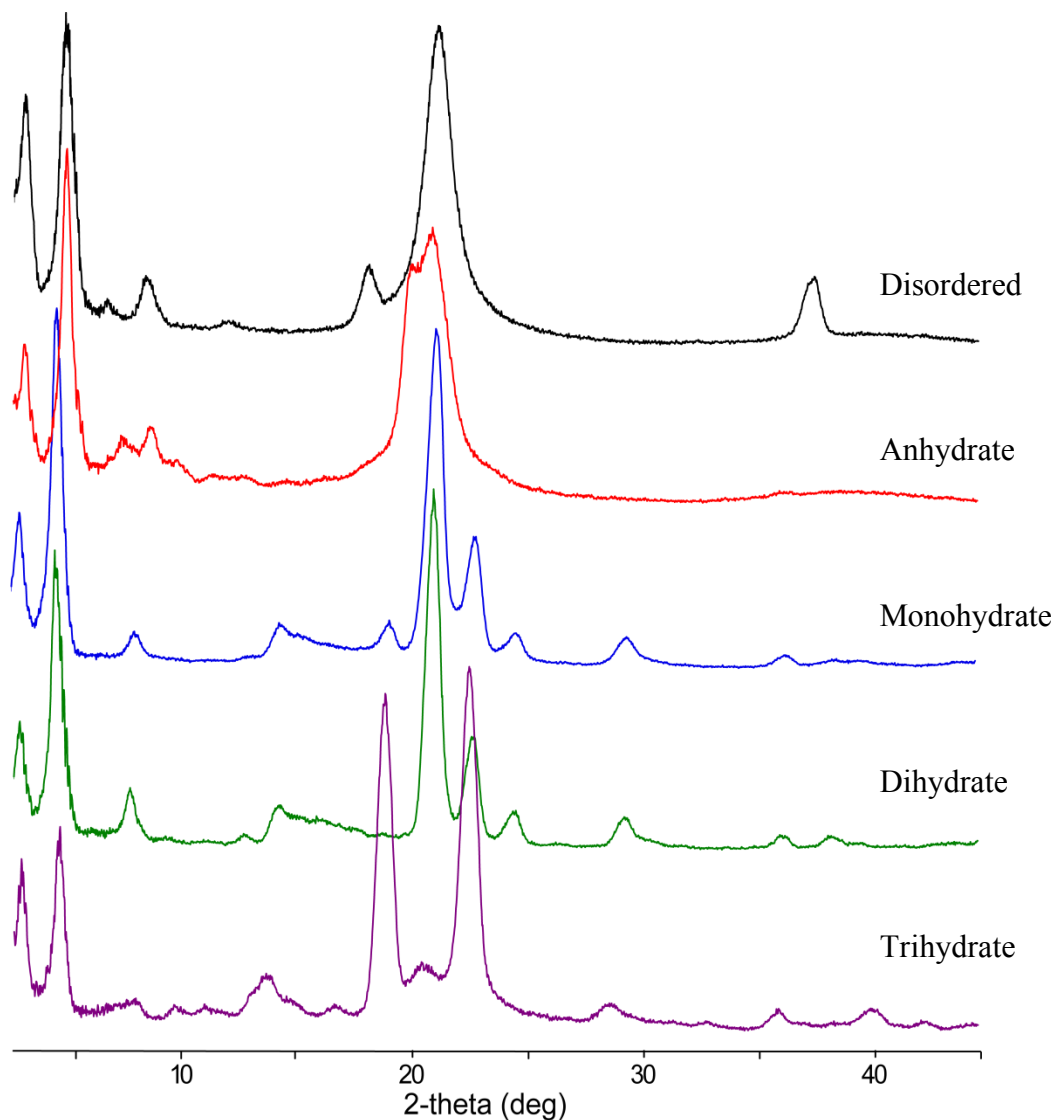
Figure 3-3. Powder X-ray diffraction patterns (PXRD) of the five different forms of magnesium stearate. Patterns from top to bottom: Disordered, Anhydrate, Monohydrate, Dihydrate and Trihydrate. Figure used with permission.

The ^{13}C CP/MAS NMR spectra of five crystalline forms of MgSt are shown in Figure 3-4. These materials were prepared according to the synthesis methods described earlier. The spectra can be divided into two sections. The left side shows the chemical shift region 170 – 190 ppm, which corresponds to the carbonyl carbon of the fatty acid chain. Four of the samples show sharp peaks, indicating an ordered, crystalline region around the carbonyl carbon. The fifth spectrum shows a broad peak, indicating disorder and a lack of long-range order in the carbonyl region. It has been designated

"disordered," rather than amorphous, due the apparent order in the aliphatic region. Multiple peaks for the carbonyl carbon indicate multiple molecules in the crystallographic unit cell. The dihydrate appears to have two molecules in the unit cell, while the anhydrate and monohydrate appear to have six molecules in the unit cell.
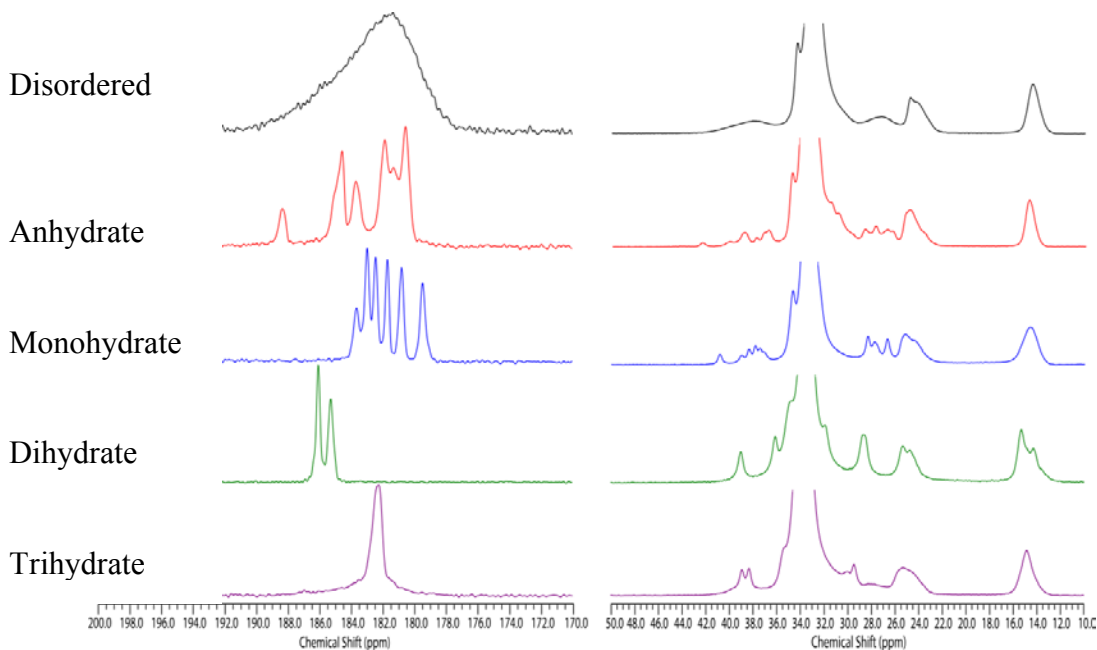
Figure 3-4. ^{13}C CP/MAS SSNMR spectra of five forms of magnesium stearate. The spectra show the carbonyl region (170–200 ppm) and the aliphatic region (10-50 ppm), as there are no other peaks in the spectrum. The forms are denoted in the figure by their hydration state, except for the disordered form, which is identified based on the disorder in the carbonyl region.

The aliphatic region of the spectrum (10 – 50 ppm) shows distinct peaks corresponding to the C_2, C_3, $C_{4-(n-2)}$, C_{n-1} and C_n carbons. The n designation refers to the carbon on the end of the fatty acid chain, e.g. n=18 for stearic acid, and n=16 for palmitic acid. The chemical shifts of the aliphatic carbon peaks can be observed for C_2 (~38 – 41 ppm), C_3 (~28 ppm), $C_{4-(n-2)}$ (33 – 36 ppm), and C_{n-1} (~25 ppm). The methyl carbon of the fatty acid chain, C_n, has a chemical shift around ~14 ppm in the aliphatic region of the spectrum. The fatty acid ratio affects the sharpness of the C_n peak, with pure samples having sharper peaks and mixed fatty acid samples having broader peaks in the aliphatic region. Pure fatty acid samples are expected to have sharper peaks than mixed fatty acid

samples, due to the overlap of peaks from different fatty acids (i.e. the C_2 peaks of stearic and palmitic). The synthesized samples in Figure 3-4 are relatively pure mixtures, and the sharper peaks in the aliphatic region reflect this.

Figure 3-5 shows the TGA weight loss and ^1H T_1 relaxation times for several monohydrate, dihydrate and disordered samples prepared in the lab. The low water content of the disordered samples reflects the fact that they were prepared by drying, as well as the extent of drying. The disordered samples also have the lowest ^1H T_1 relaxation times reflecting the lack of order in the sample particles. The monohydrate and dihydrate samples have TGA around 3% and 5.5% water loss, respectively. The corresponding ^1H T_1 relaxation times for the monohydrate cluster around 3s, while the dihydrate ^1H T_1 relaxation times range from $5 - 17$ s. It is interesting that the points for each form cluster together, suggesting distinctly different structural properties for each form. Figure 3-6 shows that the scatter in the dihydrate ^1H T_1 relaxation values appears to be impacted by the fatty acid composition (% stearate), with lower ^1H T_1 relaxation values correlating with lower stearate content. This suggests a higher amount of order in the dihydrate samples with higher stearate content and lower order in the mixed fatty acid samples. The lack of spread in ^1H T_1 relaxation values for the monohydrate suggests that the order in monohydrate crystal structure is less affected by fatty acid composition, likely due to higher mobility in the carbonyl region due to relaxation sinks. It appears that the higher amount of water in the MgSt crystal structure gives the molecules less mobility and leads to longer relaxation times. Additionally, the ^1H T_1 relaxation values in Figure 3-5 are notably higher than those observed for the commercial samples, indicating that the particles in the samples have less order, possibly from smaller particles or other processing that may have affected the order in the commercial samples.
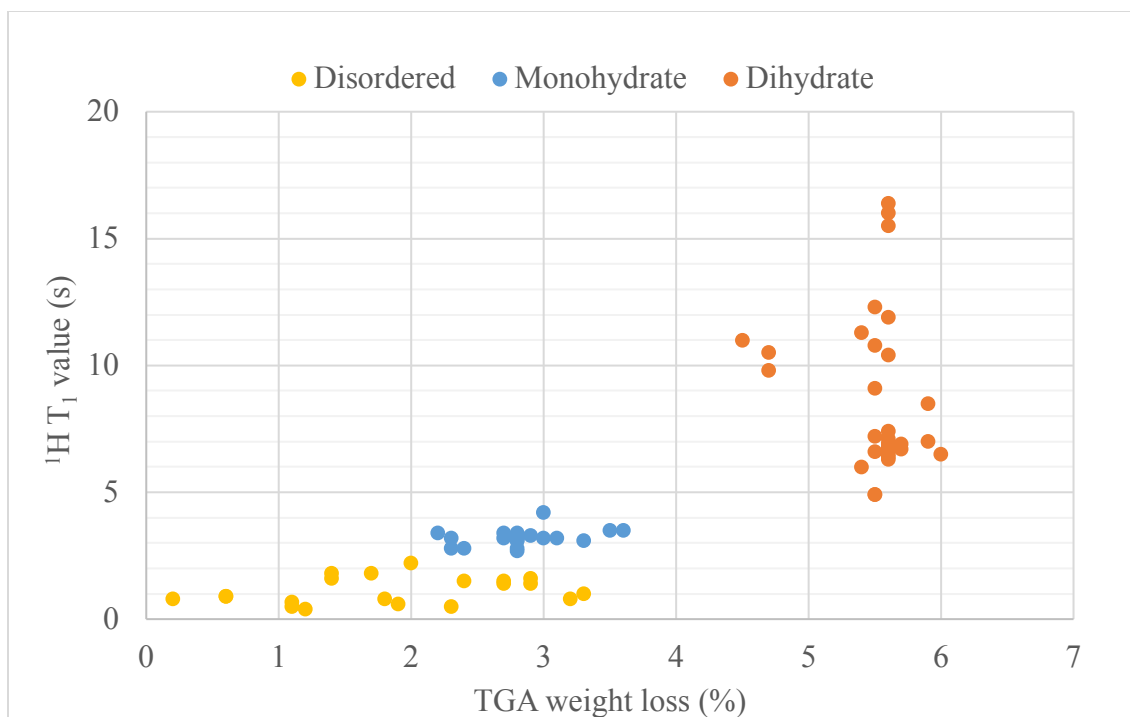
Figure 3-5. TGA weight loss and ^1H T_1 values for lab-synthesized MgSt samples, comparing pure monohydrate, pure dihydrate and disordered forms.
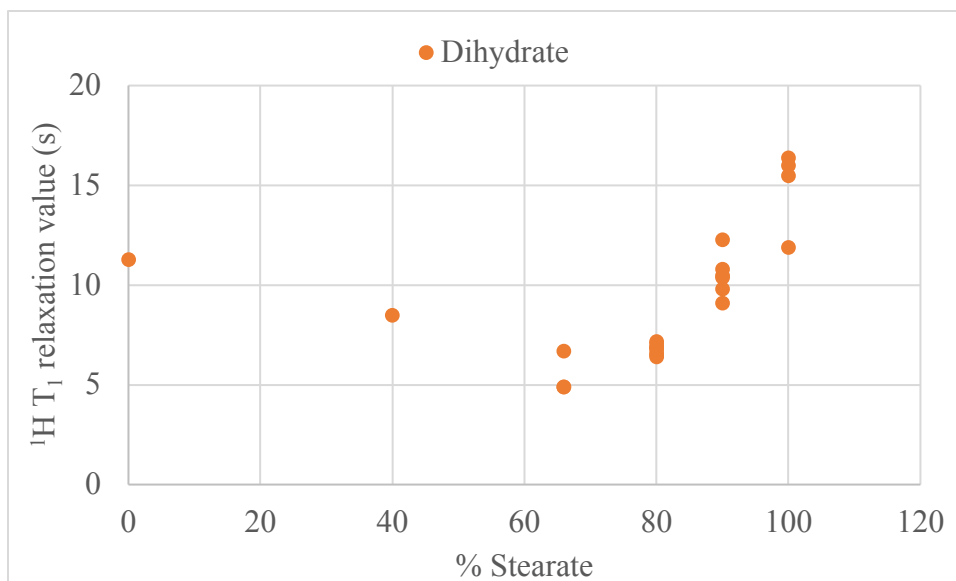
Figure 3-6. ^1H T_1 relaxation values for MgSt dihydrate samples prepared with varying compositions of stearic acid.

The ^{13}C SSNMR of a representative dihydrate sample from each stearate:
palmitate composition is shown in Figure 3-7 with the ^{1}H T_1 relaxation values listed in
Table 3-1. The carbonyl region (160 – 190 ppm) indicated the double peaks characteristic
of the dihydrate form of MgSt, with no obvious differences in crystal form between fatty
acid compositions. However, the aliphatic region (0 – 50 ppm) showed a trend with fatty
acid composition, particularly with the methyl peak ~ 14 ppm. The 100:0 St:Pa spectrum
showed a single, sharp methyl peak. Notably, the C16 peak of the pure palmitate (0:100
St:Pa) sample also has a single, sharp peak. For the mixed fatty acid concentrations, a
broader, double peak was observed, indicating a mixture of stearate and palmitate, with
the C18 and C16 methyl carbons having slightly different chemical shifts. The
implication of this is that fatty acid composition differences can be detected in the
aliphatic region of the ^{13}C SSNMR spectrum, and the extent of fatty acid mixture is
reflected in the lower relaxation times.

Table 3-1. ^{1}H T_1 relaxation values for lab-synthesized dihydrate samples

St:Pa	^{1}H T_1 (s)	Std dev
0:100	11.3	n/a
40:60	8.5	n/a
66:34	5.8	1.3
80:20	6.8	0.3
90:10	10.5	1.1
100:0	15.0	2.1
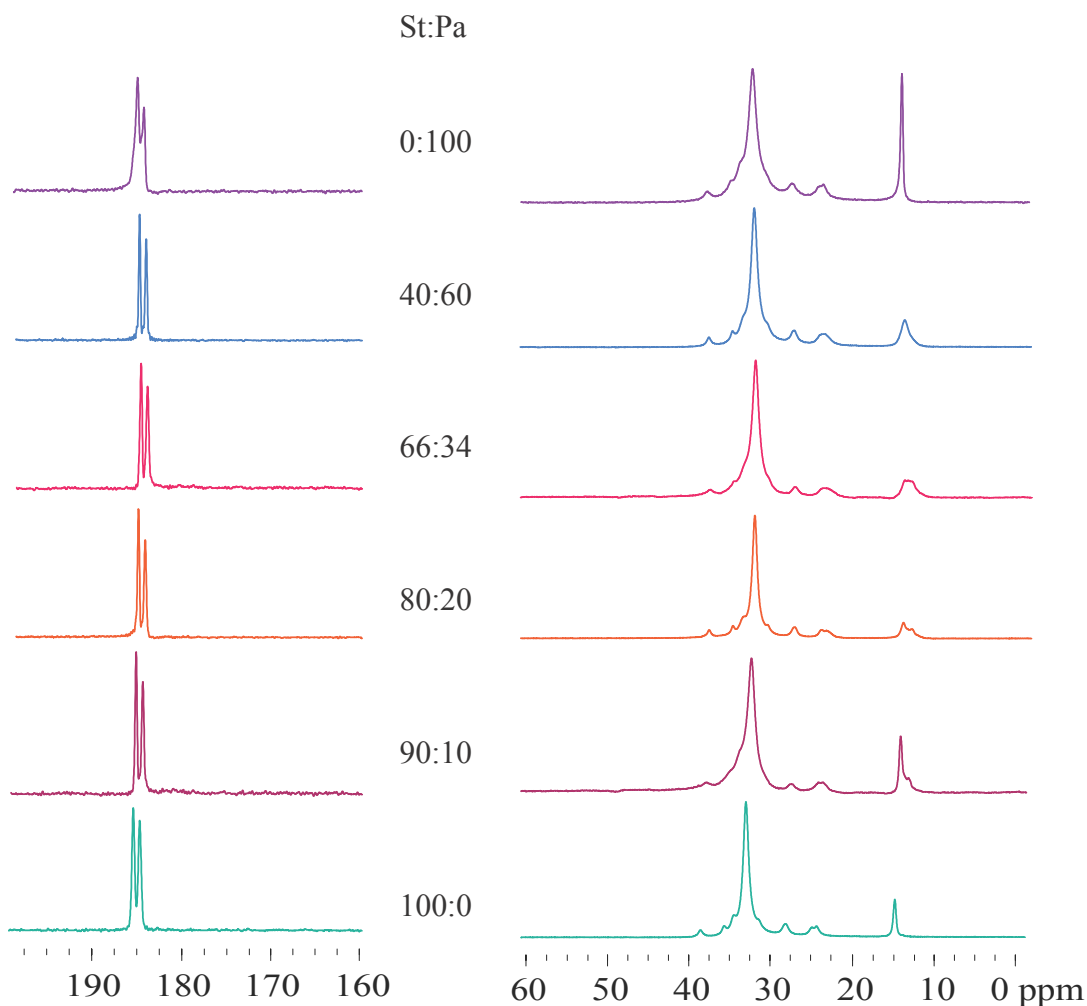
Figure 3-7. ^{13}C SSNMR for lab-synthesized dihydrate samples with various St:Pa compositions

This section has shown the different forms of MgSt may be identified by ^{13}C SSNMR, DSC, TGA, and XRPD. Additionally, it is shown that ^{13}C SSNMR is the only technique which can easily identify the unique forms of MgSt for samples when mixtures of fatty acids and form are present in the sample. ^{13}C SSNMR also makes it possible to quantify mixtures of forms in MgSt, based upon the carbonyl region of the spectrum. Additionally, ^{1}H T_1 relaxation times appear to generally correlate with TGA weight loss for the different forms, with a possible influence of fatty acid composition on ^{1}H T_1 relaxation times.

3.5.2 Commercial MgSt Samples

Eight samples of MgSt from several different suppliers were characterized for physical form, to determine the typical variety of forms present in commercial MgSt materials. The ^{13}C SSNMR spectra of these eight commercial MgSt is shown in Figure 3-8. The two Alfa Aesar samples have a disordered form, as indicated by the broad peak in the carbonyl region between 170 – 200 ppm. The spectra of the Fisher and Acros A0235781 samples show a distinctive pattern of 6 peaks shown 178 – 184 ppm region, which corresponds to the monohydrate form. The spectra from MP Biomedicals, Chem-Impex, Aldrich and Acros A0288107 samples show mixtures of monohydrate and dihydrate. The clear distinction between the monohydrate peaks and the two dihydrate peaks between 185 – 187 ppm allows for quantification of the forms in these samples, although quantitation analysis was not performed for these samples.

In addition to the differences in the carbonyl region, there are also differences in the aliphatic region of the spectra. The disordered Alfa samples appear to have a sharper peak at the methyl group ~ 14 ppm, indicating increased order in the aliphatic end of the molecules. If the fatty acid chains are ordered in the aliphatic region, it could explain the disorder observed in the carbonyl region. However, all of the other aliphatic peaks are also broad, suggesting that the structure of the disordered material is not straight-forward. In the C_2 region, differences between the monohydrate and dihydrate are observed, with several peaks for the monohydrate in the 38 – 41 ppm region, but only the samples showing dihydrate in the carbonyl region have a C2 peak at 36 ppm.
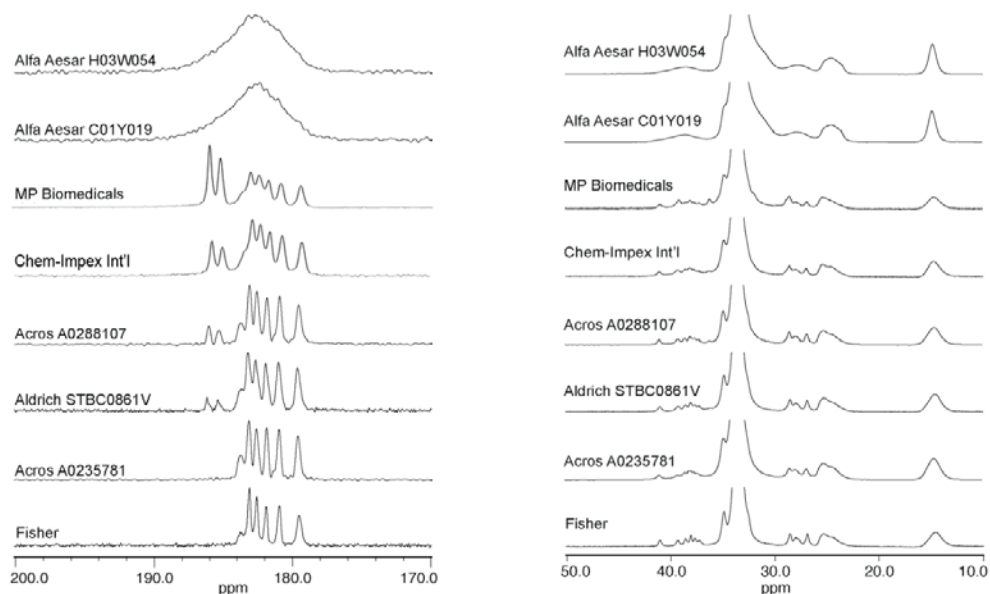
Figure 3-8. ^{13}C CPMAS NMR spectra of the eight samples of commercial magnesium stearate. The spectra show the carbonyl region (170–200 ppm) and the aliphatic region (10-50 ppm), as there are no other peaks in the spectrum. The samples are denoted in the figure by their source and, if two samples were obtained from the same source, lot number. Used with permission from Delaney et al.

The ^1H T_1 relaxation times for the carbonyl peaks in the commercial samples were also measured and shown in Figure 3-9. A higher ^1H T_1 relaxation time typically indicates higher order in the crystal. The low ^1H T_1 values for the disordered samples are consistent with this idea, having ^1H T_1 values of 0.8 ± 0.2 s and 0.9 ± 0.2 s. Comparing the relaxation times for the mixed samples, we see that the dihydrate peaks have different relaxation times than the monohydrate peaks, indicating that the forms are not intimately mixed in the sample. Because the ^1H T_1 relaxation times are different for the two sets of peaks, these two forms are not intimately mixed at the 50 nm level in these samples.(148) It is likely that the samples are mixtures of monohydrate and dihydrate particles rather than crystals with large domains of both forms.
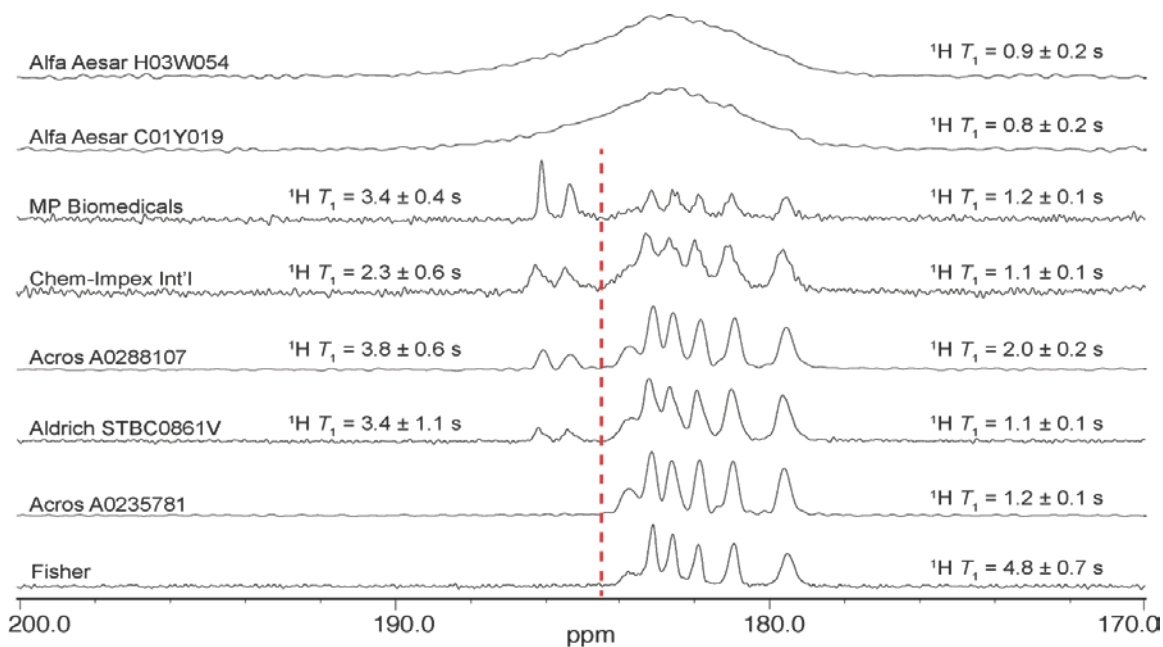
Figure 3-9. ^{13}C CPMAS NMR spectra of the carbonyl region (170–200 ppm) of the eight samples of commercial magnesium stearate. The ^{1}H T_1 relaxation times for the monohydrate and dihydrate peaks are shown in the figure. Figure used with permission from Delaney et al.

Figure 3-10 shows the DSC thermograms for the eight commercial samples. The forms observed in the thermograms for these samples are consistent with the DSC results in Figure 3-2. The Alfa Aesar samples assigned as disordered form from SSNMR show broad thermal events in the DSC and broad weight loss of ~ 3% in the TGA plots. The Acros and Fisher samples, which are both designated as monohydrates, have thermal events with onset around 105 °C, as well as weight loss events around the same temperature. The four samples with mixtures of monohydrate and dihydrate have overlapping peaks in the DSC thermograms consistent with the dehydration events described for the pure MgSt forms in Figure 3-2. These four monohydrate-dihydrate mixtures also show at least two weight loss dehydration events in each TGA plot, corresponding with the relative amounts of dihydrate and monohydrate present in each sample. From the DSC, the qualitative amount of dihydrate in the mixed form samples is MP Biomedicals > Chem-Impex > Acros ~ Aldrich, which is consistent with the SSNMR data. Although in general, it is possible to correlate the thermal data with the known forms of the MgSt samples, it is very challenging to identify the forms in the mixtures

49

from the complicated thermograms alone. Using the SSNMR and thermal data together, the differences between the forms of MgSt can be clearly identified and quantified.
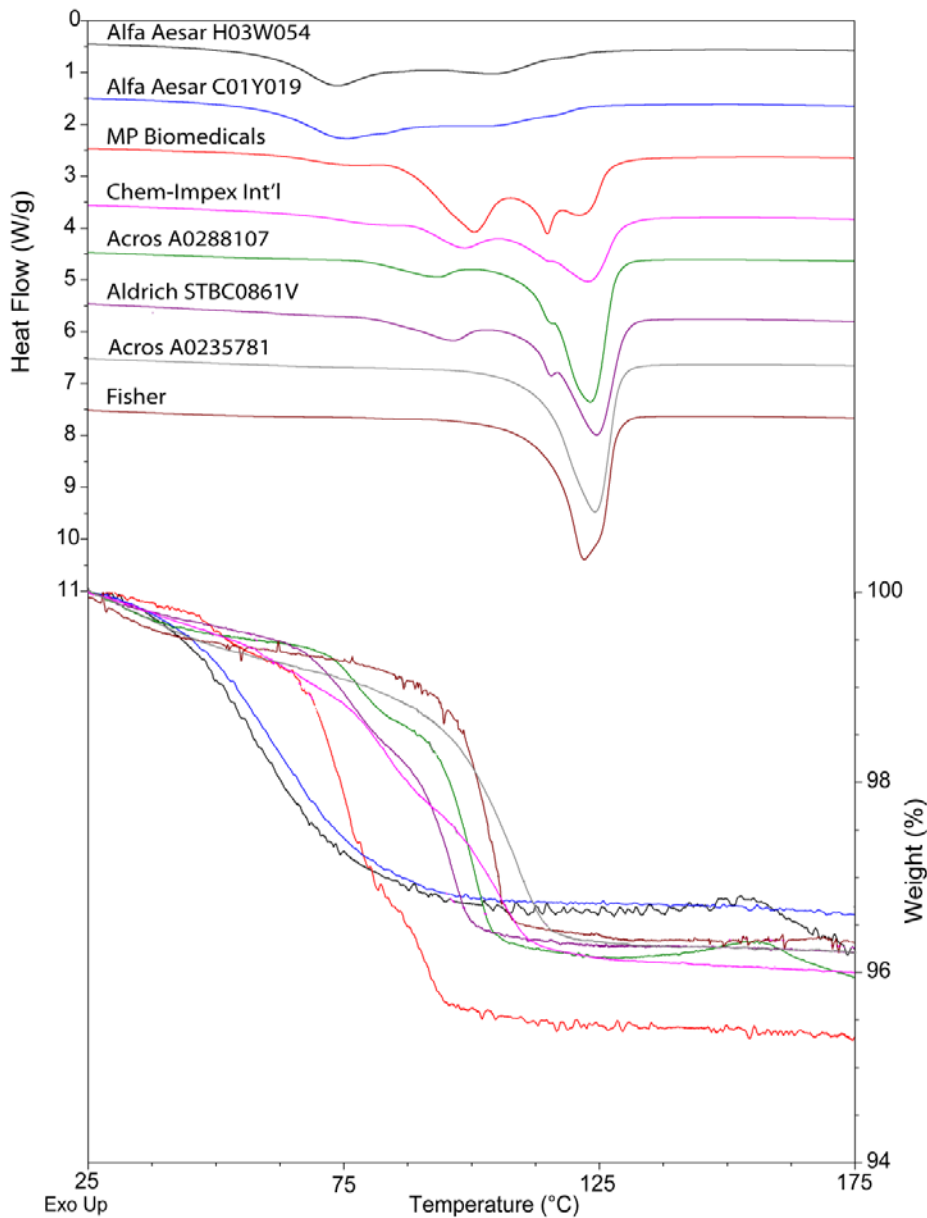
Figure 3-10. Differential Scanning Calorimetry (DSC) thermograms and Thermogravimetric Analysis (TGA) gravimetric weight loss plots for the eight samples of commercial magnesium stearate. DSC thermograms from top to bottom are listed by source and lot number, but are ordered as: Disordered, mixtures of dihydrate and monohydrate going to monohydrate. TGA plots from top to bottom are plotted in the same color as the DSC thermograms. Figure used with permission.

XRPD diffraction patterns for the eight commercial samples are shown in Figure 3-11. There are a few differences that can be observed between the samples, particularly between the disordered and monohydrate forms. The two Alfa Aesar samples show broad peaks indicating disorder, while rest of the samples have multiple sharp peaks. The Aldrich and Acros monohydrate samples show slight differences from the monohydrate/dihydrate mixtures, with the appearance of a peaks around 23° 2θ and 30° 2θ indicates the dihydrate form. The relative ratios of the peaks for the Acros A0235781 and Fisher monohydrate samples initially appear different, but this is likely due to preferred orientation in the sample preparation. Overall, the mixture of monohydrate and dihydrate forms is difficult to deconvolute using XRPD.
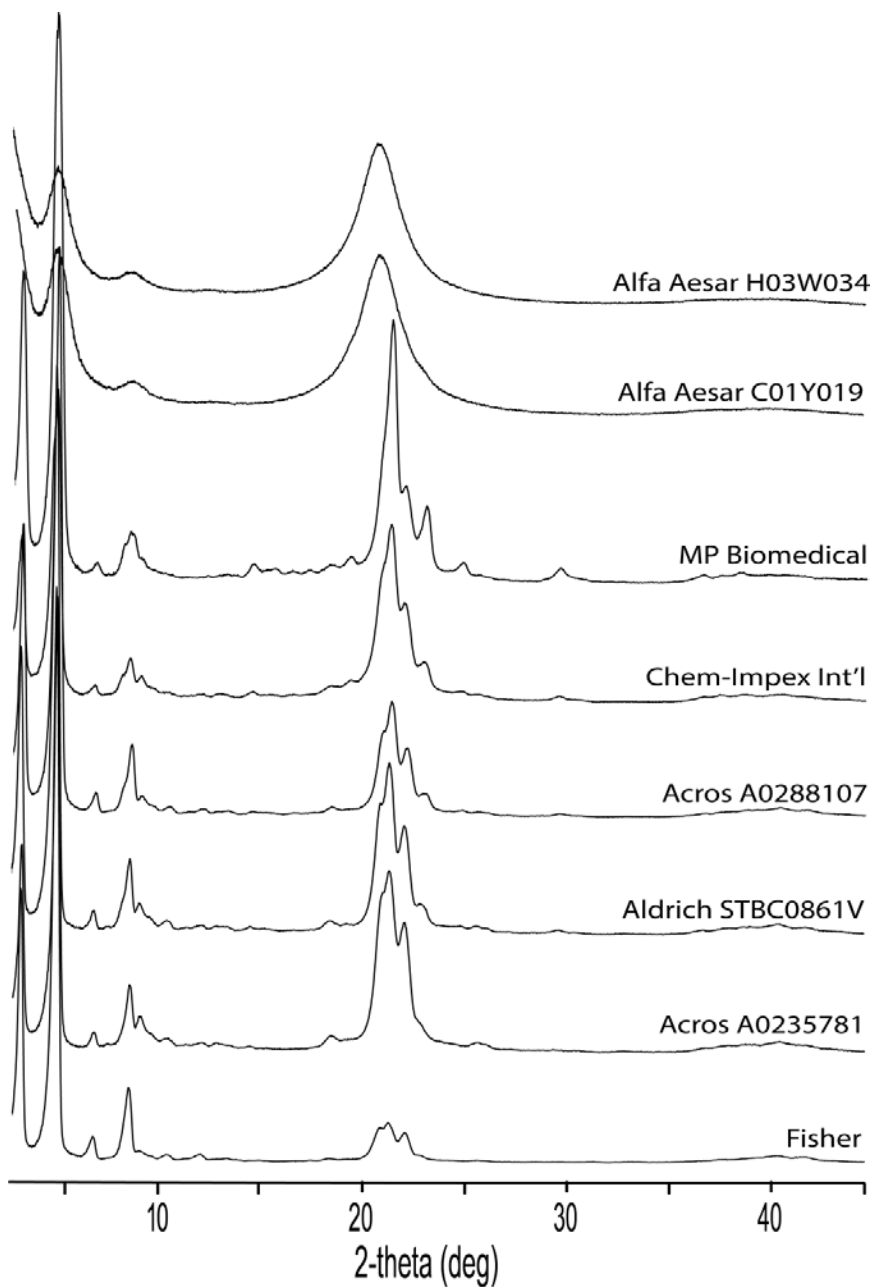
Figure 3-11. Powder X-ray diffraction patterns (PXRD) of the eight samples of commercial magnesium stearate. Patterns are labeled based upon their source and lot number. Figure used with permission.

This section has presented data characterizing the physical forms of eight commercial MgSt samples. DSC and TGA thermal data indicate differences between MgSt samples having different forms, but it is difficult to interpret mixtures of forms. XRPD also shows differences between samples having different forms, but mixtures of

forms and samples of mixed fatty acid compositions were difficult to interpret. In contrast, ^{13}C SSNMR was able to clearly distinguish between monohydrate, dihydrate and disordered forms in the commercial MgSt samples.

3.6   Conclusions

This chapter presented solid-state characterization for eight commercial MgSt samples and five lab-synthesized samples having five different pure forms of MgSt. Five different crystalline forms of MgSt were identified using ^{13}C SSNMR. The TGA water loss dehydration peaks were used to assign the proposed hydration states for monohydrate, dihydrate and trihydrate samples. DSC and XRPD data were consistent with SSNMR form trends and it was possible to identify the forms, especially for the pure forms. However, it is much more challenging to distinguish and/or quantify for mixtures of MgSt forms with traditional techniques, compared with ^{13}C SSNMR. The additional correlation of ^{1}H T_1 relaxation values with TGA weight loss and potentially fatty acid composition may provide insight into structural aspects of the various forms.

3.7   Acknowledgements

CHAPTER 4.   PREPARATION OF CRYSTAL HYDRATE FORMS OF
MAGNESIUM STEARATE BY VARYING SYNTHESIS CONDITIONS

4.1   Author Information

Julie L. Calahan, University of Kentucky, KY

Daniel F. DeNeve, Purdue University, IN

Sean P. Delaney, US Pharmacopeia, MD

Benjamin J. Munson, Eastern Kentucky University, KY

Christopher J. Mays, Ross University, Roseau, Dominica, West Indies

Manish Sethi, Tergus Pharma, NC

Nick Winquist, Humana, KY

Eric J. Munson, Purdue University, IN

4.2   Abstract

Magnesium stearate (MgSt) is a popular pharmaceutical lubricant, but batch-to-
batch variations in physical properties can cause variability in performance. In order to
understand the variability of MgSt properties, it is important to understand how MgSt is
prepared and the effects of various factors on the crystal form produced from the
synthesis reaction. Two synthesis reactions were investigated: the "melt method", a one-
step spontaneous reaction of magnesium hydroxide with melted stearic and palmitic acids
and the "bath method", a two-step reaction involving addition of magnesium chloride to
ammonium stearate soap. Samples of MgSt were prepared to investigate various reaction
conditions: 1) including the effect of fatty acid content on the crystal form produced for
both methods, 2) the amount of reaction water for the melt method, 3) reaction
temperature for the bath method and 4) drying method. It was found that the synthesis
method, fatty acid composition and reaction temperature all affect the crystal form
yielded from synthesis, where high stearate content at 70 ° with the bath method is most

likely to produce the dihydrate form and 50:50 ratio of fatty acids at 90 °C with the melt method is likely to produce the monohydrate form. Addition of 10 mL of water during the melt reaction appeared to aid formation of the monohydrate form. In terms of drying, the monohydrate sample was less affected by drying method than the dihydrate and mixed form samples. The air-drying condition was found to affect the synthesized form the least and the nitrogen drying tends to dehydrate the dihydrate form. Overall, synthesis conditions likely to produce pure monohydrate and pure dihydrate were determined.

4.3   Introduction

The variability of MgSt can be a result of several key factors that influence the physicochemical properties (fatty acid composition, crystal form/hydration state and particle size) of the material, all of which are related to preparation and processing: synthesis conditions, mixing, milling and form conversion and/or stability conditions. In order to understand the variability of MgSt, it is important to understand the effect of each of these factors. The synthesis is the first step in the material preparation process and will be the primary focus in this chapter.

A wide range of chemical composition is allowed for magnesium stearate samples. The USP monograph for MgSt allows for "variable proportions of magnesium stearate and magnesium palmitate"(19). To meet USP standards, the MgSt sample must be derived from at least 40% stearic acid and at least 90% of the sample must come from a combination of stearic and palmitic acids. The remaining 10% of the sample may be derived from other fatty acids, such as myristic, pentadecanoic, margaric, arachidic and behenic acids. This leads to a Mg metal content between 4-5%, depending on the chain lengths of the fatty acids and their ratios. The content of stearic and palmitic acids in a MgSt sample can be determined using a boron trifluoride-methanol extraction method to convert the stearate and palmitate to their methyl esters and separate and identify them using GC-MS. (19-22) Although commercial MgSt samples have a range of chemical compositions, and USP has set broad guidelines for chemical composition requirements, several researchers have suggested that within these guidelines the fatty acid composition

55

does not seem to affect lubrication. Interestingly, Rajala et al. found that two lots with similar chemical composition behaved very differently, possibly due to their hydration state differences.(23) The significance of fatty acid composition in relation to synthesis is being investigated and reported here.

The synthesis preparation of MgSt has been described in the literature using two basic reaction methods. Equation 1-1 is the most basic reaction for MgSt synthesis, and was noted in Kahner's 2017 review as one of two methods to make MgSt.(17) The second reaction, shown in Equation 1-2, is a two-step reaction published by Miller and York in 1985, Ertel et al. 1987 and Rajala et al. in 1995. (23-25)

$$2 \text{ H-St} + \text{Mg(OH)}_2 \rightarrow \text{Mg-St}_2 + 2 \text{ H}_2\text{O} \qquad \text{Equation 4-1}$$

$$2 \text{ H-St} + 2 \text{ NaOH} \rightarrow 2 \text{ Na-St} + \text{MgCl}_2 \rightarrow \text{Mg-St}_2 + 2 \text{ NaCl} + \text{H}_2\text{O} \quad \text{Equation 4-2}$$
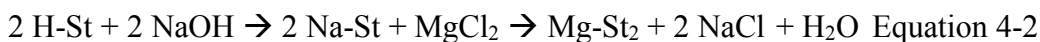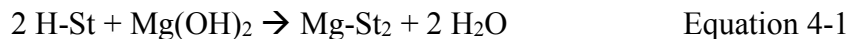
Aspects of the reaction shown in Equation 4-1 and Equation 4-2 have subsequently been patented by Mallinckrodt for manufacturing use with high ratios of stearate to prepare the dihydrate form of MgSt with a plate morphology. (26, 27) It is noted that other alternative salts, such as NH_4OH, may be substituted for NaOH in Equation 4-2. Additionally, Mallinckrodt has also presented the same synthesis reaction substituting $MgSO_4*7H_2O$ for the $MgCl_2$.(28) As Mallinckrodt recognized, the most important effect of chemical composition appears to be its effect on the hydrate form produced during synthesis.(29) Marwaha and Rubenstein suggested that the alignment of fatty acid chains in a crystal is governed by the chain length in the crystal packing structure, which would affect the shearing potential of MgSt.(98) This chapter addresses some of the trends observed in MgSt synthesis, for both reaction methods, using varying fatty acid ratios.

4.4   Materials and Methods

4.4.1   Materials

Stearic and palmitic acids were purchased from TCI. Magnesium hydroxide, ammonium hydroxide and magnesium chloride were purchased from Fluka (St. Louis, MO) , JT Baker (Radnor, PA) and EMD (Darmstadt, Germany), respectively.

4.4.2   MgSt Synthesis Procedures

Two preparation methods can be used to make MgSt. In this chapter they are referred to as the "melt method" and the "bath method". The melt method is a straight-forward, spontaneous reaction which entails melting the acids (stearic, palmitic, other) together above 70 °C, then adding $Mg(OH)_2$ and water to the melted acids. Solid magnesium stearate (the magnesium salt of stearic acid) has a lower solubility than the melted fatty acids and is formed from the reaction, according to Equation 4-1.

The bath method is a two-step reaction in which the acids are dissolved in a water bath heated to 70-90 °C. The pH of the system is adjusted to ~ pH 9 using ammonium hydroxide to create the ammonium soap of the fatty acids. Magnesium stearate is then precipitated out in a replacement reaction with magnesium chloride, as outlined in Equation 1-2. Alternative reactants may be substituted for the various salts, such as replacing NH_4OH to make the calcium soap using Ca_2OH. Or, NH_4OH versus NaOH to adjust pH and make soap, or $MgCl_2$ versus $MgSO_4$ for the replacement step. The specific reaction in this study utilizes NH_4OH in place of NaOH:

Stearic acid + NH_4OH → NH_4-Stearate

2 NH_4(Stearate) + $MgCl_2$ → Mg(Stearate)$_2$ + 2 NH_4Cl Equation 4-3

Following synthesis, the solid MgSt particles were subjected to a washing procedure involving a reflux with water and/or acetone, to remove any unreacted acids and impurities, such as excess MgO or Mg(OH)$_2$. The samples were then dried to remove excess water. Drying procedure was either air drying at ambient conditions for a week or vacuum dried at 25 °C for 24 hours.

4.4.3   SSNMR Method

^{13}C CP/MAS data were collected using a Tecmag Redstone NMR Spectrometer (Houston, TX), Bruker 400 MHz magnet (Billerica, MA), and a rebuilt H-X Chemagnetics (Ft. Collins, CO) NMR probe with 7.5 mm rotors spinning at 4000 Hz. A relaxation delay of 10 - 30s seconds was used with 2K acquisition points and 512, 1024 or 2048 scans. TNMR software (Houston, TX) was used to process the data. 3-methylglutamic acid was used as a reference standard, with the methyl peak referenced to 18.84 ppm.

4.4.4   Thermogravimetric Analysis (TGA)

TGA weight loss was measured using TA Q50 (TA Instruments, Newcastle, DE) with a 10 °C/min ramp from 25 °C to 250 °C.

4.4.5   Differential Scanning Calorimetry (DSC)

DSC thermal analysis was performed using Q2000 DSC (TA Instruments, Newcastle, DE). The heating rate was 10 °C/min ramp from 25 °C to 250 °C.

4.5 Results and Discussion

4.5.1 Effect of Chemical Composition on Crystal Form Produced from Synthesis

Several batches of MgSt were prepared with the melt method at various St:Pa ratios, as shown in Figure 4-1. SSNMR of lab-synthesized MgSt prepared using the melt method. It appears that there is a trend in preferred form that correlates with fatty acid ratio. Specifically, 50:50 St:Pa ratio shows a clean monohydrate form, with dihydrate character increasing with increasing stearate content. This was observed to be a general trend for the melt method in our MgSt synthesis experiments.
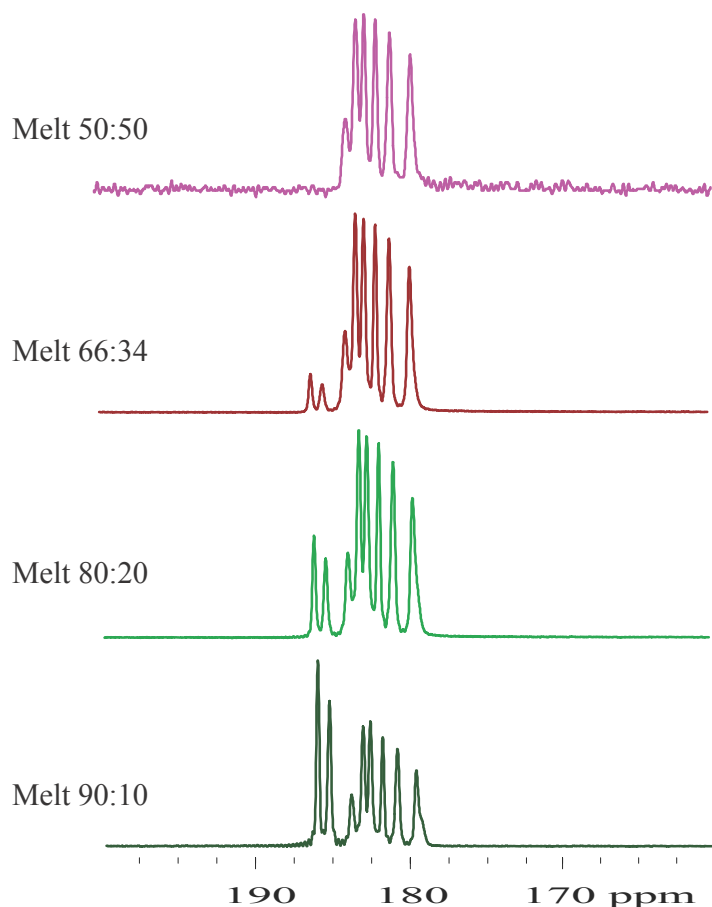
Figure 4-1. SSNMR of lab-synthesized MgSt prepared using the melt method

Several batches of MgSt were prepared with the bath method at various St:Pa ratios, as shown in Figure 4-2. For the bath method, it appears that there is a trend in

preferred form that correlates with fatty acid ratio, which is different from that of the melt method. For the bath method, the 50:50 St:Pa ratio shows mostly the trihydrate form, with the dihydrate form dominating with increasing stearate content, with 90:10 showing pure dihydrate form. Additionally, significant amounts of a new form of monohydrate is observed in the 70:30 and 80:20 samples. These general trends for the bath method were observed repeatedly in our MgSt synthesis experiments, particularly with higher stearate ratios, such as the 90:10 ratio, yielding the dihydrate form from the bath method.
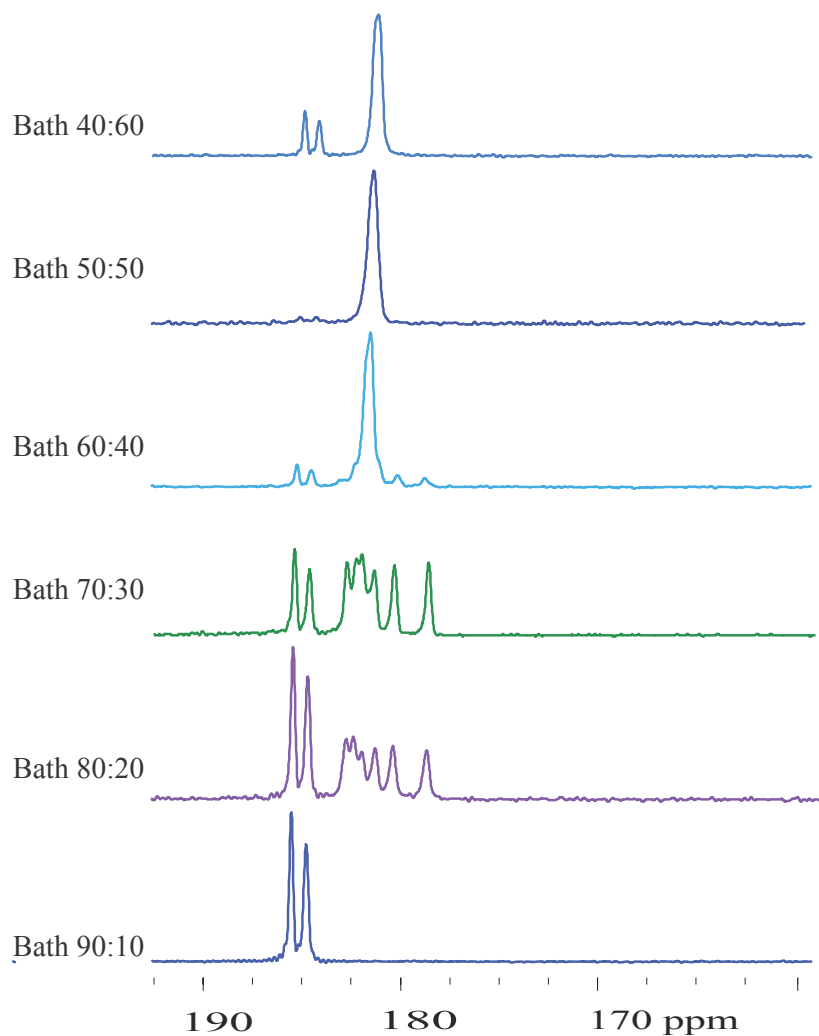
Figure 4-2. ^{13}C SSNMR of Lab-synthesized MgSt prepared using the bath method

In order to investigate differences between the synthesis methods, pure magnesium stearate and pure magnesium palmitate, as well as 50:50 stearate: palmitate

mixtures were prepared using both the melt and the bath method. The SSNMR for these samples are shown in Figure 4-3. Overall, it appears that the melt method easily yields the monohydrate form for 50:50 mixture, while the bath method yields dihydrate for the pure acids.
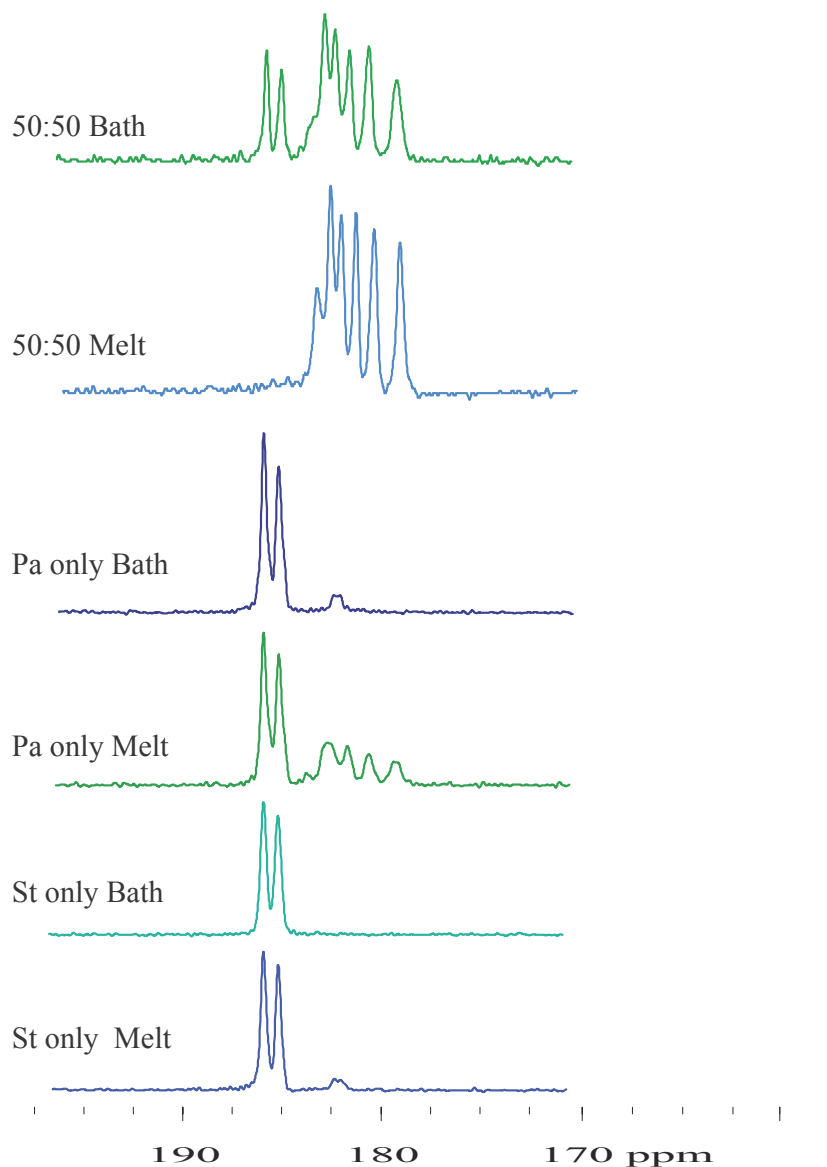
Figure 4-3. ^{13}C SSNMR for MgSt batches showing the carbonyl region, 160-200 ppm

It is also noted that the "Pa only Bath" and "St only Melt" samples have a small peak around 182 ppm. The trihydrate form of MgSt and the unreacted stearic and

palmitic acids have chemical shifts in this region, so thermal data is necessary to identify the small 182 ppm peak for these two samples. The DSC in Figure 4-4 shows the "Bath, Pa only" sample has a small peak with a melting onset ~ 65 °C, consistent with unreacted palmitic acid. Figure 4-5 also reveals a slight weight loss in the TGA for the "Bath, Pa only" sample, consistent with a small amount of trihydrate. For the "Melt, St only" sample, there is no visible melt in the DSC and no weight loss in the TGA. The melting point of stearic acid is ~ 70 °C, and a trace amount may be hidden under the larger dihydrate dehydration. The TGA is expected to show no weight loss for stearic acid, and the small peak at 182 ppm in the "Melt, St only" sample is more likely to be stearic acid than the trihydrate form.
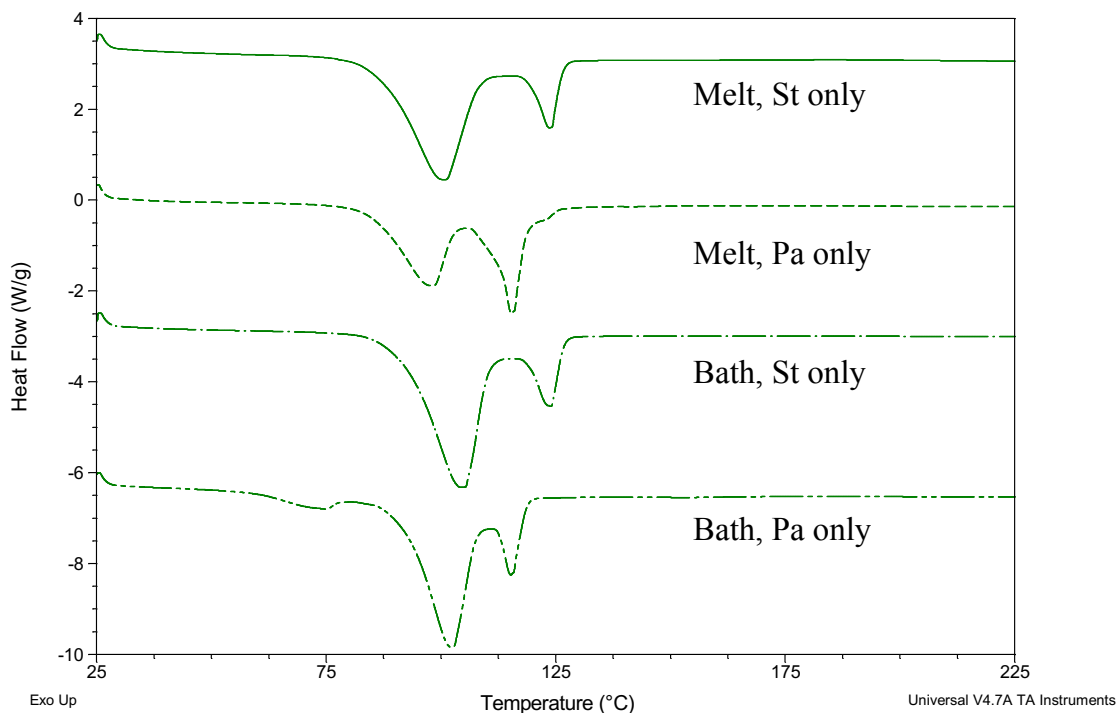
Figure 4-4. DSC of lab-synthesized MgSt samples, prepared with pure stearate and pure palmitate
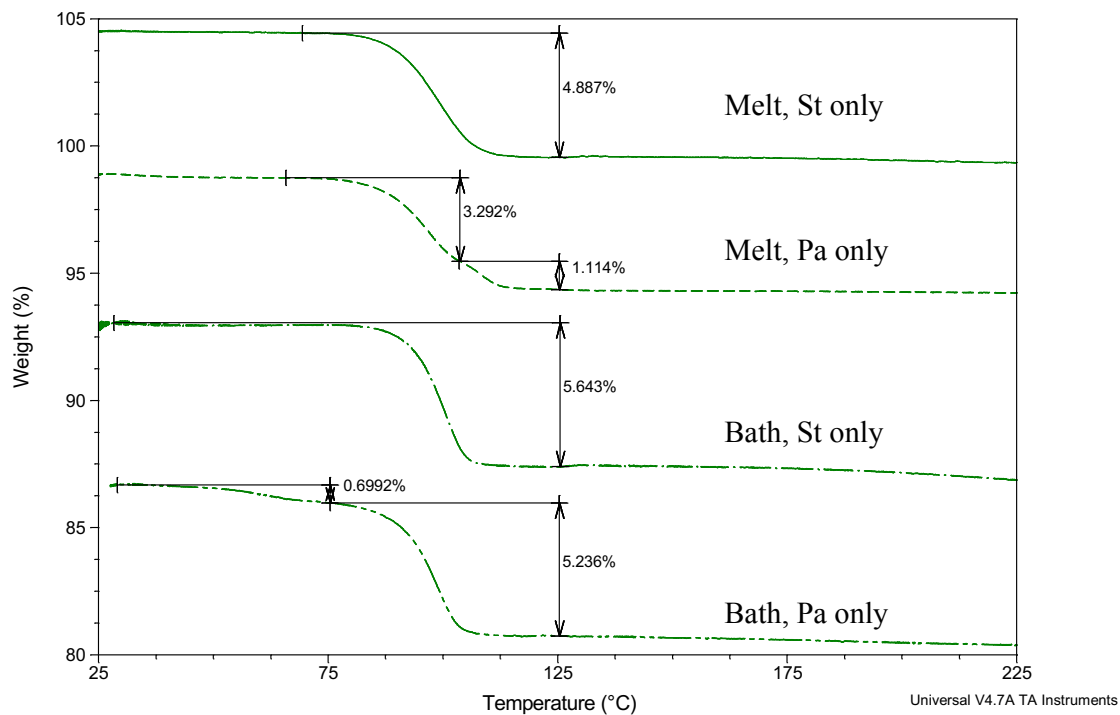
Figure 4-5. TGA of lab-synthesized MgSt samples, prepared with pure stearate and pure palmitate

The melt method tends to generate more monohydrate form, especially at stearate: palmitate ratios closer to 50:50, while the bath method generates more of the dihydrate form, especially for samples with a higher stearate content. The melt method crystallization is an immediate reaction of melted acids with magnesium hydroxide, where the bath method is a slower reaction from ammonium fatty acid salts with magnesium chloride. At first, the dihydrate appears to have delayed crystallization kinetics, suggesting that the monohydrate form may be metastable compared to the dihydrate form, but thermal data shows that monohydrate should be more stable at these temperatures.

From Figure 4-3, it appears that pure acids prefer to crystallize as the dihydrate form, whereas fatty acid mixtures are more likely to crystallize as the monohydrate form. In other words, the monohydrate form was preferred when fatty acid mixtures were present, and higher St:Pa ratios had a higher relative concentration of dihydrate. The higher stearate ratio had more unmixed fatty acid content and more of the dihydrate form,

whereas mixed composition samples had more of the monohydrate form. This basic understanding enables synthesis of pure dihydrate with high stearate content and synthesis of pure monohydrate with 50:50 mixtures of stearate: palmitate.

An important aspect of the synthesis method is to ensure that the crystal habit/ form of the acid starting material does not impact the form produced. The unit cell of MgSt crystal forms are not yet known, due to the shearing tendency of MgSt and the difficulty growing single crystals without twinning that are large enough to perform single crystal analysis. If the acids are not completely dissolved or melted prior to making the soap (or reacting with $MgOH_2$ for the melt), the solid form of the acids could act as seeds for the MgSt, impacting the crystal form of MgSt generated. However, this is not likely to affect the observed trends in fatty acid composition. The thermodynamic driving force for the reaction for stearic vs. palmitate is similar: 1) The pK_as for stearic acid and palmitic acid are both approximately 4.75. 2) The solubility of stearic acid is 0.6 μg/mL and palmitic acid is 0.04 μg/mL, giving stearic acid a slightly higher driving force, but both substances are virtually insoluble in water. Melting points are also similar, with 68.8 °C for stearic and 61.8 °C for palmitic acid, and both acids will be melted at the reaction temperature range of 70 – 90 °C, for both synthesis methods.

From Figure 4-3, we may speculate that the kinetics of crystal formation for the monohydrate and dihydrate are different, with the monohydrate crystals forming faster and the dihydrate crystals forming preferentially with longer time. This scenario would be reasonable if the dihydrate is the more stable form. However, thermal data is clear that the monohydrate has a dehydration temperature of 90 - 105 °C while the dihydrate dehydration temperature is lower, around 70 - 90 °C. Based on thermal stability, we would expect the dihydrate to form first as a metastable form, followed by the more stable monohydrate. It is possible that the molecules are oriented as pure strands (St-St) or mixed (St-Pa) and may crystallize out in that formation. This scenario fits with the observation that a higher stearate content yields a higher percentage of dihydrate form.

4.5.2 Effect of Reaction Water on MgSt Form for Melt Method

For an investigation of the impact of water on the form produced from the melt method, six samples were synthesized at 50:50 St:Pa ratio with the melt method. Conditions were varied between 0 mL water, 10 mL water and 50 mL water and compared at 70 °C and 90 °C reaction temperatures. The results are shows in Figure 4-6. Monohydrate was produced at both 0 mL water conditions, with trace amounts of dihydrate in both 10 mL samples, as well as the 50 mL 90 °C sample. The 50 mL – 70 °C had significant dihydrate and this increase in dihydrate with additional water added is not unexpected for the 70 °C, as the dihydrate form requires more water to be incorporated into the crystal lattice. The 50 mL – 70 °C condition had significant dihydrate character, 50 mL - 90 °C condition had only a small amount of dihydrate. Here it is reasonable that the 90 °C condition produces less dihydrate than the 70 °C condition because the monohydrate form is more stable at 90 °C. This is discussed in more detail in Chapter 5 in relation to form conversions.
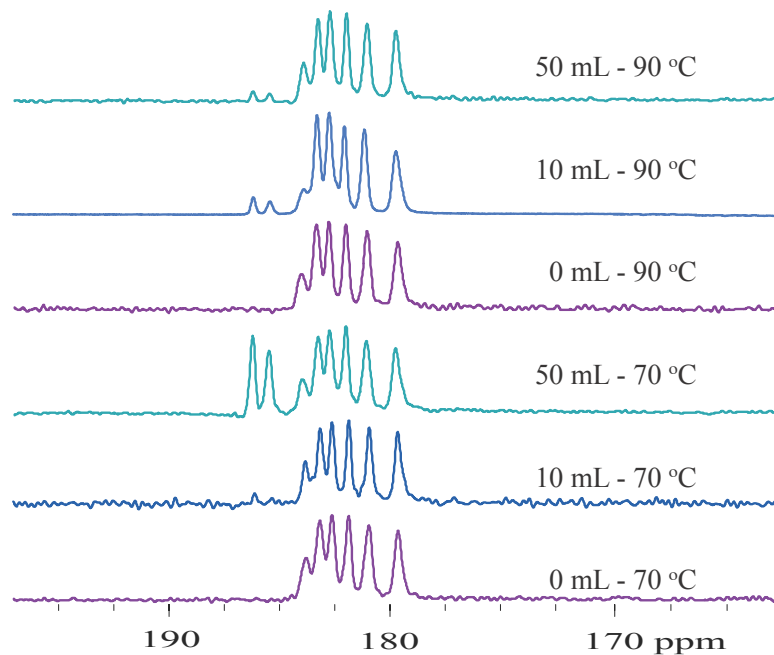
Figure 4-6. ^{13}C SSNMR of MgSt samples synthesized at 70 °C and 90 °C, using various amounts of water

4.5.3 Effect of Synthesis Reaction Temperature on MgSt Form

To evaluate the effect of reaction temperature on form, a single lot of material was synthesized to make MgSt at 90:10 ratio with the bath method. Half of the sample was reacted at 70 °C and isolated as dihydrate after filtration. The remaining half of the sample was boiled at 100 °C, then filtered and subsequently isolated as monohydrate, as shown in Figure 4-7. The only difference between the two samples was the reaction temperature.

The TGA clearly shows that the dihydrate form dehydrates around 70 °C and the monohydrate dehydrates around 100 °C. Between 70 – 90 °C, the dihydrate is expected to be the stable form based on its thermal properties. Above 100 °C, the monohydrate is expected to be the stable form, which is what we observe for this sample, with the preferential synthesized form of dihydrate between 70 – 90 °C and the monohydrate above 100 °C. This phenomenon suggests that the reaction temperature for MgSt synthesis is critical in controlling the physical form yielded from the synthesis.

70 °C Dihydrate   90 °C Monohydrate

200 190 180 170 160 ppm   200 190 180 170 160 ppm
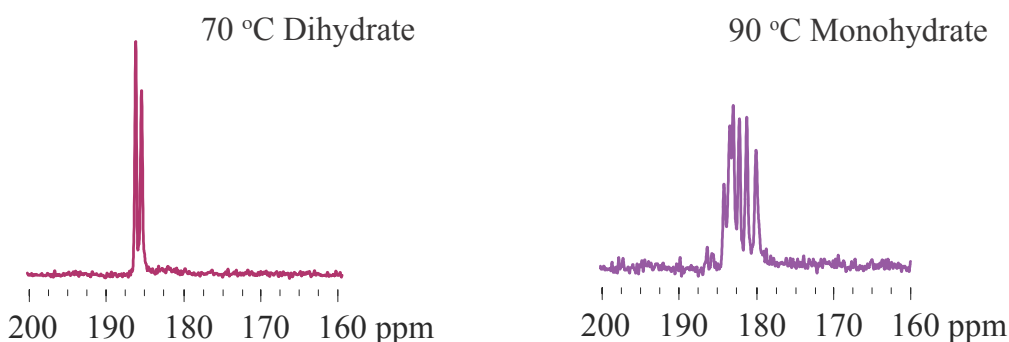
Figure 4-7. SSNMR of a batch of 90:10 St:Pa prepared using the bath method. The batch was split into two portions, the first portion with reaction temperature at 70 °C and the second portion boiled at ~100 °C.

Four samples were synthesized at 66:34 St:Pa ratio, shown in Figure 4-8. The reaction temperature was varied between 70 °C and 90 °C for melt and bath methods. At

70 °C, the melt method produced monohydrate with trace dihydrate and the bath method had a higher amount of dihydrate content. At 90 °C, the melt method produced monohydrate with trace dihydrate and the bath method produced dihydrate. Overall, these results are consistent with the previous trends where 1) mixtures of stearate and palmitate tend to produce monohydrate, but 2) the bath method produces higher amounts of dihydrate and 3) higher reaction temperature produces higher amounts of dihydrate. These three variables in the synthesis process appear to be simultaneously impacting the crystal form of MgSt produced.
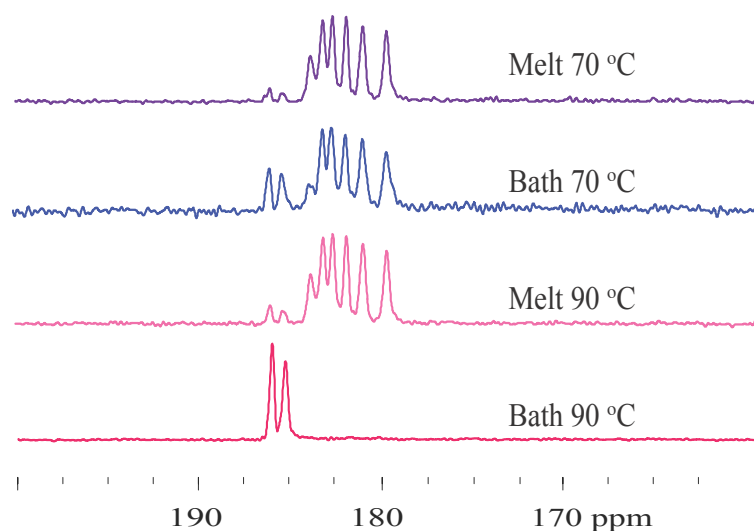
Figure 4-8. ^{13}C SSNMR of MgSt 66:34 St:Pa samples, synthesized with variations in temperature and synthesis method

4.5.4   Effect of Drying Conditions on Crystal Form

The last step of the synthesis involves drying the samples. To evaluate the conditions of the drying process, two samples were synthesized: 90:10 St:Pa using the bath method and 50:50 St:Pa ratio using the melt method, shown in Figure 4-9 and Figure 4-10, respectively. Each sample was split into aliquots for drying at various conditions: 1) air drying in a covered, open pan at ambient condition for 7 days, 2) vacuum drying in a covered, open pan in a vacuum oven for 24 hours, 3) nitrogen drying in a vial with

flowing dry nitrogen gas for 7 days, 4) desiccated drying in a vial placed in a desiccator for 7 days.
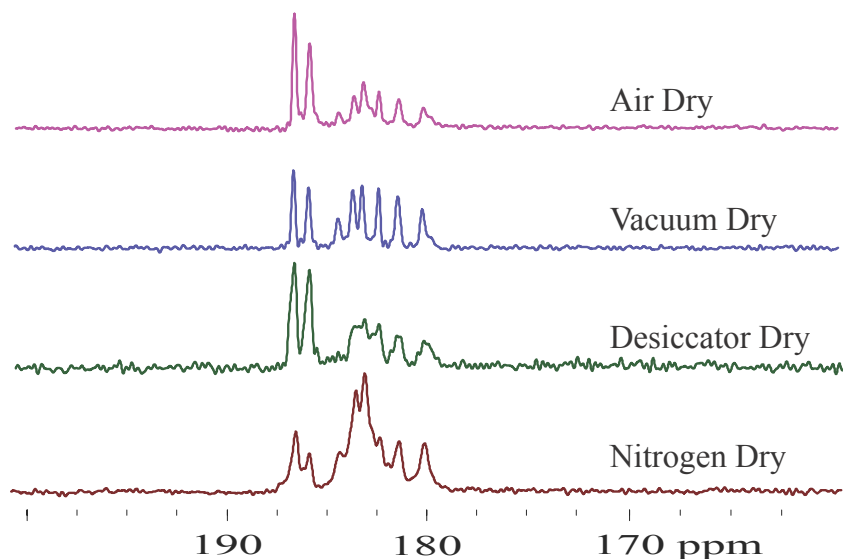
Figure 4-9. ^{13}C SSNMR for MgSt samples from Bath method 90:10 after drying via various methods

Figure 4-9 shows the drying for a 90:10 sample using the bath method. The air-dry method is the least harsh and is the best representation of the material produced from the synthesis. The vacuum drying condition appeared to show higher monohydrate content and reduced dihydrate, suggesting possible rearrangement from dihydrate to monohydrate. The desiccator condition showed some evidence of dehydration, with the monohydrate peaks becoming less defined. Under nitrogen flow, the dihydrate appeared to partially dehydrate into the disordered form, accompanied by rearrangement of the monohydrate peaks. This behavior is consistent with other N_2 drying data and this phenomenon is discussed at length in Chapter 6, as nitrogen drying may inhibit the normal lubricating effect of MgSt and result in fast dissolution and poor tablet lubrication properties.
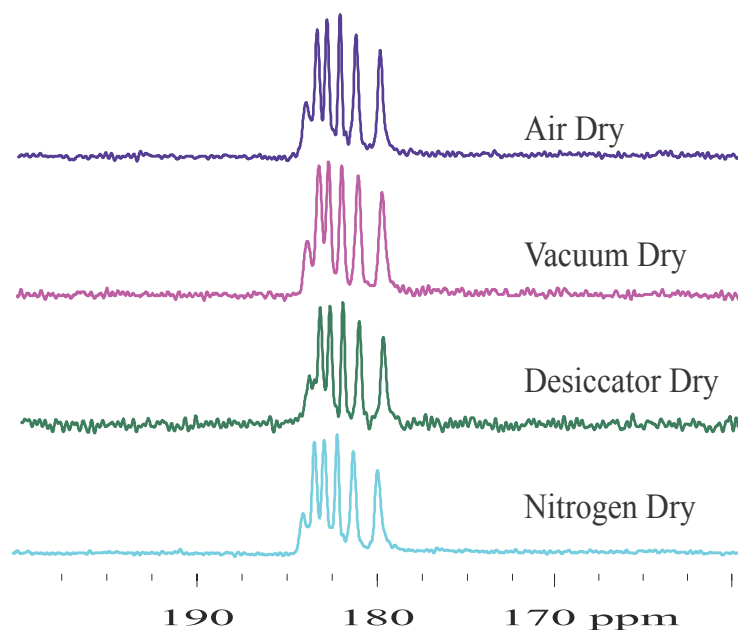
Figure 4-10. ^{13}C SSNMR for MgSt samples from Melt method 50:50 after drying via various methods

For the 50:50 melt material, SSNMR showed a similar form for all four melt method samples dried in different ways, which are all monohydrates. (Figure 4-10) The drying method did not appear to significantly affect the crystal form for the monohydrate samples. However, it appeared from the 90:10 bath sample that the dihydrate, and mixtures containing the dihydrate form, were more sensitive to the drying method and conditions that may promote dehydration of the MgSt physical forms.

4.5.5   Reproducibility of Lab-Synthesized MgSt Monohydrate and Dihydrate

The primary goal of the synthesis study was to create samples to be studied. Therefore, it was important to evaluate reproducibility with regard to consistency of crystal form produced from MgSt synthesis. Additional lab-synthesized samples were prepared using the melt method at fixed fatty acid compositions of 55:45 and 90:10 stearate: palmitate. Figure 4-11 and Figure 4-12 show monohydrate produced from 55:45 melt condition and dihydrate produced from the 90:10 bath condition, with only very minor differences between the samples.
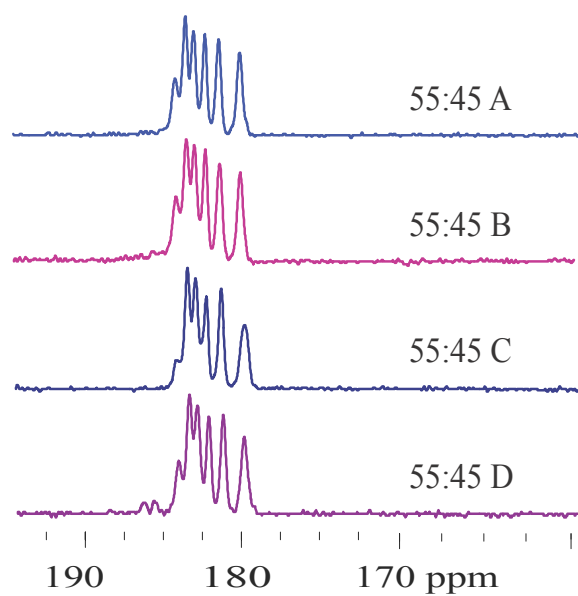
Figure 4-11. ^{13}C SSNMR of monohydrate MgSt synthesized from melt method at 55:45 St:Pa
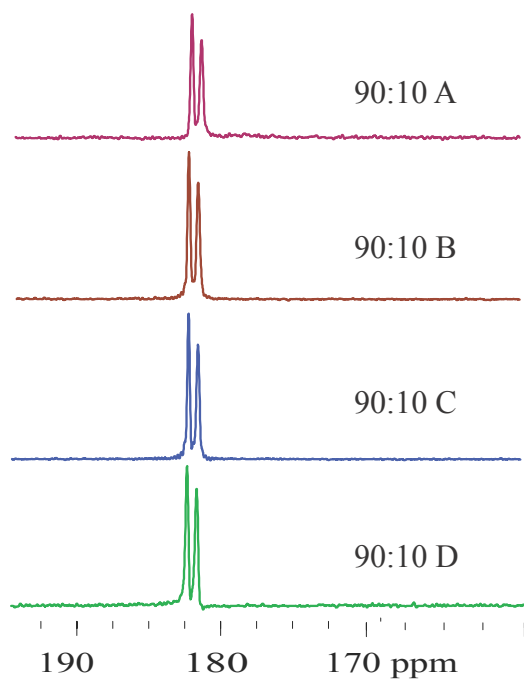
Figure 4-12. ^{13}C SSNMR of dihydrate MgSt synthesized from bath method at 90:10 St:Pa

However, additional samples were prepared at 55:45, shown in Figure 4-13 with some variations in crystal form produced. This illustrates the challenge of preparing consistent materials. Conditions believed to influence the form and morphology of the

material obtained from the synthesis process include reaction temperature, the amount of water present during the synthesis and impurities in the synthesis reagents. Stirring rate is also believed to impact the particle size of the MgSt formed. However, there was no clear explanation for the observed variation from the synthesis conditions for the samples in Figure 4-13. It was later discovered that some of the glassware contained residual solids from previous experiments, which may have contributed to inadvertent seeding with the dihydrate form.
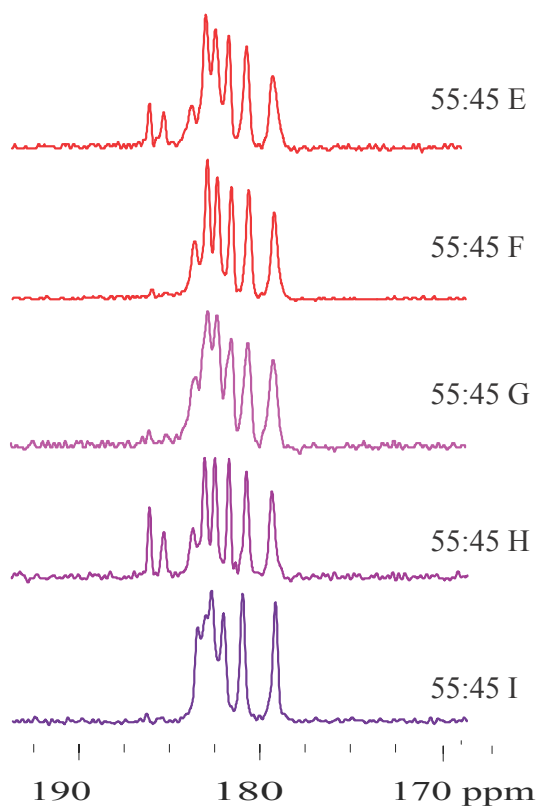
Figure 4-13. ^{13}C SSNMR of additional lab-synthesized prepared with the melt method at 55:45 St:Pa

4.6   Conclusions

There are several conclusions from this investigation of MgSt synthesis. First, the chemical composition (stearate: palmitate ratio) and the reaction method both affect the crystal form of magnesium stearate that is produced from synthesis reactions. Pure fatty

acid compositions (i.e. stearate only or palmitate only) showed a preference to produce the dihydrate form and fatty acid mixtures tended to yield more of the monohydrate form. The melt method, a spontaneous reaction of fatty acids with magnesium hydroxide, preferentially produced the monohydrate form, with increasing amounts of dihydrate yielded from higher stearate content samples. The bath method, a two-step reaction precipitating MgSt from soap and magnesium chloride, also yielded higher amounts of dihydrate form at higher stearate content samples. Combining the observed trends with fatty acid composition and method, it was found that the monohydrate form could be most easily produced from the melt method with a 50:50 St:Pa composition and the dihydrate form could most easily be produced from the bath method at 90:10 St:Pa composition.

Second, addition of a small amount of water during the melt method reaction appeared to aid formation of the monohydrate form. Additionally, the reaction temperature in the bath method was found to affect the crystal form produced. For a 90:10 St:Pa composition, dihydrate was yielded at 70 °C, but monohydrate was yielded when the temperature was increased to 100 °C.

Additionally, drying magnesium stearate may affect the physical form of the material, with more significant effects seen for the dihydrate and form mixtures. On a practical level, air drying for a few days was found to be the most gentle and effective drying method for lab-scale synthesis of MgSt. The dihydrate appears to be more sensitive to drying than the monohydrate form, but both forms can dehydrate in harsh drying conditions such as nitrogen drying or desiccation. Further investigation of the effect of drying on magnesium stearate are discussed in Chapter 6.

CHAPTER 5. PREDICTING THE HYDRATE FORM CONVERSIONS OF MGST IN BULK POWDER AND TABLET FORMULATIONS

5.1 Author Information

Julie L. Calahan, University of Kentucky, KY

Daniel DeNeve, Purdue University, IN

Sean P. Delaney, US Pharmacopeia, MD

Eric J. Munson, Purdue University, IN

5.2 Abstract

Magnesium stearate (MgSt) is a popular pharmaceutical lubricant, but batch-to-batch variations in physical properties can cause variability in performance. It is proposed that the variability in the dissolution and lubrication properties of MgSt can be related back to its complicated structural properties, specifically the crystal hydrate forms of MgSt. The crystal hydrate forms are believed to interconvert, which may affect performance of MgSt in formulations. Thermal analysis was used to choose temperature conditions to investigate the interconversions between the crystal forms. Dehydration temperatures for the trihydrate ranges from 60 - 80 °C, from 80 – 100 °C for the dihydrate and the monohydrate dehydrates around 105 °C. ^{13}C SSNMR was used to identify the crystal forms at different temperature and humidity conditions. The dihydrate was found to dehydrate to the anhydrate form with a disordered intermediate form with heating to 105 °C. The disordered form was rehydrated to the monohydrate form at 105 °C, 100 %RH and to the trihydrate form at 25 °C, 100 %RH. Direct conversions at 80 °C, 100 %RH reflected increasing thermal stability from trihydrate < dihydrate < monohydrate. An updated schematic for MgSt form conversions was proposed, encompassing form conversions from the intermediate disordered form as well as from direct form conversions. Finally, tablet formulations stored at typical stability conditions

showed an increase in the dihydrate form at 40 °C/ 75% RH and dehydration of the dihydrate to the disordered form at 40 °C/ 0% RH. Overall, it was shown that the crystal form of MgSt can change under varying temperature and humidity conditions, both in bulk and in tablet formulations.

5.3   Introduction

Magnesium stearate (MgSt) is the most commonly used excipient for pharmaceutical tablet formulations, and is used in over half of the marketed formulations.(1) MgSt is typically added to tablet formulations as a lubricant at a 0.25 - 5% level to prevent powder from sticking to the tablet die and manufacturing equipment during the tableting process. Many formulation labs have experienced unexplained batch-to-batch and lot-to-lot variation with MgSt, where the lubrication capability and/or the dissolution rate varies unexpectedly.(16, 97) For example, one lot from a manufacturer may show picking and sticking after several thousand tablets are made as powder builds up on the equipment, but other lots do not show the same extent of picking and sticking. In addition, tablets manufactured from different lots of MgSt may have different dissolution properties. The reasons for the inconsistencies between lots and types of MgSt are still poorly understood, (8, 149-151) but it is proposed that the variability in the dissolution and lubrication properties of MgSt can be related back to its complicated physicochemical properties.(98, 126)

One of the physicochemical properties of MgSt that have been proposed to have a significant effect on its lubrication and dissolution is the crystalline hydrate form.(152) Magnesium stearate is currently known to exist in multiple pseudo-polymorphic forms, but it has taken a few decades to reach this understanding. In 1977, Mueller noticed that the amount of water in a MgSt sample was related to its lubrication properties and that thermal drying can change its polymorphic properties. They suggested that drying changes the crystal structure from an orthorhombic or monoclinic crystal structure to hexagonal structure.(31) A few years later, Miller and York began to investigate the physical characterization of MgSt powders by preparing and characterizing pure

74

magnesium stearate and magnesium palmitate samples. They identified that both pure samples were associated with two molecules of water, and suggested that synthesis conditions such as pH played a role in hydration state.(25) Ertel and Carstensen also studied the physical properties of pure MgSt throughout the 1980s.(24, 32, 33) They determined that preparation conditions affect the hydration state and modifying the relative humidity (RH) and/or temperature can convert to a different hydration state. For example, heating at 105 °C led to water loss as well as crystal lattice collapse. In addition, they noted the importance of the long spacing of the crystal lattice structure, which was dependent on the hydration state. Wada specifically looked at MgSt pseudo-polymorphism and hydration using DSC,(34) but it was not until 1997 that Sharpe et al. identified the pseudo-polymorphs as anhydrate, dihydrate and trihydrate (without mention of a monohydrate form).(35) They proposed structures for the dihydrate and trihydrate phases based on the long crystal spacing from XRPD and deduced that the pseudo-polymorphism is a result of "changes in the angle of inclination of the hydrocarbon chains relative to the plane of the Mg atom head groups, brought about by the water content in the lattice."(35) Bracconi et al. perform a thorough XRPD investigation of two commercial lots without single crystals to fully elucidate the crystal structure,(36) and two years later, their DSC evaluation of the same two lots did not "fully clarify the relation between thermal and structural properties."(37) In 2001, Swaminathan and Kildsig published a schematic showing form conversions between the different hydrate forms,(39) which was later expanded to include the monohydrate form along with extensive evaluation of MgSt dihydrate properties from a commercial manufacturer's point of view.(28)

Although the single crystal structures of MgSt forms are still elusive, Delaney et al. showed that SSNMR can uniquely and reliably identify the crystalline forms of MgSt. Using SSNMR, five forms were identified as anhydrous, ordered monohydrate, dihydrate and trihydrate forms and an additional disordered monohydrate.(38) The ability to identify MgSt crystal forms using ^{13}C SSNMR by Delaney et al. not only clarifies the existing hydrate variability, but also provides a foundation for studying MgSt hydrate form conversions.(38) This research provides a study of the MgSt form conversions based on the dehydration and rehydration temperatures of the isolated MgSt hydrate

forms. Using ^{13}C SSNMR, we were able to easily identify form conversions in neat MgSt samples. Additionally, we were able to study MgSt form conversions in tablet formulations at low levels of MgSt, using ^{13}C labeled stearic acid to synthesize MgSt. In this chapter, we investigated in greater detail the form conversions of MgSt upon exposure to different relative humidity conditions, temperature and processing conditions.

5.4   Materials and Methods

5.4.1   Materials

Stearic acid and palmitic acid were purchased from TCI (Tokyo, Japan). Labeled stearic and palmitic acids were purchased from Aldrich. Magnesium hydroxide was purchased from Fluka (St. Louis, MO). Magnesium chloride hexahydrate was purchased from EMD (Darmstadt, Germany). Tablet excipients Avicel (microcrystalline cellulose, MCC) and alpha-Lactose monohydrate were obtained as a complimentary sample from FMC Biopolymer (Philadelphia, MA) and purchased from Sigma (St. Louis, MO), respectively. The commercial samples used in this study were obtained from Peter Greven.

5.4.2   Thermogravimetric Analysis (TGA)

TGA weight loss was measured using TA Q50 (TA Instruments, Newcastle, DE) with a 10 °C/minute ramp from 25 °C to 250 °C. TGA

5.4.3   Differential Scanning Calorimetry (DSC)

DSC thermal analysis was performed using Q2000 DSC (TA Instruments, Newcastle, DE). The heating rate was 10 °C/min ramp from 25 °C to 250 °C.

5.4.4   Solid-state NMR Spectroscopy (SSNMR)

^{13}C CP/MAS/TOSS SSNMR data were collected using a home built Tecmag Redstone NMR Spectrometer (Houston, TX), Bruker 400 MHz magnet (Billerica, MA), and Chemagnetics (Ft. Collins, CO) NMR probe with 7.5 mm rotors spinning at 4000 Hz. A relaxation delay of 12 s was used with 2K acquisition points and 1024 scans. TNMR software (Houston, TX) was used to process the data. 3-methylglutamic acid was used as a reference standard, with the methyl peak referenced to 18.84 ppm.

5.4.5   Conditions for Form Conversions

Form conversions for MgSt samples were performed by placing ~ 500 mg powder samples in an aluminum pan and heating in an oven at defined temperatures. Humidity samples at 75 %RH condition were prepared using jars containing saturated salt solutions of sodium chloride. Drying was performed by placing powder in a vial and holding under nitrogen flow or in a desiccator.

5.4.6   MgSt Synthesis

Magnesium stearate lots were synthesized in various stearate: palmitate ratios of 50:50, 55:45, 66:34, 70:30, 80:20, 90:10 and 100:0. Two synthesis methods were used. For the "melt" method, stearic and palmitic acids were melted at 70 °C, then reacted with magnesium hydroxide and water. For the "bath" method, stearic and palmitic acids were dissolved in a 90 °C water bath, ammonium hydroxide was added to adjust the pH above pH 9, then magnesium chloride was added to precipitate magnesium stearate. The

recovered solids from both methods were washed using a reflux bath of 1:1 acetone: water for 24 hours to remove impurities and any unreacted starting materials. The MgSt samples were air-dried and/or dried in a vacuum oven at 25 °C to remove surface water.

5.4.7   Mixing and Tableting

Indomethacin tablet formulations were prepared by adding MgSt to a "Premix" mixture containing 16.7% indomethacin (Sigma, St. Louis, MO), 47.3% alpha-lactose monohydrate (Sigma, St. Louis, MO), 34% Avicel (FMC Biopolymer, Philadelphia, PA) in a ratio of 2:98 MgSt: Premix. The tablet powders were mixed as 1 g batches in 40 mL glass vials for 60 minutes using a Turbula T-2C mixer (WAB, Basel, Switzerland) on the highest setting. Six individual 150 mg tablets were made from each 1 g formulation batch and pressed using a single tablet press (Globe Pharma, North Brunswick, NJ) at 50 bar for 30 seconds. The tablet weights were recorded, and the dissolution results were adjusted for tablet mass. Ball mixing was performed by adding 1g of MgSt to a 40 mL glass vial with ten ¼-inch plastic balls and mixed for 60 minutes using the Turbula T-2C mixer.

5.5   Results and Discussion

5.5.1   Thermal Analysis for MgSt Form Conversions

Magnesium stearate is known to be a physically stable powder at ambient conditions. It was observed that each of the hydrate forms is stable for > 2 years at 25 °C in closed vials. However, the hydrate forms have been reported to interconvert under specific temperature and relative humidity conditions,(39) so investigation was undertaken to confirm and define the conditions for interconversion of the MgSt crystal forms. Thermogravimetric weight loss data for the five forms of MgSt is displayed in Figure 5-1, showing the dehydration temperatures, which can be used to select appropriate temperature conditions to promote interconversions between forms. The

dehydration temperatures for the different hydrate forms are different, with trihydrate dehydration between 60-80 °C, dihydrate between 80-100 °C and monohydrate dehydration between 100-120 °C. The disordered form has a broad weight loss temperature, ranging from 40-125 °C, indicating surface bound water or a possible channel hydrate. It appears that all the hydrate forms can be completely dehydrated when heated above 105 °C and can then be converted from the dehydrated state to the desired hydrate form at selected temperature and humidity conditions.
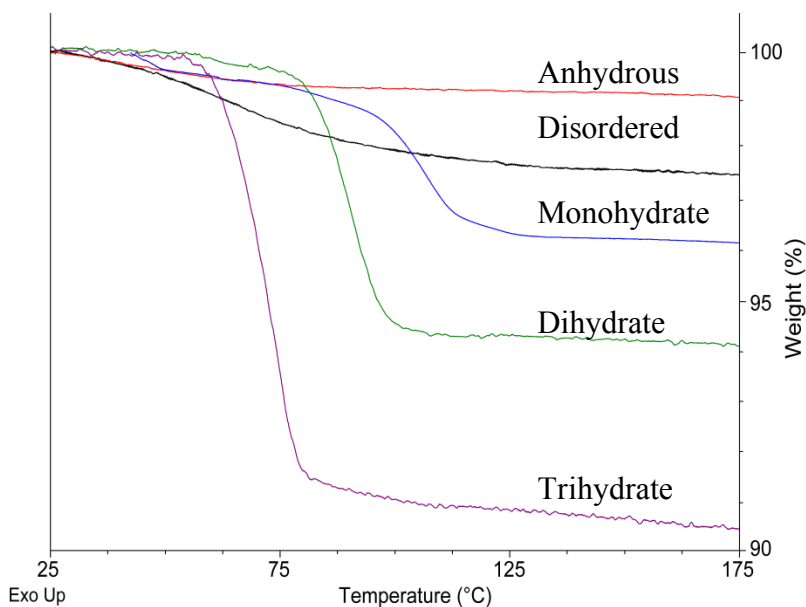
Figure 5-1. Thermal data showing the melting and dehydration temperature for different MgSt forms. Used with permission from Delaney et al.

5.5.2 Form Conversions in MgSt with 100% Stearate Content

Figure 5-2 shows the SSNMR for the form conversions of a MgSt sample, originally prepared as the dihydrate form, with 100% stearate content. When a portion of this material was heated at 105 °C in an oven without humidity control, it visually appeared melted. As this material was brought to room temperature, it solidified into an anhydrous form with apparent crystalline order, as determined by ^{13}C SSNMR. This intermediate anhydrous melt was then rehydrated at 105 °C, 100%RH and recovered as

the monohydrate form of MgSt. It was clear from this experiment that a single sample of MgSt can undergo changes in hydrate form using the temperature and RH conditions.
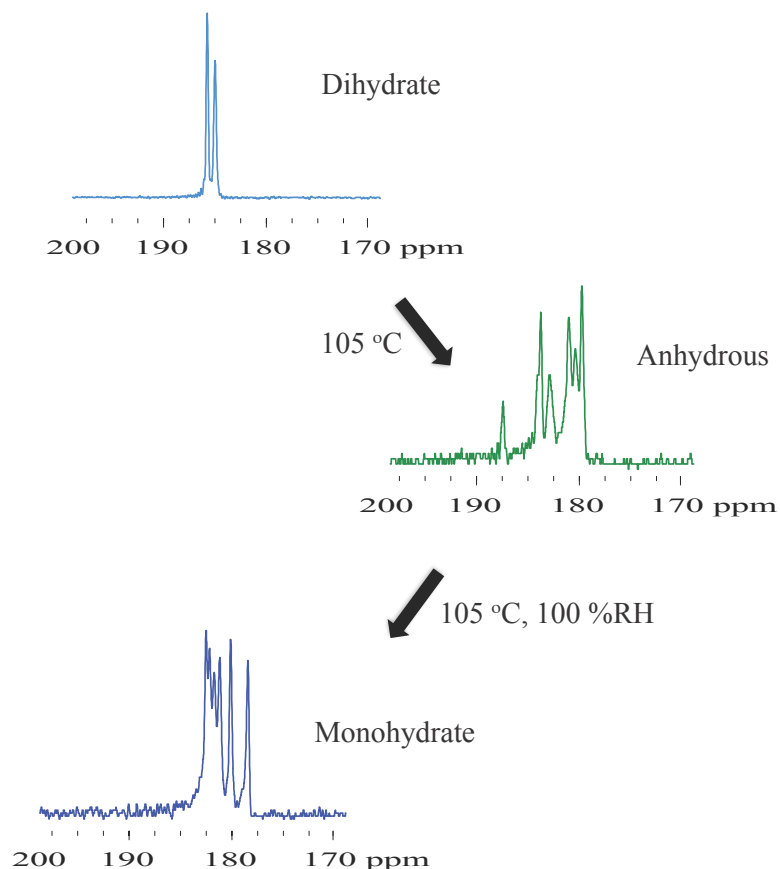
Figure 5-2. Form conversions for MgSt prepared from 100% stearic acid

5.5.3 Form Conversions of MgSt due to Dehydration at 105 °C

The first step in understanding the form conversions observed in Figure 5-2 is an examination of the dehydration process. Based on the thermogravimetric analysis in Figure 5-1, the different forms of MgSt will dehydrate at different temperatures, and all three hydrate forms will be dehydrated above 105 °C. Figure 5-3 shows a dihydrate sample after heating at 105 °C. After 3h heating, the material was changed to the disordered form. An additional 5h of heating, for a total of 8h, generated the anhydrous

form. The disordered form appears to be an intermediate form, with the anhydrous form as the stable form at 105 °C under dry conditions.
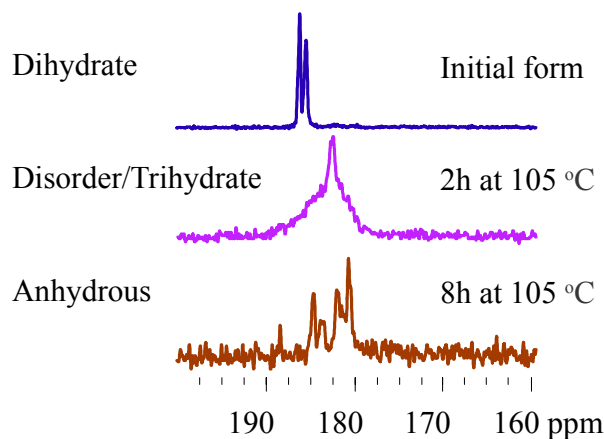
Figure 5-3. ^{13}C SSNMR of a MgSt dihydrate sample after drying at 105 °C

5.5.4 Form Conversions of MgSt due to Rehydration at 100% RH

Having established that dehydration by heating can generate the disordered form, the rehydration process was investigated. Rehydration temperature conditions were chosen with the aim of converting to specific forms of MgSt. Specifically, 105 °C, 100 %RH was chosen as a rehydration condition which was expected to convert to the monohydrate form, since it is close to the dehydration temperature of monohydrate. Similarly, 25 °C, 100 %RH was chosen as a rehydration condition expected to convert to the trihydrate form, being below the dehydration temperature of the trihydrate form.

Figure 5-4 shows the dehydration and rehydration conversions at 105 °C, 100% RH for several MgSt hydrate mixtures with a range of fatty acid ratios. These samples were dried at 105 °C to promote dehydration, followed by rehydration at 105 °C, 100% RH. As predicted from the thermal data, the monohydrate form was yielded at the 105 °C, 100% RH condition. Furthermore, it appeared that the starting form was irrelevant when converting to the monohydrate form via the dehydration-rehydration process. This made sense, since the trihydrate and dihydrate were expected to dehydrate into the

disordered form at 105 °C. The disordered material rehydrated into the form dictated by the rehydration temperature, which in this case was the monohydrate form.
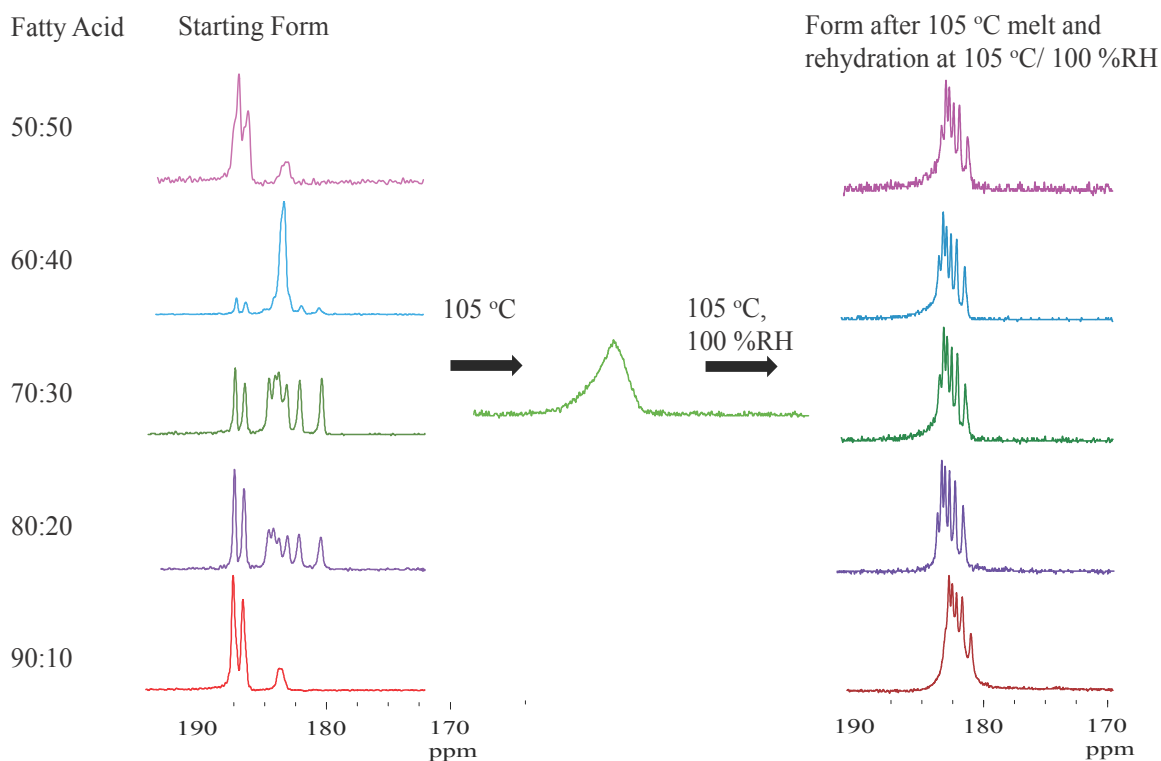
Figure 5-4. ^{13}C SSNMR of MgSt form conversions to monohydrate after heating at 105 °C and subsequent rehydration at 105 °C/100% RH

Figure 5-5 shows the dehydration and rehydration MgSt form conversions at the 25 °C, 100 %RH condition. The starting materials contained mixtures of dihydrate and monohydrate and were dehydrated to the disordered form at 105 °C prior to the rehydration step at 25 °C, 100 %RH. The starting materials all had a 66:34 fatty acid composition and were labeled with about 30% palmitic acid ^{13}C label on the C1 carbon. It was expected that the trihydrate would predominantly form from the disordered form at these conditions, since the temperature was below the dehydration temperature for the dihydrate and monohydrate. The results showed mixtures of the trihydrate form (indicated by the single sharp peak around 183 ppm) and/or the disordered form

(indicated by the broad peak). There appeared to be more of the disordered form when the starting material was predominantly monohydrate, and more of the trihydrate form with traces of the high melting anhydrate form when the starting material contained large amounts of dihydrate. This may be due to partial conversion to the anhydrate intermediate form during the drying step at 105 °C, if it was held at 105 °C for an extended period of time. The implication of this set of experiments is that the disordered form can be converted to the trihydrate form at moderate conditions of 25 °C/ 100 %RH, conditions which may be relevant to storage conditions for the bulk raw materials.
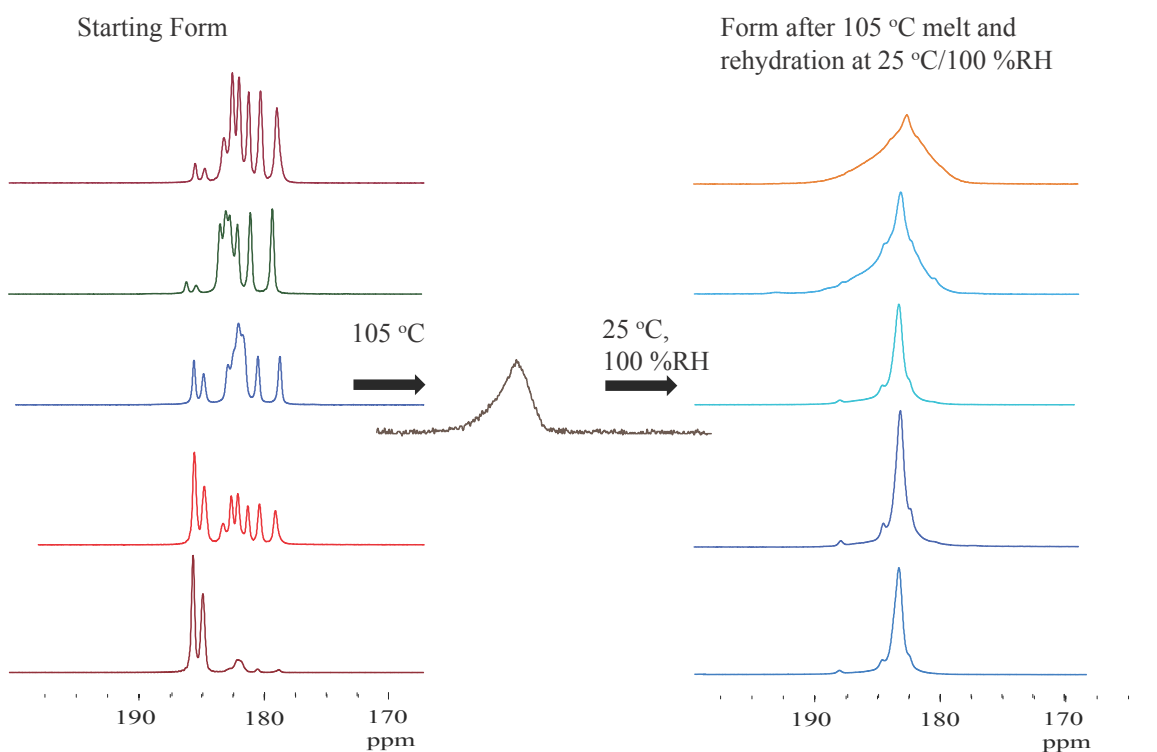
Figure 5-5. MgSt conversions to trihydrate and/or disordered form by melting at 105 °C, then rehydrating at 25 °C/100% RH

5.5.5   Direct Form Conversions at 80 °C/100%RH

Thus far we have seen that MgSt form conversions readily occur from the dehydration of the hydrate forms to the disordered form, followed by rehydration of the

disordered form at temperatures corresponding to the hydrate forms. This section addresses the "direct" form conversions, without an intermediate disordered step.

Dihydrate interconversions are expected to occur at conditions around 80 °C/ 100 %RH. This condition represents the dehydration temperature of the dihydrate form and is intermediate between the monohydrate and trihydrate hydration temperatures, which are 105 °C and 25-40 °C, respectively. Several MgSt mixtures of dihydrate-trihydrate were placed at 80 °C/ 100 %RH for one week (without the melt intermediate prior to rehydration). Figure 5-6 shows an increase in dihydrate content for these samples after storage at 80 °C/ 100 %RH, but complete conversion is not attained in these experiments after a week of storage. In addition to the increase in dihydrate, the trihydrate content appears to partially convert into monohydrate under these conditions. These results support the expected MgSt form conversions at this temperature and humidity. It is challenging to convert completely to the dihydrate form, with the hydration temperature transition existing between monohydrate and trihydrate hydration temperatures.
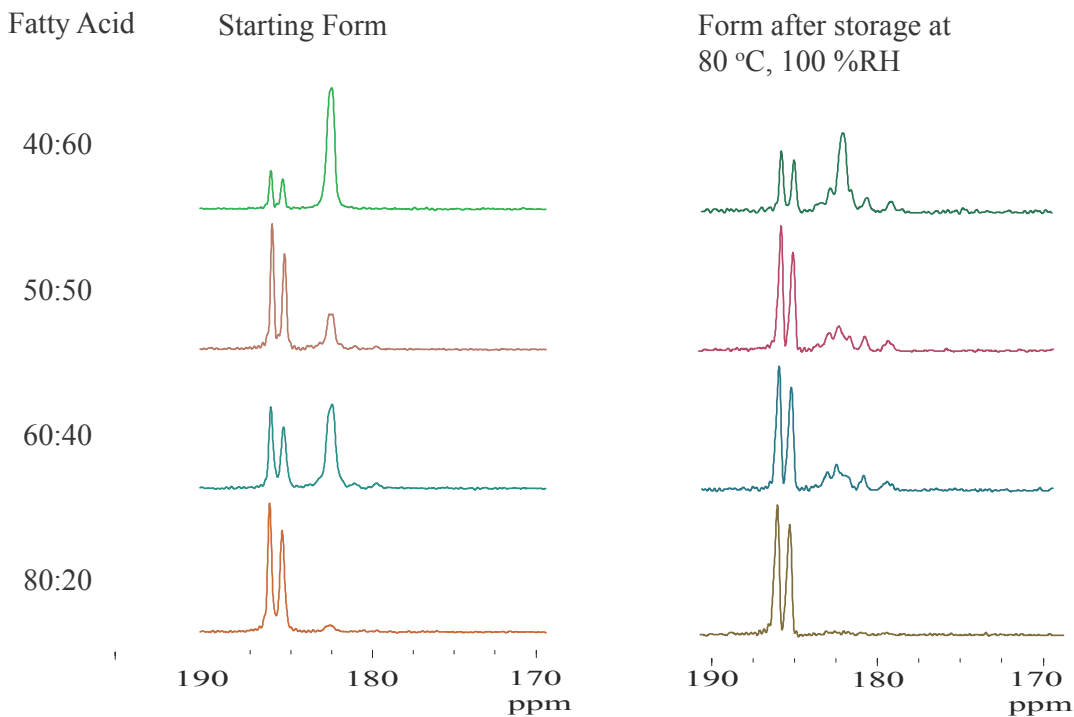
Figure 5-6. MgSt form conversions to dihydrate after storage at 80 °C/100% RH

5.5.6   Form Interconversion Schematic

As mentioned earlier, MgSt hydrate conversion schematics have been put forth by previous researchers.(39) Our study revealed a form conversions which can be organized into the schematic illustrated in Figure 5-7. The outer ring shows the conditions for direct conversions between hydrate forms, while the inner ring shows conditions for form conversions through the disordered or anhydrous intermediate step. This schematic shows the conversions in a systematic manner and is more elegant than previous MgSt form conversion schematics.

The intermediate form is a melt which forms upon dehydration at 105 °C and solidifies when removed from the oven and can be recovered as either the disordered form or the anhydrous form. The disordered form is generated with heating for ~ 2 hours. If the material is heated for longer periods of time, the equilibrium shifts further and the more crystalline anhydrate is formed. In the presence of water, both the disordered and anhydrous forms readily sorb water to form the trihydrate at 25 °C, the dihydrate around 80 °C or the monohydrate at 105 °C.

The dehydration temperatures of MgSt hydrates are unusual in that the higher order hydrates dehydrate at lower temperatures. In the presence of water, the trihydrate converts to dihydrate and/or trihydrate above the trihydrate dehydration temperature, and the dihydrate form converts to the monohydrate above the dihydrate dehydration temperature. Removing the water dehydrates all of the forms, and both the disordered form and the anhydrate will sorb water and form the hydrate that is most stable at the given temperature condition. Temperature is the primary driver for determining the crystal form, but the presence of water is required to form the hydrates. In the presence of water, the monohydrate is the most stable hydrate form of MgSt, with dehydration around 105 °C, followed by the dihydrate at 70 – 90 °C and trihydrate below 50 °C. These conditions are relevant for formulation development processes such as wet granulation and the impact of MgSt form conversions should be considered when using processing techniques which introduce water into the system at elevated temperatures.
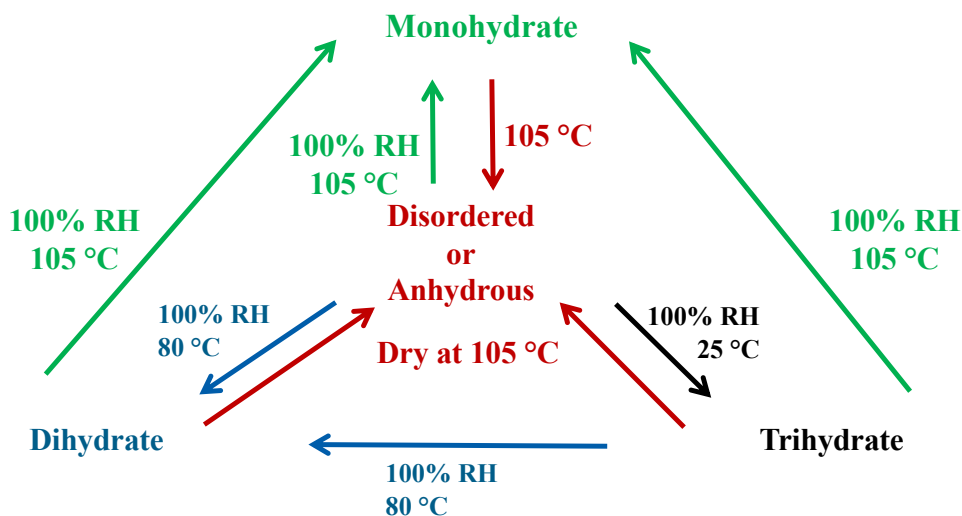
Figure 5-7. Proposed Schematic of MgSt Form Interconversions

5.5.7   Form Conversions at 75 %RH

The MgSt potential for form conversions in dry conditions and in 100 %RH conditions has been discussed in the previous sections. The interconversion of MgSt crystal forms may be a potential formulation stability concern. Therefore, storage conditions are also an important consideration in formulation development situations. Conditions such as 25 °C, 75 %RH, 40 °C, 75 %RH and 60 °C, 75 %RH may be evaluated for storage and stability. This section briefly addresses the 75 %RH condition at various temperatures, including some conditions commonly used in pharmaceutical stability studies.

Figure 5-8 shows the conversion to monohydrate at 60 °C, 75 %RH, as well as a partial conversion at 40 °C, 75 %RH. Under high humidity conditions, the disordered form of MgSt was observed to convert to the monohydrate form. It was slightly curious that the dihydrate was not formed at 60 °C, instead of the monohydrate. This data suggests that the monohydrate is the more stable form at these temperatures, even though the dihydrate was expected at intermediate temperatures around 60 °C. It is speculated

that 75 %RH is not a high enough relative humidity to preferentially form the dihydrate crystal form at 60 °C.
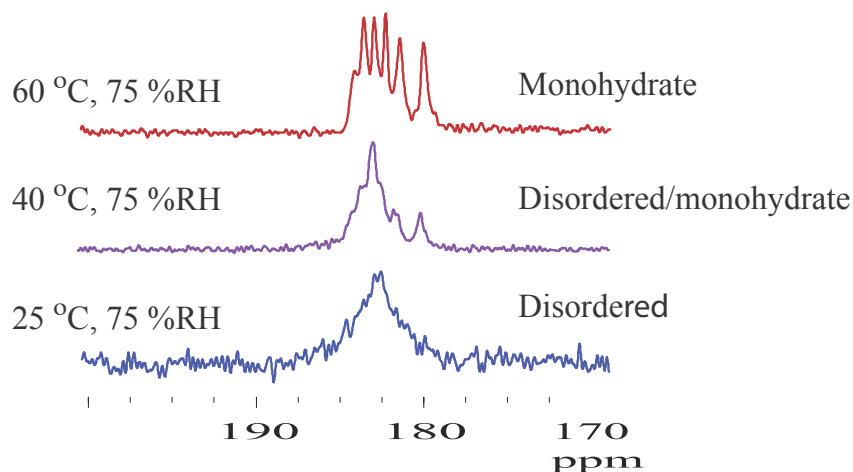
Figure 5-8. MgSt form conversions from disordered starting material under various temperature conditions at 75% RH

5.5.8   Form Conversions in Tablets after Storage at Stability Conditions

In addition to determining the form conversions in bulk MgSt, the possibility of form conversions of MgSt in tablets was investigated. Due to the low level of MgSt in most tablet formulations, it is often difficult to detect the MgSt in formulations. For this reason, several lots of MgSt were synthesized in the lab using labeled stearic acid. The stearic acid was ^{13}C labeled at the C1 carbon of the carbonyl. This allows for enhanced sensitivity of MgSt in the carbonyl region and MgSt form differences can be detected in formulations prepared using labeled MgSt. For this study, the tablets were made on a hydraulic, single tablet press using 200 bar compaction pressure. The starting form of neat MgSt was compared with the form of MgSt in tablets.

Figure 5-9 shows tablets containing 2% MgSt after storage at various temperature and humidity conditions. The starting form was a mixture of monohydrate, dihydrate and trihydrate. Form conversions were observed, corresponding with the forms expected at the temperature and humidity of each storage condition. The 25 °C, 75 %RH condition showed a slight change in the form of MgSt, with the trihydrate peak decreasing relative

to the dihydrate peaks, but this is can be attributed to an increase in resolution due to the effects of tablet compression. At 40 °C/ 75% RH, there is significant increase in the dihydrate peak relative to the monohydrate and trihydrate peaks. The dihydrate increase at 40 °C/ 75% RH is nominally consistent with the dihydrate dehydration conditions, suggesting the dihydrate is expected to exist at 40 °C/ 75% RH, which is in between the conditions to form the monohydrate and trihydrate. At 40 °C/ 0% RH, the dihydrate peak shrinks and almost disappears, accompanied by a small growth of disorder in the baseline, indicating dehydration. Additionally, a decrease in the trihydrate peak and shifting of the monohydrate peaks is observed, indicating a new form of MgSt. The effects of dehydration on the monohydrate form will be discussed further in Chapter 6. This dehydration and loss of crystallinity is particularly relevant for formulation development, as solid oral dosage forms are often packaged in 0% RH conditions.
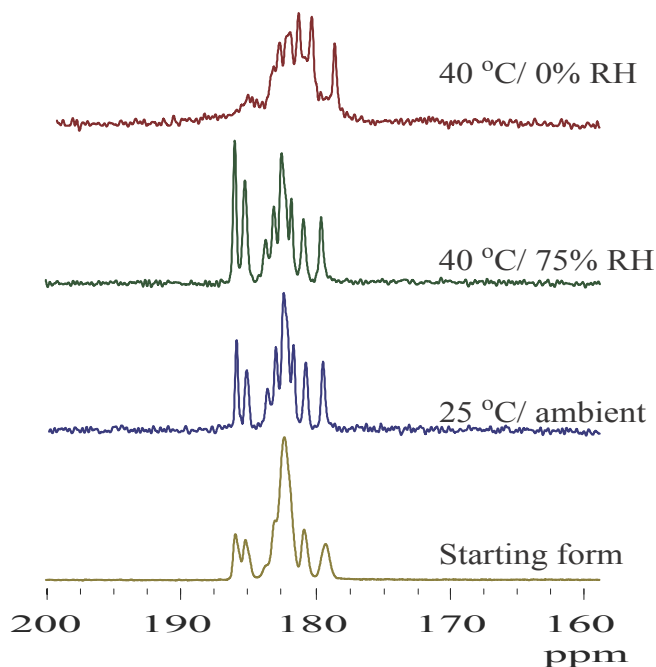
Figure 5-9. SSNMR of MgSt in tablet formulations after storage at various stability conditions

Stability conditions can clearly impact the form of MgSt in tablet formulations, even at low levels of MgSt. Dehydration in particular is an important issue to be aware of for tablet formulations, as storage at 40 °C/ 0% RH for just 7 days can impact the forms

of MgSt. Dehydrating the sample pulls the water out of the crystal lattice, which may collapse the crystal structure and disrupt the lubrication ability. This is bad for lubrication efficiency, so the storage conditions prior to tableting should be chosen with this in mind. However, the dehydration of MgSt after tableting may be beneficial in decreasing the effect of MgSt on dissolution. After the tablets are made, this structure change may still affect the particle-particle interactions inside the tablets, with implications for dissolution and absorption, with the MgSt potentially affecting the ability of the drug to be released into the body. The MgSt coverage of particles in the formulation will be less effective after dehydration, increasing particle-particle adhesion and allowing for easier release and faster dissolution. All of these things should be considered in developing the best tablet formulations incorporating MgSt, with particular attention to the potential for form conversion at elevated temperature and relative humidity conditions.

5.6   Conclusions

This chapter provides an increased understanding of the form conversions of MgSt, both in bulk and in tablet formulations. Thermal data can be used as a guide to choose likely conversion conditions based on the dehydration temperatures of the MgSt hydrate forms. In dry conditions at 105 °C, the hydrates can be dehydrated into the disordered form. The disordered form may then be rehydrated at 100 %RH at temperatures corresponding to the various hydrate forms. It was shown that at 80 °C, 100 %RH, the trihydrate converts into the dihydrate and/or monohydrate form, showing that in the presence of excess water, the crystal form depends on temperature. A form conversion schematic for MgSt is presented, proposing conditions for direct conversions between MgSt crystal hydrate forms, as well as form conversions through an intermediate disordered or anhydrous form. Stability conditions for bulk MgSt samples were briefly investigated and showed the monohydrate form was formed over the dihydrate form at 40 °C/ 75%RH and 60 °C/ 75 %RH. Tablet formulations also showed MgSt form conversions at 40 °C/ 75%RH, with an increase in dihydrate form, and at 40 °C/ 0%RH with dihydrate being dehydrated. Overall, it is shown that the crystal form of MgSt can change under varying temperature and humidity conditions, both in bulk and in tablet

formulations. Understanding the form conversions of MgSt in bulk and in tablets is potentially relevant to formulation stability and storage conditions.

5.7   Acknowledgements

CHAPTER 6. THE IMPACT OF DRYING ON MGST SURFACE AREA AND HYDRATE FORM

6.1 Author and Journal Information

Julie L. Calahan[1], Evelyn G. Yanez[3], Daniel DeNeve[1,2], Joe Lubach[3], Eric J. Munson[1,2*]

[1] University of Kentucky, Lexington, KY

[2] Current address: Purdue University, Lafayette, IN

[3] Genentech, Inc., South San Francisco, CA

*Corresponding author: Address: Purdue University, Robert E. Heine Pharmacy Bldg Rm 124D, 575 Stadium Mall Drive, West Lafayette, IN 47907-2091, Phone: (765) 494-1450, Email: munsone@purdue.edu

Abbreviations

Magnesium stearate (MgSt)

Thermogravimetric analysis (TGA)

Solid-state nuclear magnetic resonance (SSNMR)

Relative standard deviation (RSD)

Monohydrate (Mono)

Dihydrate (Di)

BET (Brunauer-Emmet-Teller)

SSA (Specific surface area)

6.2 Abstract

Purpose: Magnesium stearate (MgSt) is a widely used pharmaceutical lubricant in tablet manufacturing. However, batch-to-batch variability of MgSt can lead to inconsistency in performance. Surface area is known to impact tablet performance. The crystal form of MgSt has also been shown to affect lubrication performance. In this work, we investigate how drying impacts the surface area results and may also induce a change in crystal form.

Methods: Surface area analysis was conducted using a Micromeritics ASAP 2460 with Smart Vac Prep attachment to vary drying time and temperature. Specific surface area was calculated using the BET method. Solid-state NMR was used to identify the crystal form of MgSt samples. ^{13}C spectra were acquired on a 9.4T spectrometer using a home-built 7.5mm MAS probe at 4 KHz at room temperature and processed using Tecmag software.

Results: The extent of drying MgSt prior to surface area analysis impacts the surface area results, as well as the fit of the BET equation. Surface area after drying for 2h at 40 °C (USP conditions) showed a notable decrease in surface area for some commercial samples, which also correlated with a physical form change in the MgSt sample. Specifically, the dihydrate form of MgSt appeared to disappear and the disordered form appeared with an increase in drying time. A similar form change for MgSt was observed in tablets after storage in desiccated conditions for 7 days.

Conclusions: Drying is shown to affect the crystal form of MgSt, both in bulk and in tablets. This has implications for appropriate storage conditions and the physical stability of MgSt used in pharmaceutical formulations.

6.3 Introduction

Magnesium stearate (MgSt) is the most common pharmaceutical excipient and is used as a lubricant in approximately half of the tablet formulations on the market. (1) In spite of its popularity as an effective lubricant, it has been repeatedly recognized that there is significant variability between MgSt samples which can cause inconsistent lubrication between lots and batches of MgSt. In addition to chemical composition variability and pseudopolymorphism variability, the particle size and surface area of MgSt have been investigated for their impact on performance variability. In 1984, Frattini and Simioni reported a correlation between MgSt surface area and tablet ejection force. (40) Phadke et al. suggested that particle size analysis would be a potential way to evaluate batch-to-batch variation in MgSt, and studied the degassing effects associated with BET surface area analysis, hypothesizing that lower surface area after degassing could be due to hydrate form conversion.(40-42) Andres et al. recognized the need for an improved understanding of MgSt degassing effects in 2001,(43) followed by Koivisto et al. who noted that although all hydrate forms converted to anhydrous at 105 °C, the hydrate surface area isotherms did not always fit properly with BET theory.(44)

Extensive investigation of the degassing of MgSt was undertaken by Lapham and Lapham, revealing dehydration and unreliable BET results with degassing as low as 40 °C. In their 2019 study, the surface area and isotherms of four commercial samples were analyzed before and after degassing at temperatures ranging from 30 – 110 °C. The hydration state of the starting materials was determined from TGA weight loss and vacuum drying, with assumptions of anhydrous and hydrated forms based on weight loss temperatures. Looking closely at isotherms and low pressure hysteresis, the differences in adsorption/desorption isotherms for the samples were found to be related to the hydrated water in the starting form for each batch and a swelling effect causing adsorbate to be entrapped in the sample during the adsorption process.(45-47) Expanding on the current understanding of the degassing process from the Lapham work, we aim to relate the dehydration to changes in MgSt crystal form. Our previous paper by Delaney at al. presents a variety of characterization techniques for several MgSt commercial samples, including SSNMR. The carbonyl region of the SSNMR spectrum clearly distinguishes between crystalline hydrate forms, as well as the anhydrate and disordered forms of MgSt.(48)

In this present chapter, we characterize the surface area of selected commercial and lab-synthesized MgSt samples, using various drying and degassing conditions prior to surface area analysis. The samples are characterized by SSNMR before and after drying, to evaluate the impact of drying conditions on neat MgSt. Drying/degassing leads to dehydration, and a form change for MgSt hydrates, with this form change being easily identified using SSNMR. It is also shown that the extent of drying time at 40 °C is critical to not only the observed surface area but also the physical form of MgSt. Finally, dissolution of tablet formulations before and after drying shows an effect of dehydration on the functional properties of MgSt.

6.4   Materials and Methods

6.4.1   Materials

Magnesium hydroxide was purchased from Fluka (St. Louis, MO). Stearic acid and palmitic acid were purchased from TCI (Tokyo, Japan). Magnesium chloride hexahydrate was purchased from EMD (Darmstadt, Germany). Phosphate buffer was prepared from sodium phosphate monobasic and sodium hydroxide, purchased from purchased from BDH Analytical (Radnor, PA). Tablet excipients Avicel (microcrystalline cellulose, MCC) and alpha-Lactose monohydrate were obtained as a complimentary sample from FMC Biopolymer (Philadelphia, MA) and purchased from Sigma (St. Louis, MO), respectively. The commercial MgSt samples were ordered through VWR from Beantown (dihydrate) and Alfa Aesar (disordered), and the Peter Greven (monohydrate) sample was purchased in bulk by Genentech.

6.4.2   MgSt Synthesis Methods

Magnesium stearate lots were synthesized in ratios using 90:10 and 55:45 stearic: palmitic acids. To synthesize the 55:45 disordered sample, a "melt method" combined

magnesium hydroxide and water with melted stearic and palmitic acids at 70-90 °C. To synthesize the 90:10 samples, a "bath" method was used, where the stearic and palmitic acids were dissolved in water and ammonium hydroxide at pH 9 to generate the sodium soap, followed by addition of magnesium chloride to precipitate out the magnesium stearate. The monohydrate 90:10 sample was subsequently heated above 100 °C before the reflux step. In each case, the recovered solids were washed using a reflux bath of 1:1 acetone: water for 24 hours to remove impurities and unreacted starting materials. The MgSt samples were dried in a vacuum oven at 25 °C overnight to remove surface water.

6.4.3   Mixing, Tableting and Sieving

MgSt tablets for dissolution were prepared by adding MgSt sample to a "Premix" mixture containing 16.7% indomethacin (Sigma, St. Louis, MO), 50% alpha-lactose monohydrate (Sigma, St. Louis, MO), 33.3% Avicel (FMC Biopolymer, Philadelphia, PA) in a ratio of 2:98 MgSt: Premix. The tablet powders were mixed as 1 g batches in 40 mL glass vials for 60 minutes using a Turbula mixer (WAB, Basel, Switzerland) on the highest setting. Individual 150 mg tablets were made from each 1 g formulation batch and pressed using a single tablet press (Globe Pharma, North Brunswick, NJ) at 50 bar for 30 seconds. The tablet weights were recorded and the dissolution results were adjusted for tablet mass. When needed, MgSt samples were sieved using ASTM sieves that range between 75 μm and 125 μm sieve sizes.

6.4.4   Dissolution

Dissolution was performed by dissolving each tablet in 900 mL of pH 7.2 phosphate buffer at 37 °C using a VanKel V7000 USP method 2 dissolution apparatus (Varian, Cary, NC). The paddles were stirred at 100 rpm. μDISS fiber optic UV probes (pION, Billerica, MA) were used to collect data at various time points from 0 - 120 minutes and processed using UV absorbance at 320 nm. The μDISS probes were

calibrated using indomethacin in phosphate buffer. The dissolution data was processed using the second derivative function to eliminate the effects of particles on the UV absorbance reading.

6.4.5   Solid-state NMR Spectroscopy (SSNMR)

^{13}C CP/MAS and ^{1}H T_1 relaxation data were collected using a home built Tecmag Redstone NMR Spectrometer (Houston, TX), Bruker 400 MHz magnet (Billerica, MA), and Chemagnetics (Ft. Collins, CO) NMR probe with 7.5 mm rotors spinning at 4000 Hz. A relaxation delay of 12 seconds was used with 2K acquisition points and 1024 scans. TNMR software (Houston, TX) was used to process the data. 3-methylglutamic acid was used as a reference standard, with the methyl peak referenced to 18.84 ppm.

6.4.6   Thermogravimetric Analysis (TGA)

TGA weight loss was measured using TA Q50 (TA Instruments, Newcastle, DE) with a 10 °C/min ramp from 25 °C to 250 °C.

6.4.7   Surface Area Analysis

Surface area analysis was conducted using a Micromeritics ASAP 2460 with a Micromeritics Smart Vac Prep attachment (Micromeritics Instrumentation Corporation, Norcross, GA, USA). A sample of about 1000 mg was dried at 40 °C and outgassed under nitrogen flow conditions. Krypton adsorption-desorption isotherms were recorded at liquid nitrogen temperatures (77K) and specific surface area was calculated by the Brunauer-Emmett-Teller (BET) method. Data was analyzed using Micromeritics MicroActive version 5.0 software.

6.5   Results

6.5.1   Surface Area Analysis for Commercial MgSt Samples

To investigate the relationship of MgSt crystalline form with surface area, several commercial MgSt samples were compared, shown in Table 6-1. Samples were analyzed for BET surface area after degassing at 2h 40 °C and 48h 40 °C. This was done to compare the USP method for MgSt with a condition where the samples were completely dry. The surface area data reported in Table 6-1 includes the BET C constant values and the correlation coefficients for the curves. In BET theory, the C value is an indicator of the interaction of the sample with the adsorbate gas. A C value of 10 is considered a minimum for a sample that behaves according to BET adsorption theory.(47) Table 6-1 shows that some of the MgSt samples have low C values (below 10) for the 2h drying condition. A second indication of suspect surface area data is the correlation coefficient. The correlation coefficients The BET curves were evaluated using 3 points in the range 0.05 - 0.30 p/p0. The USP chapter for surface area analysis for MgSt specifies a minimum of 3 points.(19) Some of these samples had a poor correlation coefficient with more than 3 points, indicating a poor BET fit, and can be an indication of incomplete drying of the samples. A degassing step is generally required to be performed prior to the gas adsorption step, to remove surface bound water and surface impurities from the samples. Table 6-1 shows the C values for 48h drying are all > 10, indicating more complete drying at 48 hours compared with 2 hours. Additionally, the % difference in surface area before and after drying ranges from 5 – 21%, suggesting there may be a reason for the surface area change. The surface area results for MgSt samples are sensitive to drying conditions, as indicated by the noted differences between the samples that were outgassed at 40 °C for 2 hours and 48 hours.

Table 6-1. Surface area data for commercial samples dried at 2h 40 °C and 48h 40 °C

| Sample | Crystal form | Drying: 2h 40 ℃ | | | Drying: 48h 40 ℃ | | | % Diff |
		BET (m^2/g)	C value	Correlation coefficient	BET (m^2/g)	C value	Correlation coefficient	
Alfa Aesar Lot C01Y019	Disordered	0.69	12.58	0.9986	0.77	14.22	0.9990	10.4
Alfa Aesar Lot H03W054	Disordered	0.79	8.54	0.9995	0.89	13.98	0.9992	11.2
MP Biomedical Lot 75281	Mono-dihydrate	3.62	5.21	0.9985	3.83	15.47	0.9989	5.5
Chem-Impex Lot 6301123019902	Mono-dihydrate	4.02	10.71	0.9995	3.78	14.74	0.9988	6.0
Acros Lot A0288107	Mono-dihydrate	4.83	9.42	0.9991	3.92	12.85	0.9987	18.8
Sigma-Aldrich Lot STBB0861V	Mono-dihydrate	5.28	9.56	0.9993	4.17	13.66	0.9989	21.0
Acros Lot A0235781	Monohydrate	6.62	12.86	0.9993	6.02	10.72	0.9996	9.1

6.5.2 Effect of Drying on MgSt Crystal Form

To investigate the cause of these differences, the 2 hour drying samples and selected 48 hour drying samples were characterized by ^{13}C SSNMR after the surface area analysis, to determine whether there was a form change during the surface area analysis. The ^{13}C SSNMR of these samples before and after drying for surface area analysis is shown in Figure 6-1. The samples that were outgassed at 40 °C for 2 hours did not show observable changes in the ^{13}C SSNMR spectra. Before drying, two of the commercial MgSt samples had a disordered form, four samples had a mixture of monohydrate-dihydrate and one sample was a pure monohydrate form. There appears to be a relationship between the crystal form and the surface area recorded in Table 6-1. The BET surface area results listed showed that the disordered samples had the lowest surface area, while the monohydrate-dihydrate mixtures had intermediate surface area and the pure monohydrate samples had the highest surface area. However, after 48h drying, clear differences in the forms were observed, with a decrease in the dihydrate form,

accompanied by the appearance of the disordered form. The monohydrate peaks also appear to shift with excess drying, indicating a form change for the monohydrate.
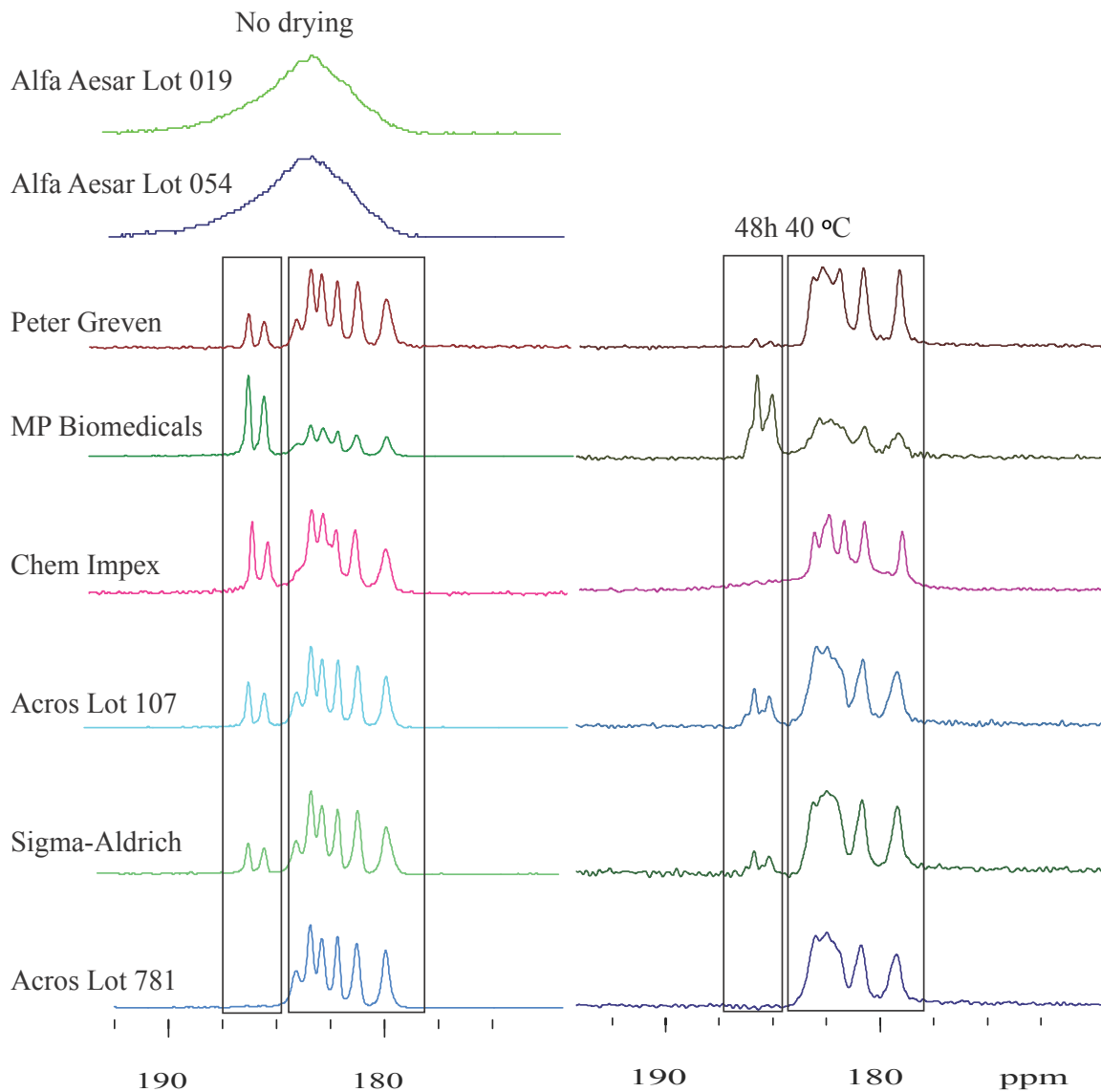
Figure 6-1. ^{13}C SSNMR for several commercial MgSt samples, before and after drying at 40 °C for 48 hours. Only the carbonyl region of the spectrum (170 - 200 ppm) is shown, to identify the crystal form of the samples. The box around 185-187 ppm indicates the dihydrate peaks, and the box around 178-185 ppm indicates the monohydrate peaks.

The ChemImpex sample in Figure 6-2 illustrates these changes well, showing a clear form change for the ChemImpex material after being outgassed at 40 °C for 48

hours. The dihydrate disappears and a broad, disordered peak appears in the spectrum. Additionally, the monohydrate peaks are clearly shifted, indicating a form change as a result of drying.
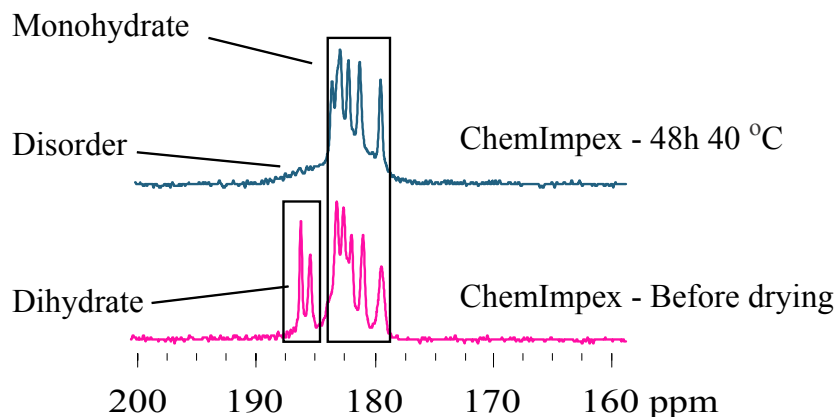
Figure 6-2. ^{13}C SSNMR of the ChemImpex MgSt lot before drying (bottom) and after drying (top) for 48h at 40 °C. After drying, the dihydrate peaks in the SSNMR spectrum disappear and a broad disordered peak appears in the spectrum.

Having observed an initial effect of drying to impact the crystal form of MgSt during surface area analysis, more intensive work was performed for a single Peter Greven commercial lot (PG). Various drying conditions were compared for the PG lot. As shown in Figure 6-3, BET surface area analysis was performed on the same lot with various outgassing conditions: no drying, 2h at 40 °C, 12h 40 °C, 24h 40 °C and 48h at 40 °C. It is clear from Figure 6-3 that the crystal form is changing with drying. The N_2 and Kr adsorption BET surface area results are shown in Table 6-2, including the correlation coefficients and C values. The surface area result decreased with additional drying, corresponding with form changes in the SSNMR spectra. The dihydrate peaks decreased and completely disappeared after 48h drying, accompanied by appearance of traces of the disordered form. There is also a change in the SSNMR spectra of the monohydrate peaks. The small peak on the left side of the monohydrate disappears at 12h and a new peak appears between the next two peaks. The space between the last two monohydrate peaks also increases slightly, as the peak on the right becomes sharper with

an increase in resolution. This shifting of the peaks of the monohydrate indicates a new crystal form, which appears in the 12h, 24h and 48h dried samples.
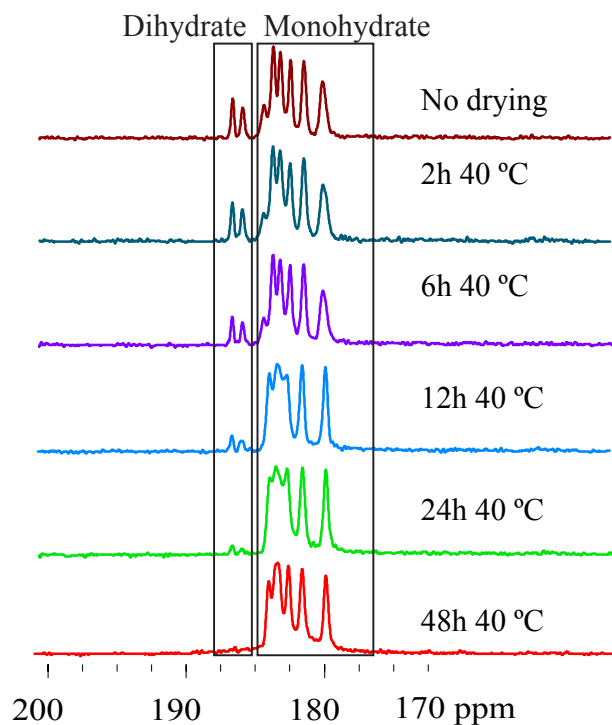
Figure 6-3. SSNMR for MgSt "PG" lot, showing the effect of the surface area drying method on MgSt hydrate forms.

Table 6-2. Surface area data for MgSt PG lot under different drying conditions

Drying conditions	N₂ gas adsorption			Krypton gas adsorption			TGA
	BET (m^2/g)	C value	Correlation coefficient	BET (m^2/g)	C value	Correlation coefficient	% loss
No drying	9.47 ± 0.66	13.87	0.9972	5.54 ± 0.21	9.24	0.9991	3.3
2h, 40 ºC	7.95 ± 0.54	15.02	0.9974	5.35 ± 0.18	10.45	0.9993	3.2
6h, 40 ºC	6.74 ± 0.11	22.48	0.9999	4.89 ± 0.15	10.42	0.9994	3.3
12h, 40 ºC	6.42 ± 0.09	23.00	0.9999	5.11 ± 0.17	8.24	0.9993	3.2
24h, 40 ºC	6.37 ± 0.09	22.00	0.9999	4.99 ± 0.08	8.45	0.9998	2.8
48h, 40 ºC	6.08 ± 0.11	20.86	0.9998	4.81 ± 0.07	6.21	0.9998	2.8

Comparing the N_2 with Kr surface area analysis in Table 6-2, it is noted that the C values are slightly lower for Kr adsorption, but the correlation coefficients are higher for Kr. It is interesting that the absolute values for BET surface area are smaller when using Kr as the adsorbate, due to the adsorbate size. That is, the Kr cross sectional area is less than N_2 cross sectional area, so the calculations of surface monolayer coverage give slightly different results. Kr also shows less variation in surface area, dropping 0.67 m^2/g (from 5.54 m^2/g to 4.81 m^2/g) after 48h, unlike N_2 which shows a significant drop in surface area from 9.47 m^2/g to 7.95 m^2/g after only 2h drying and 6.08 m^2/g after 48h drying. From the SSNMR in Figure 6-3, we see that 2h drying does not appear to change the crystal form significantly, where drying for 12 - 48h appears to significantly change the crystal form. In this case, the Kr adsorption surface area results appear to track better with the crystal form change.

6.5.3   Effect of Drying on Tablet Dissolution

To evaluate the impact of the drying (dehydration) on functional property, dissolution was performed for tablet formulations prepared using MgSt from the before and after samples. Figure 6-4 shows the dissolution results indicate faster dissolution for the dried samples, with up to 20% difference at 5 minutes and 5-10% difference at 15 minutes using this method. For clarity, 30 minutes dissolution is shown, but 95-100% dissolution is achieved for all samples before 2 hours. From previous work, it is known that the disordered form of MgSt leads to faster tablet dissolution, likely due to less effective lubrication of the formulation particles.
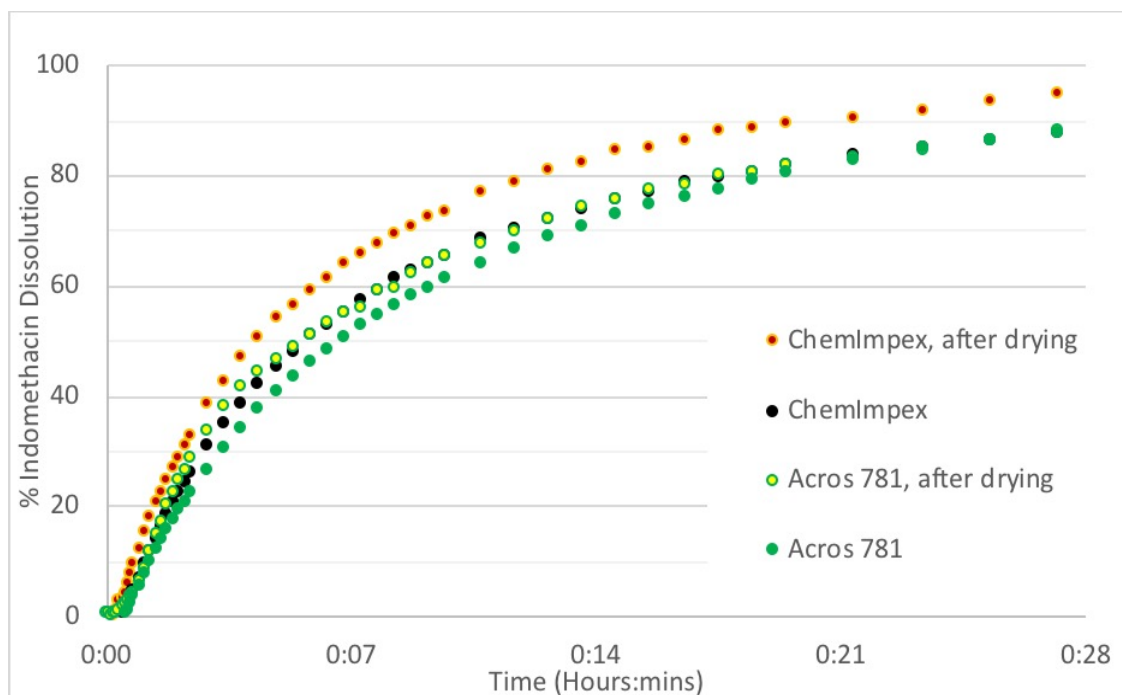
Figure 6-4. Tablet dissolution comparing formulations prepared with MgSt before drying (closed circles) and after drying (open circles). Drying appears to cause ~10% faster dissolution rate and may lead to less effective lubrication by MgSt.

6.6   Discussion

6.6.1   Correlation of MgSt Crystal Form with Surface Area

The surface area for several commercial MgSt samples appears to trend with the crystal form of the material. The disordered samples have the lowest surface area, which is consistent with poor lubrication ability. Monohydrate MgSt has higher surface area above 5 m^2/g, suggesting that this material may have the most effective lubricating ability compared to the other samples in this data set. The monohydrate-dihydrate mixtures of MgSt show an intermediate surface area in the range 3 - 5 m^2/g. Looking closely at the height of the peaks corresponding to the MgSt forms in the SSNMR spectra for the monohydrate-dihydrate mixtures, it appears that the amount of dihydrate character in the mixtures may affect the surface area as well.

The surface area analysis for MgSt, as shown in Table 6-1, was challenging with respect to obtaining consistent and reliable data for the "as is" commercial samples. Even though the C values and correlation coefficients were met using 3 points, they were on the borderline of acceptability for meeting the USP criteria for reporting surface area. The difficulty of determining surface area for MgSt is well-known to those in the field(45) and it is believed that surface water can freeze during the analysis and cause an artificially high and often variable result. Outside of additional drying, the typical way of dealing with the analysis is to focus on the lower p/p0 region between 0.05 - 0.1 p/p0 and to use fewer points for the BET analysis to get an acceptable fit. The lower p/p0 region is more likely to be before a complete adsorbate monolayer coverage of the particles, and hydrated MgSt often behaves erratically with additional adsorbate added. The reasons for this are not well understood, but several possible explanations are discussed in Lapham and it is beyond the scope of this paper to pursue further.(46)

6.6.2   Correlation of Crystal Form with Drying

The ^{13}C SSNMR for MgSt PG commercial material clearly shows the effect of drying MgSt on the crystal form. Specifically, the dihydrate character of the material is dehydrated. SSNMR clearly shows the decrease and disappearance of the dihydrate, with the appearance of disordered form conversion upon dehydration Figure 6-3. Additionally, a new form was observed in the shifting of the monohydrate peaks with drying. The significance of these changes is not only that the surface area changes, but that the lubrication ability of the MgSt sample also is likely to change as a result of the crystal form change. Other studies have shown that the presence of both the disordered form and the new monohydrate form, decreases the effect of MgSt on dissolution, and by extension, the lubrication ability of MgSt. It is possible that a batch of MgSt that is stored at 40 °C condition for an extended period could undergo a change in form, which could adversely affect its lubrication performance.

6.6.3 Effect of Drying on Dissolution

The dissolution of tablet formulations using MgSt before and after drying shows a clear effect of drying and dehydration on dissolution. The disordered form has faster dissolution compared to the monohydrate and hydrate mixtures, possibly due to less effective lubrication ability of the disordered form. It is suggested in the literature and we hypothesize that the drying removes the bound water from the crystal structure, causing dehydration and disrupting the crystal structure. The crystal structure can then collapse, resulting in the disordered form. This is consistent with the observed decrease in surface area with drying Table 6-2, which could be due to the removal of water, as well as the change in crystal structure. Overall, the dissolution is consistent with the effects of drying on MgSt, with increased dissolution rate for tablets using dried MgSt compared to non-dried MgSt. The dissolution behavior supports the expectation that drying MgSt can affect its performance.

6.7 Conclusions

Several conclusions can be drawn from this study. First, there appears to be a significant correlation between MgSt crystal form and surface area. The disordered form shows low surface area and the monohydrate form shows higher surface area. Second, drying MgSt at 40 °C leads to dehydration of the material, with a decrease in surface area being accompanied by an increase in the amount of disordered form in the sample. In addition to the form change with drying, dissolution showed that drying MgSt can also have an impact on tablet performance.

6.8 Acknowledgements

CHAPTER 7.   DEVELOPMENT OF A DISCRIMINATING DISSOLUTION METHOD FOR MGST TO STUDY THE EFFECTS OF OVER-LUBRICATION

7.1   Author Information

Julie L. Calahan, University of Kentucky, KY

Daniel DeNeve, Purdue University, IN

Job K. Limo, Berea College, Berea KY

Christopher J. Mays, Ross University, Roseau, Dominica, West Indies

Jonathan Gerzberg, University of Michigan, MI

Kanika Sarpal, Vertex Pharmaceuticals, Boston, MA

Sean P. Delaney, US Pharmacopeia, MD

Eric J. Munson, Purdue University, Robert E. Heine Pharmacy Bldg Rm 124D, 575 Stadium Mall Drive, West Lafayette, IN 47907-2091, Phone: (765) 494-1450, Email: munsone@purdue.edu

7.2   Abstract

Magnesium stearate (MgSt) is the most common pharmaceutical excipient and is used as a lubricant in approximately half of the tablet formulations on the market.(1) In spite of its popularity as an effective lubricant, it has been repeatedly recognized that there is significant variability between MgSt samples which can cause inconsistent lubrication and/or dissolution between lots and batches of MgSt. Dissolution is an important functional property for pharmaceutical formulations. Differences in dissolution for different crystal forms of MgSt have been reported, but an exhaustive study of the influence of MgSt hydrate form on dissolution has not yet been published. In this study, a dissolution method is developed for an indomethacin direct compression tablet

formulation. The method development discussed here covers: 1) manual dissolution sampling, 2) formulation mixing methods, 3) use of fiber optic UV probes, 4) calibration curves comparing UV spectrometer analysis and fiber optic probes, 5) effect of MgSt concentration on dissolution, 6) powder vs. tablet dissolution profiles, 7) effect of tablet compaction pressure, 8) effect of vial type and turbula speed, 9) effect of formulation mixing time on dissolution for monohydrate and dihydrate forms, 10) reproducibility and differentiation of tablets using various commercial MgSt lots, 11) sample homogeneity, 12) effect of MgSt particle size sieve fractions on dissolution rates and 13) effects of grinding, sieving and ball-mixing of MgSt on tablet dissolution. A dissolution method is developed which can distinguish between MgSt samples with different physicochemical properties.

7.3   Introduction

Magnesium stearate (MgSt) is the most common pharmaceutical excipient and is used as a lubricant in approximately half of the tablet formulations on the market.(1) In spite of its popularity as an effective lubricant, it has been repeatedly recognized that there is significant variability between MgSt samples which can cause inconsistent lubrication and/or dissolution between lots and batches of MgSt. Incomplete lubrication can cause picking and sticking, so MgSt is typically added as a solid lubricant to tablet formulations as a lubricant at a 0.25 - 5% level to prevent powder from sticking to the tablet die and manufacturing equipment during the tableting process. Many formulation labs have experiences with MgSt where the lubrication capability and/or the dissolution rate varies unexpectedly, with unexplained batch-to-batch and lot-to-lot variation.(16, 97) For example, one lot from a manufacturer may show picking and sticking after several thousand tablets are made as powder builds up on the equipment, but other lots do not. In addition, tablets manufactured from different lots of MgSt may have different dissolution properties. The reasons for the inconsistencies between lots and types of MgSt are still poorly understood, (149-151) but it is proposed that the variability in the dissolution and

lubrication properties of MgSt can be related back to its complicated structural properties.(98, 126)

Dissolution is an important functional property for pharmaceutical formulations. It is known since 1963 that MgSt causes slowed dissolution of API formulations(89) and that formulation mixing time and compression force affect the dissolution rate(90, 91) as well as the amount of MgSt in the formulations. The mechanism was investigated and the effect of MgSt on mixing time and compression force was attributed to lamination and adhesion of MgSt to the other particles in the formulation, along with the flaking of MgSt causing an increase in surface area.(90, 92) Hussain et al. suggested that the extent of surface coverage of the hydrophobic film on the particles is the most important factor in affecting dissolution.(83) Patra et al. studied the effect of MgSt concentration and granule size on the dissolution rate of ciprofloxacin HCl and found that a hydrophobic lubricant like MgSt decreases the drug-solvent interface, causing slower dissolution due to decreased wettability and increased dissolution rate with smaller granules.(93) Possible interactions with MgSt have been explored for their effects on dissolution, including the addition of colloidal silica by Johansson et al.,(94) the interactions of surfactants with MgSt during mixing,(50) and the interaction of MgSt with HPMC-AS in ASDs and hydrogen bonding with itraconazole ASDs.(95, 96) The effects of acidic media was also investigated by Ariyasu et al. and indicates conversion of MgSt to stearic acid during dissolution.(97, 98) Additionally, other lubricants were explored as alternatives to MgSt, including calcium stearate,(98) glycerin fatty acid esters,(99, 100) Stear-o-Wet,(101) talc.(102) Hussain, York and Timmins compared the dissolution of paracetamol tablets with different grades of MgSt. No relationship between physical properties such as surface area and dissolution was found. (83) In 2013, Okoye et al. observed differences in dissolution between naproxen and acetaminophen comparing MgSt dihydrate, monohydrate and anhydrate.(87) However, an exhaustive study of the influence on MgSt hydrate form on dissolution has not yet been published.

In this study, a dissolution method is developed for an indomethacin direct compression tablet formulation. An appropriate dissolution method is needed to show distinguish between different MgSt samples, to enable a comprehensive investigation of the properties of various MgSt samples. This method is specifically designed to be an

over-lubricated situation, to differentiate between varying types of MgSt in the tablet formulations. The method development discussed here covers: 1) manual dissolution sampling, 2) formulation mixing methods, 3) use of fiber optic UV probes, 4) calibration curves comparing UV spectrometer analysis and fiber optic probes, 5) effect of MgSt concentration on dissolution, 6) powder vs. tablet dissolution profiles, 7) effect of tablet compaction pressure, 8) effect of vial type and turbula speed, 9) effect of formulation mixing time on dissolution for monohydrate and dihydrate forms, 10) reproducibility and differentiation of tablets using various commercial MgSt lots, 11) sample homogeneity, 12) effect of MgSt particle size sieve fractions on dissolution rates and 13) effects of grinding, sieving and ball-mixing of MgSt on tablet dissolution.

7.4   Materials and Methods

7.4.1   Materials

Magnesium hydroxide was purchased from Fluka (St. Louis, MO). Stearic acid and palmitic acid were purchased from TCI (Tokyo, Japan). Indomethacin was purchased from Sigma (St. Louis, MO). Magnesium chloride hexahydrate was purchased from EMD (Darmstadt, Germany). Phosphate buffer was prepared from sodium phosphate monobasic and sodium hydroxide, purchased from purchased from BDH Analytical (Radnor, PA). Tablet excipients Avicel (microcrystalline cellulose, MCC) and alpha-Lactose monohydrate were obtained as complimentary samples from FMC Biopolymer (Philadelphia, MA) and purchased from Sigma (St. Louis, MO), respectively. The sources of the commercial samples were reported previously.(48)

7.4.2   Tablet Composition

The tablet formulation composition is 16.7% indomethacin, 50% alpha-lactose monohydrate, 33.3% microcrystalline cellulose (Avicel PH 102) and 2% magnesium

stearate (MgSt). Lactose is a commonly used filler/diluent known to have good compressibility. Avicel PH 102 is a binder often used in direct compression in tablet formulations. A "premix" containing all the formulation ingredients except MgSt was prepared first, to minimize the formulation variation in each tablet due to the other ingredients. The type of magnesium stearate was intentionally varied from batch to batch, to study the impact of MgSt properties on the functional properties of the tablets. Formulations of 1g size were prepared. The 1g size allows for six 150 mg tablets to be prepared from each formulation batch.

7.4.3   Mixing and Tableting

Indomethacin tablet formulations were prepared by adding MgSt to a "Premix" mixture containing 16.7% indomethacin (Sigma, St. Louis, MO), 47.3% alpha-lactose monohydrate (Sigma, St. Louis, MO), 34% Avicel (FMC Biopolymer, Philadelphia, PA) in a ratio of 2:98 MgSt: Premix. The tablet powders were mixed as 1 g batches in 40 mL glass vials for 60 minutes using a Turbula T-2C mixer (WAB, Basel, Switzerland) on the highest setting. Six individual 150 mg tablets were made from each 1 g formulation batch and pressed using a single tablet press (Globe Pharma, North Brunswick, NJ) at 50 bar for 30 seconds. The tablet weights were recorded and the dissolution results were adjusted for tablet mass. Ball mixing was performed by adding 1g of MgSt to a 40 mL glass vial with ten ¼-inch plastic balls and mixed for 60 minutes using the Turbula T-2C mixer.

7.4.4   Drug Properties and Buffer Selection

Indomethacin is a popular model NSAID drug, with low aqueous solubility of 0.9 mg/L(153) and pK_a of 4.5. The buffer for this project was potassium phosphate, pH 7.2. This is a simple and commonly used buffer for pharmaceutical drug development studies. This pH is more than 2 pH units above the pK_a of indomethacin, to maximize the

solubility of the drug in the buffer. The solubility of indomethacin in the buffer at this pH is > 30 µg/mL. Each 150 mg tablet contains 25 mg of indomethacin (16.7% drug load). If the entire 25 mg of drug is completely dissolved in 900 mL of buffer, the concentration of indomethacin in the buffer is 27.8 µg/mL. This is below the solubility of the drug in the buffer, allowing for complete dissolution. Potassium phosphate buffer was prepared in 9 L batches by adding 2.0 L of 0.2M potassium phosphate solution, 1.4 L of 0.2M sodium hydroxide solution and 5.4 L of deionized water. The pH was confirmed to be 7.2 +/- 0.2 with a pH meter.

7.4.5   Dissolution

Dissolution was performed by placing each tablet in 900 mL of pH 7.2 phosphate buffer at 37 °C using a VanKel V7000 USP method 2 dissolution apparatus (Varian, Cary, NC). The paddles were stirred at 100 rpm. µDISS fiber optic UV probes (pION, Billerica, MA) were used to collect data at various time points from 0 - 120 minutes, and processed using UV absorbance at 320 nm. The µDISS probes were calibrated using indomethacin in potassium phosphate buffer. The dissolution data was processed using the second derivative function to eliminate the effects of particles on the UV absorbance reading.

7.4.6   Grinding, sieving and ball mixing

Grinding was performed using a mortar and pestle. Ball mixing was performed by adding 1g of MgSt to a 40 mL glass vial with ten ¼-inch plastic balls and mixed for 60 minutes using the Turbula T-2C mixer. MgSt samples were sieved on a Gilson Performer Model SS-3 sieve shaker for approximately 60 minutes, using ASTM sieves that range between 20 micron and 250 micron sieve sizes.

7.5   Results and Discussion

7.5.1   Effect of Manual Sampling and Hand-mixing

Method development was initiated with a simple experimental design. Tablets were prepared using four different commercial lots of MgSt and mixed by hand for two minutes. Dissolution samples were pulled at various time points and the drug concentration was analyzed by UV-vis. Figure 7-1 shows similar dissolution for the four formulations, after 2 minutes of mixing by hand.
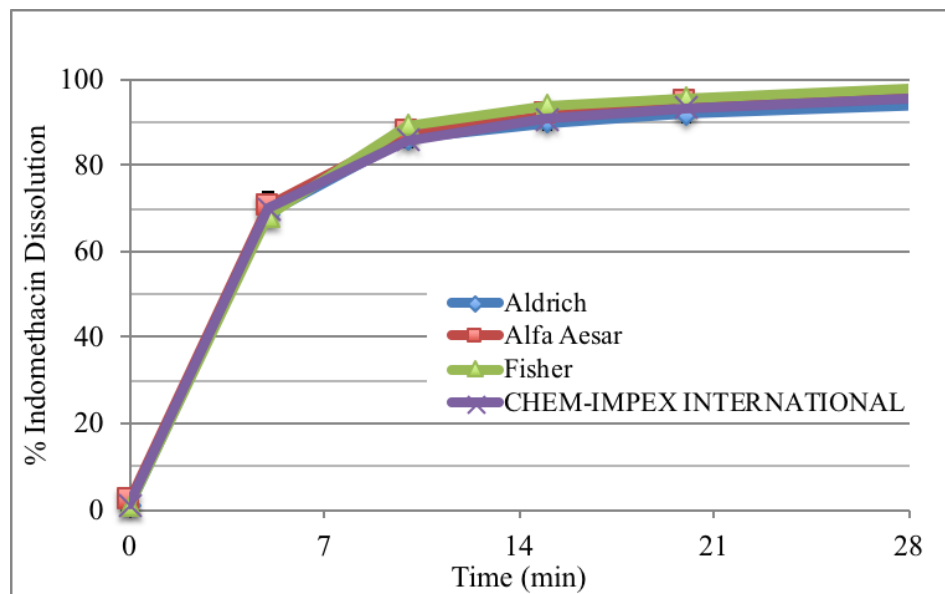
Figure 7-1. Indomethacin dissolution of tablet formulations comparing four commercial samples of MgSt. The formulations were hand-mixed for 2 minutes.

A short mixing time is normal for formulation development, but it does not address the fundamental reason that MgSt variability sometimes causes dissolution failure. Over-lubrication is the underlying issue for MgSt dissolution failure, so to investigate MgSt with dissolution, we need to be looking at an over-lubricated state. The easiest ways to create an over-lubricated state is to increase the formulation mixing time or the % MgSt in the formulation. If some types of MgSt are more susceptible to over-

lubrication than other types of MgSt, those differences will be observed by increasing the mixing time and the % MgSt in the formulation.

Extending the formulation mixing time to 30 minutes of hand-mixing resulted in the dissolution shown in Figure 7-2. Five batches of tablets containing ChemImpex brand of MgSt performed similarly, with ~ 80% dissolution at 15 minutes. However, there was more variation between the five batches of tablets containing Fisher brand MgSt. Additionally, it is unclear whether 100% dissolution is reached for all of these curves, even after 60 minutes.
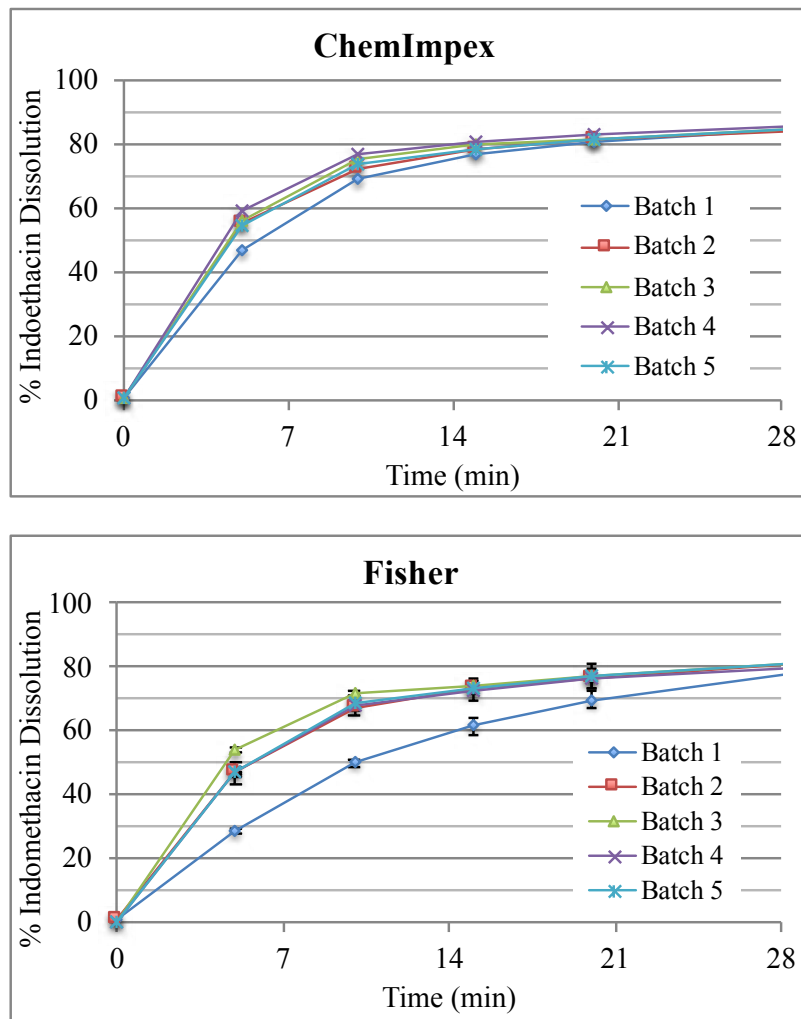
Figure 7-2. Comparison of indomethacin dissolution for tablet formulations using ChemImpex (top) and Fisher (bottom) brands of MgSt. The formulations were hand-mixed for 30 minutes.

Investigating the method details revealed several potential sources of error and/or variability in the method. First, hand-mixing could introduce inconsistency in mixing, depending on the angle of shaking and how rigorously the shaking was performed. This would be expected to vary between batches and analysts. A standardized mixing method is preferred. To address this, a Turbula mixer was obtained and used for subsequent studies. Second, the tablet weights were not tracked for these early studies, leaving room for significant error in calculating % dissolution. A large tablet weight variation could also affect the tablet hardness and disintegration of the tablets. Clearly, it would be preferred to compare tablets of a similar weight. Going forward, the tablet weights were recorded and % dissolution was adjusted accordingly for each individual tablet.

7.5.2 Advantages of uDISS Fiber Optic UV Probes for Direct Sampling

Manual sampling for dissolution studies can have several drawbacks. First, removing aliquots for sampling at various time points affects the total volume of the dissolution bath. If the volume is replaced after sampling, then the concentration in the bath is changed. Second, manual sampling is time consuming and labor-intensive, limiting the time points that can be collected in the early section of the curve. Third, transferring the aliquots of sample to another apparatus for concentration analysis can introduce error. In particular, for samples that need to be filtered to remove particle prior to HPLC analysis, the filtering process may affect the concentration of the aliquot, skewing the results of the experiment. For all these reasons, an in situ method is preferred. For this project, fiber optic UV probes were available to use with the dissolution bath, by placing the probes in the vessels at an appropriate height for sampling. The accompanying software was programmed to take many more points in every section of the curve, allowing for a more complete dissolution curve with minimal labor. A second-derivative function is built into the software to address concerns with un-dissolved particles in the solution. Table 7-1 shows aspects of the traditional dissolution method compared with the new dissolution method being developed.

Table 7-1. Components of Traditional dissolution method vs. New dissolution method

Traditional method	New method
Hand-mixing	Turbula mixing
Tablet weights uncontrolled	Adjust for tablet weight
Labor-intensive	Automated
Manual sampling	Direct sampling
Sample each time point	Multiple probes, more replicates
Volume corrections	In situ sampling
UV-vis spectrometer	Fiber optic probes
Need to filter samples	2nd derivative option

7.5.3 Calibration Curves Comparing UV-vis Spectrometer with UV Fiber Optic Probes

To confirm the reliability of the fiber optic probes, indomethacin calibration curves for the manual sampling method using UV-vis analysis were compared with calibration curves for the fiber optic UV probes. The absorbance of indomethacin was measured at 320 nm wavelength. As shown in Figure 7-3 both curves are linear through 30 μg/mL, with acceptable correlation coefficients for both curves. Additionally, the y-intercepts are close to zero for both curves. This data allows us to be confident in the ability of the fiber optic probes to provide acceptable quantitative analysis for our indomethacin tablets using the dissolution method.
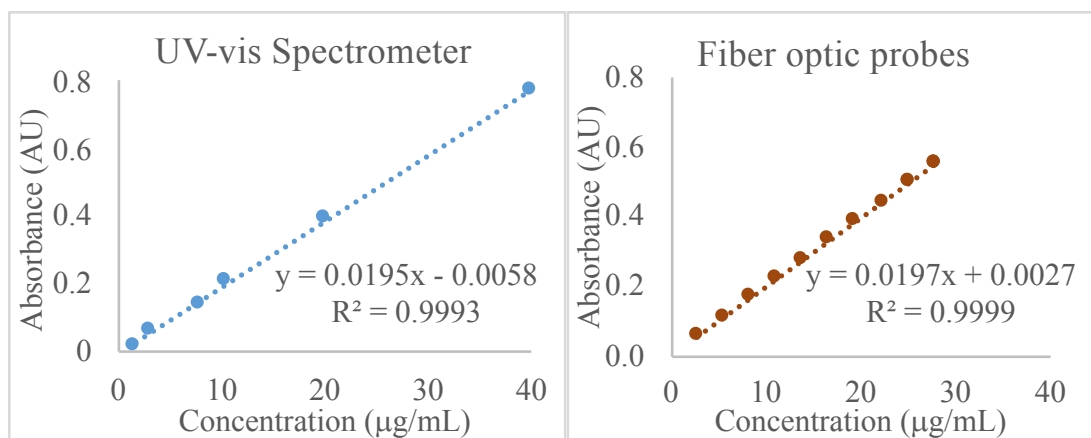
Figure 7-3. Indomethacin curves comparing data from UV-vis spectrometer and fiber optic UV probes.

7.5.4 Effect of MgSt Concentration in Indomethacin Tablet Formulations

The concentration of MgSt in the formulation is known to affect the performance of tablets, so this % of MgSt used in the formulation was varied to determine the effect in our dissolution method. Figure 7-4 compares tablet formulations containing 0.5%, 1%, 2% and 7% MgSt, using a commercial monohydrate MgSt designated "PG 193". Decreased dissolution was observed for increasing amounts of MgSt in the formulations, with 7% MgSt having less than 30% dissolution at 15 minutes. Clearly, the amount of MgSt in the formulation has an effect on dissolution. In order to promote over-lubrication in this study, a 2% level of MgSt was chosen for the formulation.
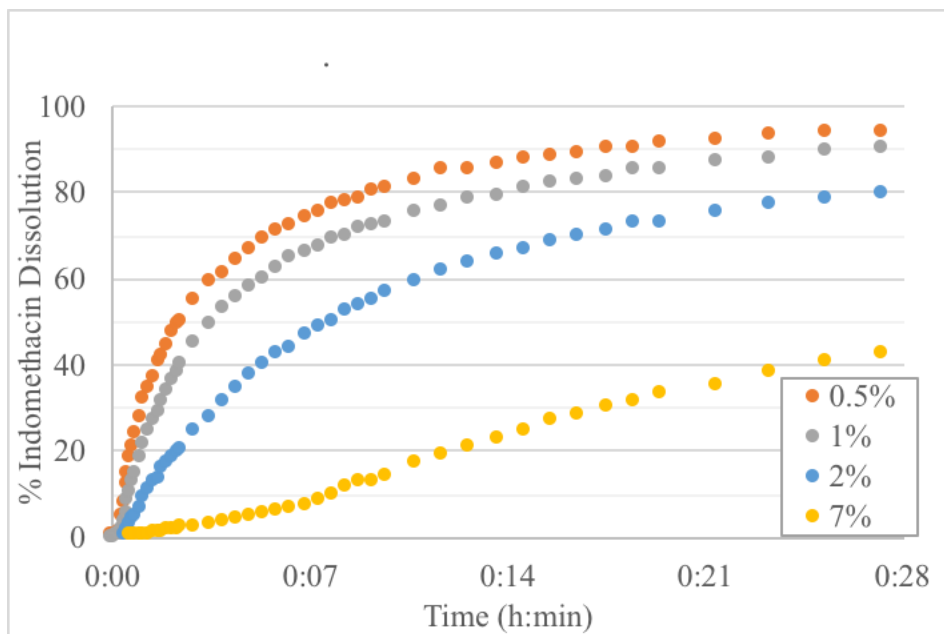
Figure 7-4. Effect of amount of MgSt on indomethacin tablet dissolution

7.5.5   Powder vs. Tablet Dissolution Profiles

As a control, dissolution was performed for samples containing no MgSt. Two different batches of premix powder and tablets were analyzed in triplicate, shown in Figure 7-5. The powder was observed to float on top of the buffer solution and dissolved slowly, due to poor wetting properties of the formulation components. The tablets sank to the bottom of the vessel and were observed to dissolve quickly. In order to investigate dissolution, rather than wetting, it was decided to focus on tablet dissolution rather than powder dissolution. The control with no MgSt shows the expected dissolution when MgSt is having no effect on tablet dissolution.
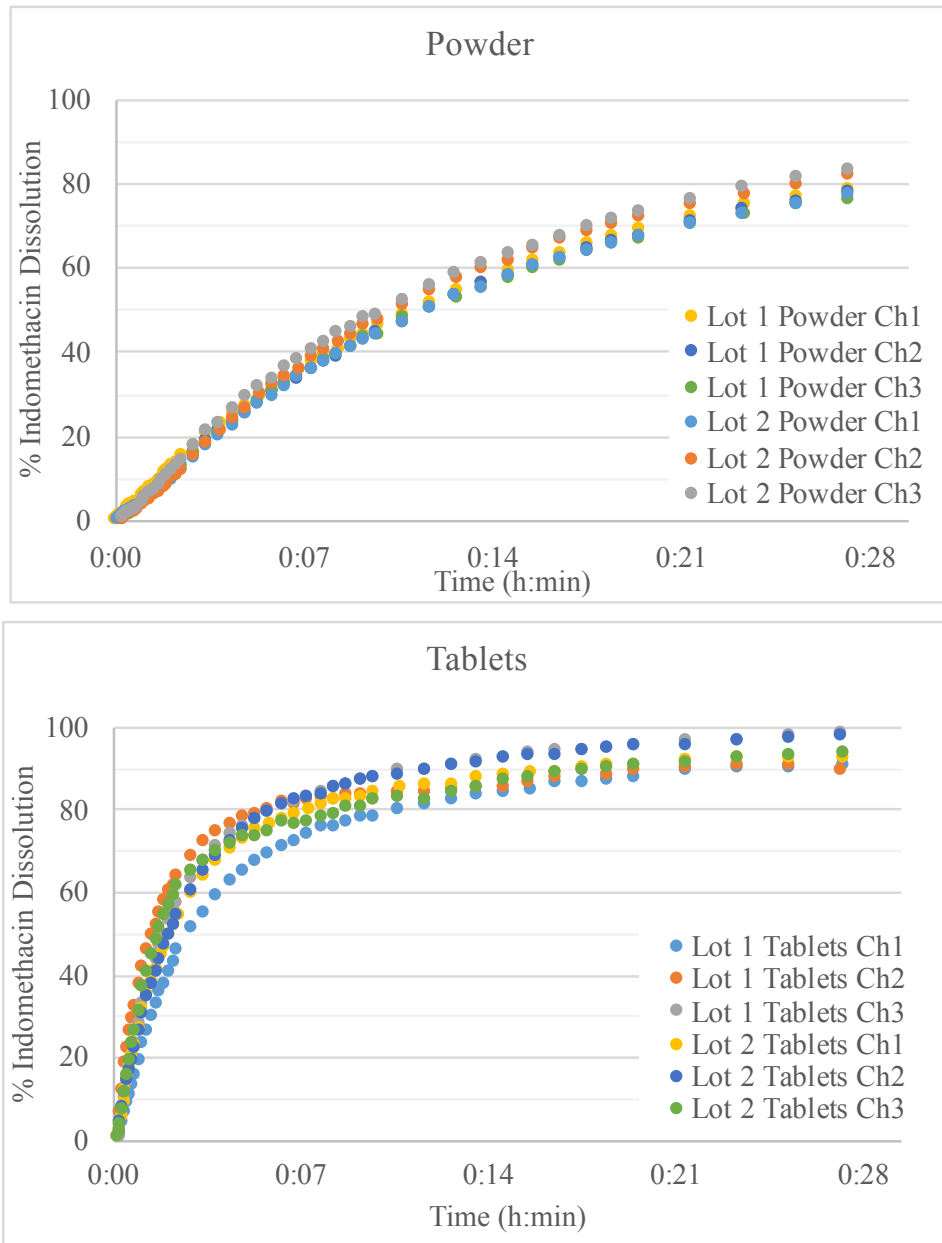
Figure 7-5. Indomethacin dissolution of premix formulation containing no MgSt, comparing powder (top) and tablets (bottom)

7.5.6 Effect of Tablet Compaction Pressure

Disintegration can also affect dissolution profiles for tablet formulations. In order to minimize the impact of disintegration on dissolution for the method here. Figure 7-6

shows the effect of compaction pressure on indomethacin tablet dissolution for Premix and tablets containing 2% MgSt from Acros. The effect of compaction pressure to delay disintegration and dissolution is seen in the first few minutes. Clearly, the Acros MgSt is causing a delay in both disintegration and dissolution, whereas the Premix only shows an effect on disintegration. The delay in dissolution due to disintegration is the relevant issue for method development. To minimize the effect of disintegration on dissolution, a low compaction pressure of 50 psi was chosen for tableting.

The solid fraction (SF) numbers show that for the premix tablets, the solid fraction is > 1. This indicates that, in the absence of MgSt, the lactose and/or Avicel is being compressed beyond the original density. However, the high solid fraction (i.e. more effective compression and likely greater hardness) does not prolong disintegration. Rather, the presence of MgSt is resulting in softer tablets and slower dissolution. This is due to the MgSt forming a hydrophobic film coating around the particles in the formulation, which has a two-fold effect. First, it keeps the formulation particles from interacting to compress like the non-lubricated particles would and second, it delays dissolution by slowing drug release from coated particles.
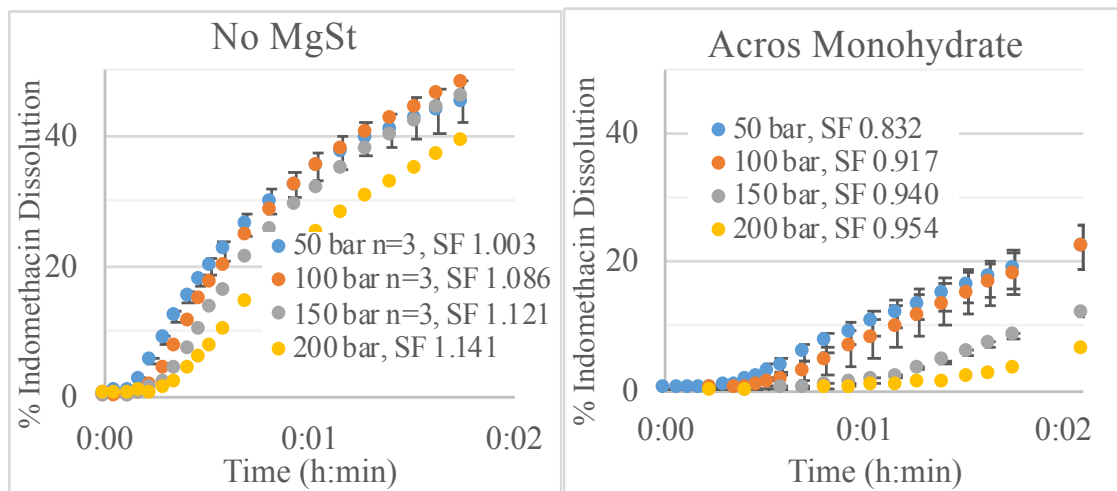
Figure 7-6. Dissolution of indomethacin tablets showing the effect of compaction pressure on disintegration and dissolution

7.5.7   Effect of Mixing Configuration and Turbula Speed

To test mixing configuration and Turbula mixing speed, three conditions were compared: a "slow-tumbling" condition where "slow" indicates a ~ 50-75 rpm setting on the Turbula, "fast" indicates ~ 100 rpm Turbula speed, and "tumbling" indicates a vial placed inside a plastic bottle to allow extra tumbling during the mixing process.

Figure 7-7 compares these three mixing conditions for a 10 min mixing time and 40 mL vial. All conditions were similar for the dihydrate formulations. However, the "fast-falling" condition was the most differentiating for the monohydrate. The "fast-falling" condition uses a 40 mL vial on the fast Turbula setting, and this is the condition used for subsequent dissolution testing.
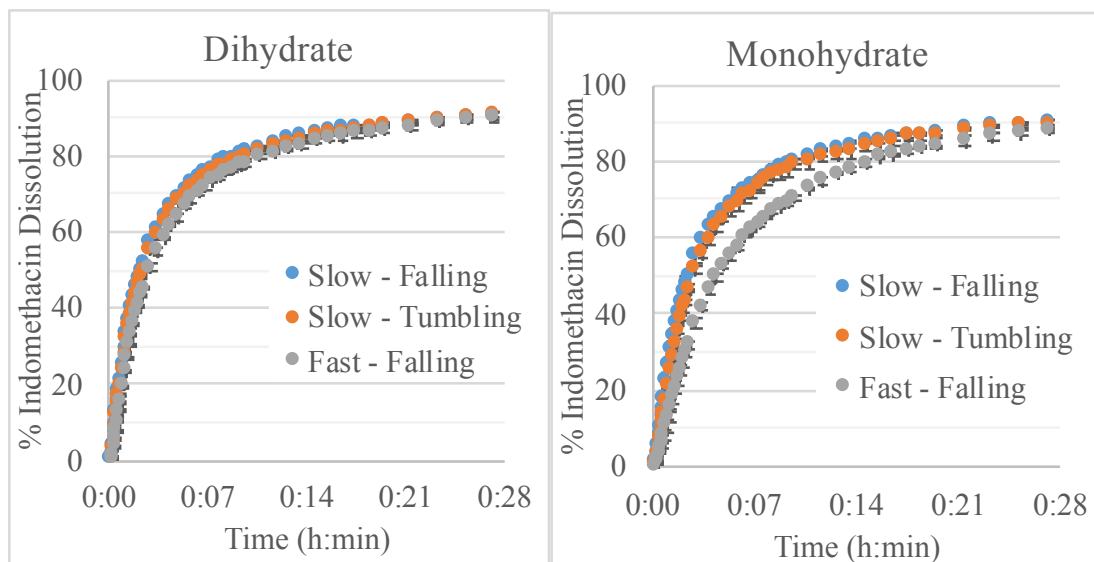
Figure 7-7. Dissolution of tablets containing lab-synthesized dihydrate and monohydrate MgSt, after mixing the formulation in various ways

7.5.8   Effect of Formulation Mixing Time on Dissolution

Another important factor in over-lubrication with MgSt is mixing time. Longer mixing times allows for a greater extent of surface coating of particles by MgSt, and this results

in slower dissolution. This effect of MgSt mixing time is well-documented in the literature.

Figure 7-8 shows the difference in dissolution as a function of mixing time. Monohydrate MgSt was compared with dihydrate MgSt after sieving to < 45 μm. The monohydrate MgSt shows greater sensitivity to over-lubrication compared to the dihydrate form of MgSt. A 60 minute mixing time was chosen as a standard mixing time for this method, to enable good discrimination between samples. This is significantly longer than the normal mixing time for formulation development and represents an over-lubricated state for many MgSt samples. As such, it enables our study to discriminate between MgSt samples which are sensitive to over-lubrication and those MgSt samples which are less sensitive to over-lubrication.
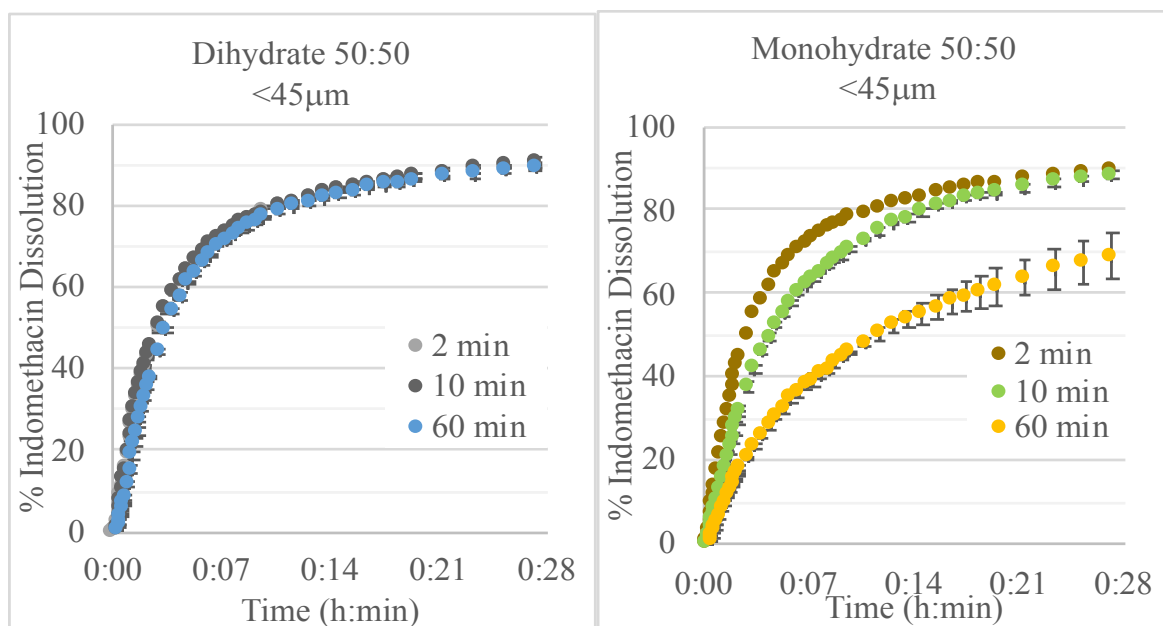
Figure 7-8. Effect of mixing time on MgSt dihydrate < 45 μm and MgSt monohydrate < 45 μm.

7.6   Conclusions

A discriminating dissolution method was developed to study the over-lubrication of indomethacin tablets using various lots of MgSt. Several different factors were

explored in the method development, including mixing method, sampling technique, the effect of MgSt concentration, compaction pressure, formulation mixing speed, formulation mixing time, reproducibility of the overall method and differentiation between samples. Using this method, differences between variations in properties of MgSt samples are addressed in Chapter 8.

7.7   Acknowledgements

CHAPTER 8.   THE IMPACT OF MGST VARIABILITY ON DISSOLUTION RATES: FATTY ACID COMPOSITION, CRYSTAL FORM, PARTICLE SIZE AND SURFACE AREA

8.1   Author Information

Julie L. Calahan, University of Kentucky, Lexington, KY

Daniel DeNeve, Purdue University, West Lafayette, IN

Evelyn G. Yanez, Genentech, Inc., South San Francisco, CA

Evan T. Liechty, University of Colorado, CO

Job K. Limo, Berea College, Berea, KY

Christopher J. Mays, Ross University, Dominica

Benjamin J. Munson, Eastern Kentucky University, KY

Jonathan Gerzberg, University of Michigan, MI

Kanika Sarpal, Vertex, Boston, MA

Job Lubach, Genentech, Inc., CA

Sean P. Delaney, US Pharmacopeia, Rockville, MD

Eric J. Munson, Purdue University, IN

8.2   Abstract

Magnesium stearate (MgSt) is a pharmaceutical excipient that is used in approximately half of all pharmaceutical tablet formulations. It is typically added as a lubricant prior to tableting to ensure proper ejection of the tablet from the press. The physicochemical properties of MgSt that have been proposed to impact lubrication and dissolution include fatty acid composition, crystalline form, and particle size and surface area. This study focuses on the dissolution properties of commercial and lab-synthesized MgSt samples. No obvious correlation between fatty acid composition and dissolution

performance was observed between commercial or lab-synthesized MgSt samples. However, higher surface area appeared to correlate with slower dissolution rate. Additionally, lab-synthesized samples showed that smaller particle size fractions correlated with slower dissolution compared to larger particle size fractions of the same starting material. A further effect of ball mixing was observed to slow dissolution rate for the disordered form, indicating the importance of processing effects by mixing and/or shearing.

8.3 Introduction

Magnesium stearate (MgSt) is the most commonly used excipient for pharmaceutical tablet formulations, with over half of the marketed formulations including MgSt as one of the formulation excipients.(1) MgSt is typically added to tablet formulations as a lubricant at a 0.25 - 5% level to prevent powder from sticking to the tablet die and manufacturing equipment during the tableting process. Many formulation labs have experiences with MgSt where the lubrication capability and/or the dissolution rate varies unexpectedly, with unexplained batch-to-batch and lot-to-lot variation.(16, 97) For example, one lot from a manufacturer may show picking and sticking after several thousand tablets are made as powder builds up on the equipment, but other lots do not. In addition, tablets manufactured from different lots of MgSt may have different dissolution properties. The reasons for the inconsistencies between lots and types of MgSt are still poorly understood, (149-151) but it is proposed that the variability in the dissolution and lubrication properties of MgSt can be related back to its complicated structural properties. (126, 154)

The physicochemical properties of MgSt that have been proposed to have the greatest effect on the functional properties of MgSt include fatty acid composition, crystalline form and particle size/surface area.(152) Magnesium stearate is historically derived from vegetable and animal sources, and is usually composed of a mixture of magnesium fatty acid salts, although in this paper the salts are also referred to as fatty acids. The USP monograph for MgSt specifies that magnesium stearate must contain at

least 40% stearate, with at least 90% being a combination of stearate and palmitate fatty acid salts.(19) The remaining 10% may be magnesium salts derived from other fatty acids, typically the C12-C22 straight-chain fatty acids.(19) A large variation in fatty acid salts can exist between magnesium stearate lots and samples, which may or may not be specified in the certificate of analysis from the manufacturer. Magnesium stearate also exists in multiple hydrate forms as well as an anhydrate form.(35, 155) The monohydrate and dihydrate forms have been reported and characterized by various techniques.(37, 39) Delaney et al. showed that there are at least five forms of MgSt, where solid-state NMR (SSNMR) spectroscopy was able to clearly distinguish between the five forms - an anhydrous form, a disordered monohydrate form, an ordered monohydrate, a dihydrate and a trihydrate.(48) Particle size and surface area have also been shown to impact performance.(151, 152, 156) In addition, some of these properties, such as particle size/surface area and crystalline form, may change upon blending time, tableting pressure and particle size reduction method and other processing operations.

Chapter 3, adapted from Delaney et al., describes a comprehensive analytical characterization of several commercial MgSt samples, where commercial refers to samples either purchased or obtained from various sources, as opposed to lab-synthesized samples. In that study, analytical techniques such as gas chromatography-mass spectrometry (GC-MS), scanning electron microscopy (SEM), differential scanning calorimetry (DSC), thermogravimetric analysis (TGA), powder X-ray diffraction (PXRD), and SSNMR were used to investigate the properties of these samples. (48) It was shown that SSNMR is very useful for identifying the crystalline form of the MgSt samples, and GC-MS could be used to characterize the fatty acid composition. However, the impact of these variables on the functional properties, specifically the lubrication and dissolution properties, was not investigated.

Dissolution is an important functional property for pharmaceutical formulations. It is known since 1963 that MgSt can cause slower dissolution of formulations(89) and that formulation mixing time, compression force, and amount of MgSt in the formulations can affect the dissolution rate(90, 91). The impact that MgSt has on dissolution rate is due to differences in mixing time and compression force was attributed to lamination and adhesion of MgSt to the other particles in the formulation, along with

the flaking of MgSt causing an increase in surface area.(90, 92) Hussain et al. suggested that the extent of surface coverage of the hydrophobic film on the particles is the most important factor in affecting dissolution.(83) Patra et al. studied the effect of MgSt concentration and granule size on the dissolution rate of ciprofloxacin HCl and found that a hydrophobic lubricant like MgSt decreases the drug-solvent interface, causing slower dissolution due to decreased wettability and increased dissolution rate with smaller granules.(93) The interactions of other formulation ingredients with MgSt have been explored for their effects on dissolution, including the addition of colloidal silica by Johansson et al.,(94) the interactions of surfactants with MgSt during mixing,(50) the interaction of MgSt with HPMC-AS in ASDs, and hydrogen bonding with itraconazole ASDs.(95, 96) The effect of acidic media was also investigated by Ariyasu et al., and their results indicated the conversion of MgSt to stearic acid during dissolution.(97, 98) Additionally, dissolution has been used to explore alternative lubricants for MgSt, including calcium stearate,(98) glycerin fatty acid esters,(99, 100) Stear-o-Wet,(101) and talc.(102) Hussain, York and Timmins compared the dissolution of paracetamol tablets with different grades of MgSt. Although marked differences between samples were noted, no clear relationship between physical properties of MgSt such as surface area and dissolution was defined. (83) In 2013, Okoye et al. observed differences in dissolution between naproxen and acetaminophen formulations comparing MgSt dihydrate, monohydrate and anhydrate. In their study, the monohydrate form slowed dissolution to a greater extent than the dihydrate and anhydrate forms of MgSt .(87) We hope to further this understanding of the effects of MgSt hydrate form on tablet dissolution with the aid of SSNMR characterization data.

This chapter will focus on the dissolution properties of both commercial and lab-synthesized MgSt samples. Dissolution was chosen as a discrimination method instead of lubrication, since formulated samples could be prepared at relatively small scales, and once the properties that impacted dissolution were identified, later studies could focus on their lubrication properties. It is important to note that the dissolution method developed for this study is only used to compare the performance of different MgSt samples. It was not designed for use in release testing, nor for meeting USP or product specifications, nor for correlations with bioavailability, but is specifically for discriminating between MgSt

lots used in tablet formulations. For this study, a simple direct compression tablet formulation comprised of 16.7% indomethacin, 35% microcrystalline cellulose, 47% lactose, and 2% MgSt was prepared with different MgSt samples, and the processing parameters (e.g. mixing time and compression forces) were optimized such that the dissolution data showed differences between MgSt samples. Each of the MgSt commercial samples characterized previously in the Delaney paper was analyzed here by dissolution.(11, 48) The commercial samples showed that the disordered form of MgSt leads to a faster dissolution rate than formulations prepared with the other MgSt hydrate forms. No clear correlation with fatty acid composition was observed, but lower surface area appeared to correlate with faster dissolution rate and higher surface with slower dissolution rates. Additionally, lab-synthesized samples showed that smaller particle size fractions correlated with slower dissolution compared to larger particle size fractions of the same material. A further effect of ball mixing was observed to slow dissolution for the disordered form.

8.4   Materials and Methods

8.4.1   Materials

Magnesium hydroxide was purchased from Fluka (St. Louis, MO). Stearic acid and palmitic acid were purchased from TCI (Tokyo, Japan). Magnesium chloride hexahydrate was purchased from EMD (Darmstadt, Germany). Phosphate buffer was prepared from sodium phosphate monobasic and sodium hydroxide, purchased from purchased from BDH Analytical (Radnor, PA). Tablet excipients Avicel (microcrystalline cellulose, MCC) and alpha-Lactose monohydrate were obtained as a complimentary sample from FMC Biopolymer (Philadelphia, MA) and purchased from Sigma (St. Louis, MO), respectively. The sources of the commercial samples were reported previously.(48)

8.4.2 MgSt Synthesis

Magnesium stearate lots were synthesized in a range of fatty acid ratios, notated using either "% stearate" or "St:Pa" to indicate the stearic acid: palmitic acid (St:Pa) ratio. Two synthesis methods were used: 1) a "melt method" combined magnesium hydroxide and water with melted stearic and palmitic acids at 70-90 °C, in a spontaneous reaction producing magnesium stearate. 2) a "bath method" dissolved the fatty acids in a heated water bath, to which ammonium hydroxide was added to create the ammonium soap, followed by a titration with magnesium chloride to precipitate out the magnesium stearate solid. These methods are described in greater detail in Chapter 4. In each case, the recovered solids were washed using a reflux bath of 1:1 acetone: water for 24-48 hours to remove impurities and unreacted starting materials. The MgSt samples were air-dried and/or dried in a vacuum oven at 25 °C to remove surface water. The disordered form was prepared by heating a dihydrate or monohydrate-dihydrate mixture to 105 °C for 48 hours. LS 1 "rehydrated" monohydrate was dehydrated and then the disordered sample was rehydrated by heating to 105 °C for 1 hour, then placing the sample in a humidity chamber at 105 °C for 24 hours. The dehydration/rehydration process produced a mixture of monohydrate with disordered forms, which appears as mostly monohydrate by SSNMR.

8.4.3 Mixing, Tableting and Sieving

MgSt tablets were prepared by adding MgSt sample to a "Premix" mixture containing 16.7% indomethacin (Sigma, St. Louis, MO), 50% alpha-lactose monohydrate (Sigma, St. Louis, MO), 33.3% Avicel (FMC Biopolymer, Philadelphia, PA) in a ratio of 2:98 MgSt: Premix. The tablet powders were mixed as 1 g batches in 40 mL glass vials for 60 minutes using a Turbula T-2C mixer (WAB, Basel, Switzerland) on the highest setting. Six individual 150 mg tablets were made from each 1 g formulation batch and pressed using a single tablet press (Globe Pharma, North Brunswick, NJ) at 50 bar for 30

seconds. The tablet weights were recorded and the dissolution results were adjusted for tablet mass. Ball mixing was performed by adding 1g of MgSt to a 40 mL glass vial with 10 ¼ inch plastic balls and mixed for 60 minutes using the Turbula T-2C mixer. MgSt samples were sieved on a Gilson Performer Model SS-3 sieve shaker for approximately 60 minutes, using ASTM sieves that range between 20 μm and 250 μm sieve sizes.

8.4.4 Dissolution

Dissolution was performed by placing each tablet in 900 mL of pH 7.2 phosphate buffer at 37 °C using a VanKel V7000 USP method 2 dissolution apparatus (Varian, Cary, NC). The paddles were stirred at 100 rpm. μDISS fiber optic UV probes (pION, Billerica, MA) were used to collect data at various time points from 0 - 120 minutes and processed using UV absorbance at 320 nm. The μDISS probes were calibrated using indomethacin in potassium phosphate buffer. The dissolution data was processed using the second derivative function to eliminate the effects of particles on the UV absorbance reading.

8.4.5 Solid-state NMR Spectroscopy (SSNMR)

^{13}C CP/MAS and ^{1}H T_1 relaxation data were collected using a home built Tecmag Redstone NMR Spectrometer (Houston, TX), Bruker 400 MHz magnet (Billerica, MA), and Chemagnetics (Ft. Collins, CO) NMR probe with 7.5 mm rotors spinning at 4000 Hz. A relaxation delay of 12 s was used with 2K acquisition points and 1024 scans. TNMR software (Houston, TX) was used to process the data. 3-methylglutamic acid was used as a reference standard, with the methyl peak referenced to 18.84 ppm.

8.4.6 Thermogravimetric Analysis (TGA)

TGA weight loss was measured using TA Q50 (TA Instruments, Newcastle, DE) with a 10 °C/minute ramp from 25 °C to 250 °C.

8.4.7   Gas Chromatography-Mass Spectroscopy (GC-MS)

MgSt samples were derivatized using a boron trifluoride-methanol procedure to convert the acids to their methyl derivatives. An Agilent 7890A GC with 5975C Mass Spec Component and 7693 autosampler was used with an HP-5 capillary column (30 m 0.320 mm bore 0.25 mm Film) and helium carrier gas at 0.9 mL/min flow rate. A 48-min program was used, with an injection temperature of 270 °C. The oven temperature was held at 70 °C for 2 min, then ramped up at 5 °C /min to 240 °C, held for 5 min, then ramped at 10 °C /min to 260 °C and held for 5 min. Data were collected using the Agilent ChemStation software, and was processed using OpenChrom software with the Agilent plugin. The identity of fatty acid derivative peaks was confirmed based on MS spectra using the NIST database.

8.4.8   Surface Area Analysis

Surface area analysis was conducted using a Micromeritics ASAP 2460 with a Micromeritics Smart Vac Prep attachment (Micromeritics Instrumentation Corporation, Norcross, GA, USA). A sample of about 1000 mg was dried at 40 °C and outgassed under nitrogen flow conditions. Krypton adsorption-desorption isotherms were recorded at liquid nitrogen temperatures (77K) and specific surface area was calculated by the Brunauer-Emmett-Teller (BET) method. Data was analyzed using Micromeritics MicroActive version 5.0 software.

8.5   Results

8.5.1   Control and Reproducibility of the Dissolution Process

In order to ensure that the dissolution data could be used to discriminate between samples, it was critical that the formulation, processing, and testing of the tablet dissolution was both extremely reproducible and gave consistent results. We found that the formulation mixing process and the dissolution measurement conditions were the critical aspects of the testing process that impacted dissolution rate, as discussed in Chapter 7. This method was used to investigate all the samples described here.

The mixing process was standardized by using an automated Turbula mixer. Kushner and co-workers have published a comprehensive comparison of the properties of a Turbula mixer and the formula necessary to translate results from a Turbula mixer to larger scale mixing equipment. (54) As Kushner has noted, the Turbula mixer does not represent the more common V-mixer blending used in many formulation labs, but it does provide a consistent and reproducible blending process. Because the Turbula mixer is a small-scale mixer, it likely does not produce the same shear forces as would be used on a manufacturing scale. For this reason, a longer mixing time is required to achieve the same shear effect with formulations containing MgSt. To accentuate differences between lots and batches, a 60-minute mixing condition was chosen as the standard method for the remaining dissolution studies. This is probably on the extreme edge of the Turbula mixing reported in the Kushner paper, but was chosen to enhance differences in the variability of the MgSt samples, and not necessarily to correlate with scale-up to larger batches.

All of the conditions for the dissolution measurement were standardized and found to be reproducible for replicate tablet formulations from the same lot when processed in the same way. Figure 8-1 shows the reproducibility of dissolution data for three commercial samples for multiple runs of the same sample. Six separate formulation samples were prepared from each lot and 3 tablets were prepared from each formulation, making a total of 18 tablets per lot. Our method shows RSD < 10% for replicate samples in each lot, as indicated by the error bars. There is also significant differentiation between

the three commercial lots presented in Figure 8-1. These three commercial samples have differences in their physicochemical properties (hydrate form, fatty acid composition and particle size) which may contribute to the observed differences in dissolution.(154, 157)
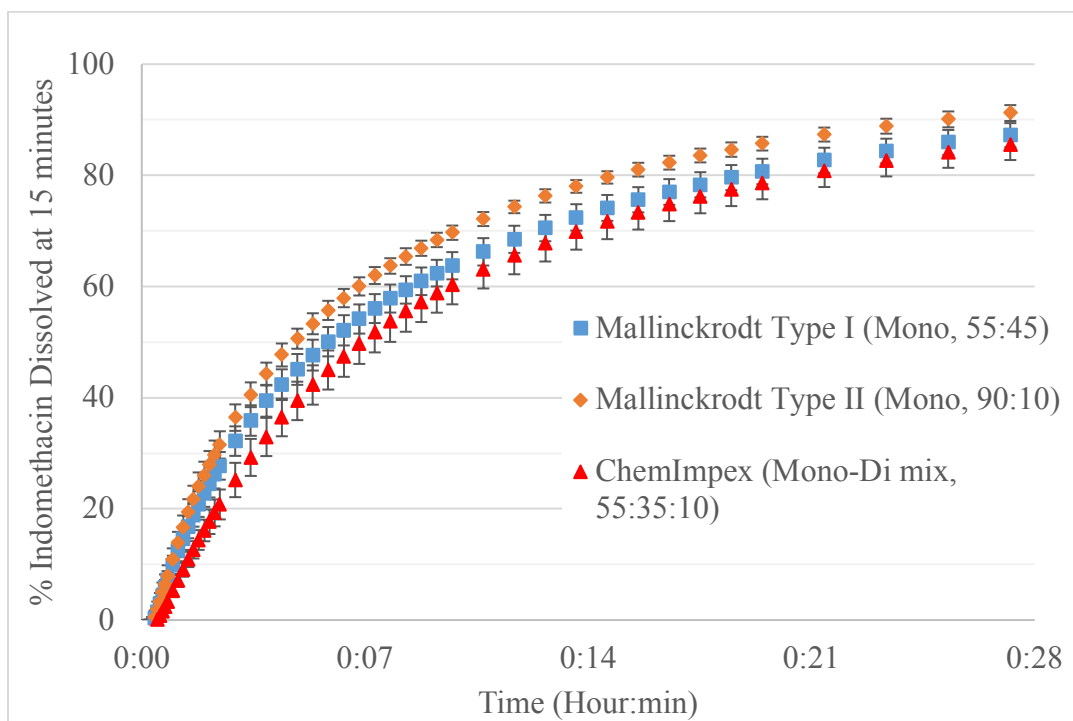
Figure 8-1. Dissolution of three commercial samples (n=18) shows reproducibility for multiple runs of each sample. Commercial lots are from Mallinckrodt 1726, Mallinckrodt 5712 and Chem-Impex suppliers, listed from fastest to slowest dissolution.

8.5.2   Variation in Dissolution using Commercial Samples

Figure 8-2 shows the dissolution profiles for eight commercial samples, all of which had been previously characterized in the literature, including determining the crystalline form from the carbonyl peak in the ^{13}C SSNMR spectrum.(48) For these samples, our dissolution method shows a tight RSD <10% for triplicate samples, as

indicated by the error bars in Figure 8-2. All the samples indicate > 95% dissolution in less than 2 hours, with most of dissolution occurring within 30 minutes.
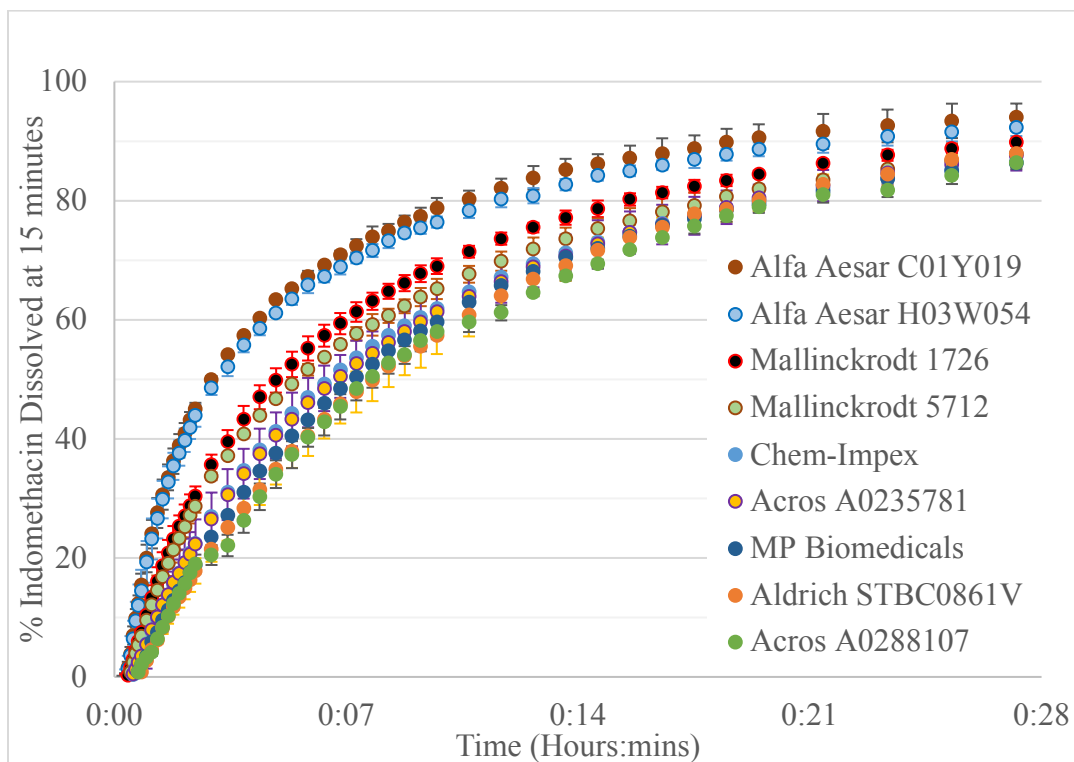
Figure 8-2. Dissolution of indomethacin tablets containing MgSt from several different commercial suppliers. Listed from fastest to slowest dissolution: Alfa Aesar Lot C01Y019, Alfa Aesar Lot H03W054, Mallinckrodt 1726, Mallinckrodt 5712, Chem-Impex, Acros Lot A0235781, MP Biomedicals, Aldrich Lot STBC0861V, Acros Lot A0288107.

The commercial samples in Figure 8-2 were evaluated with respect to how their physicochemical properties related to dissolution. Previous studies have suggested that the dissolution performance may be related to different crystalline forms, chemical composition and/or particle size. Accordingly, crystal form, fatty acid composition, particle size, surface area and dissolution rate characterization data for these samples are indicated in Table 8-1. For commercial MgSt samples, it can be particularly challenging to define the properties of the sample, since the sample preparation and manufacturing process of the samples is largely unknown, aside from what may be listed in a certificate

of analysis from the manufacturer. In particular, the processing is unknown, including how the materials were prepared and the extent to which the particles were milled. Both of these types of processing can affect the dissolution.

Table 8-1. Physicochemical properties of MgSt commercial samples: Crystal form, fatty acid composition, surface area and dissolution

Supplier	Crystal Form	Fatty Acid Composition	Surface Area (m^2/g)	% Dissolution at 15 min
Alfa Aesar Lot 019	Disordered	64:27:9	0.77	86.1
Alfa Aesar Lot 054	Disordered	66:28:6	0.89	84.2
Mallinckrodt 1726	Monohydrate-dihydrate	90:10	2.83	78.6
ChemImpex	Monohydrate-dihydrate	55:35:10	3.78	73.1
MP Biomedical	Monohydrate-dihydrate	58:36:6	3.83	72.0
Acros Lot 107	Monohydrate-dihydrate	64:34:2	3.92	69.3
Sigma-Aldrich	Monohydrate-dihydrate	63:34:3	4.17	71.6
Mallinckrodt 5712	Monohydrate	55:45	4.31	75.3
Acros Lot 781	Monohydrate	63:35:2	6.02	72.7

A significant correlation between the disordered form and fast dissolution was observed. The two lots with the fastest dissolution are from Alfa Aesar, with 84 - 86% dissolution at 15 minutes. The Alfa Aesar lots shown in Figure 8-2 have a disordered crystal form, and indomethacin tablets made with these MgSt samples had the fastest dissolution. There is a large variability between the rest of the commercial samples, with dissolution from 69 - 79% at 15 minutes. As indicated in Table 8-1, these samples are

monohydrate and monohydrate-dihydrate mixtures by SSNMR. It is difficult to draw any further conclusions about the relationship between MgSt crystal form and dissolution with these commercial samples, largely because crystal form appears not to be the only variable affecting dissolution. Fatty acid composition and surface area also need to be investigated for correlation with dissolution rate.

8.5.3   Effect of Fatty Acid Composition on Indomethacin Tablet Dissolution

In addition to analyzing the commercial MgSt samples, and in order to better elucidate the effects of fatty acid composition, crystalline form and particle size/surface area on dissolution rate, additional MgSt samples were synthesized under controlled conditions to enable better control and identification of each of these properties individually. Table 8-2 lists these lab-synthesized samples and their properties. Specifically, the fatty acid composition (stearate: palmitate ratio) was controlled by the fatty acids used in synthesis and the crystal form was identified by ^{13}C SSNMR. To assess the influence of particle size within an individual sample, the sample was sieved into different size sieve fractions prior to preparing the formulations. For comparison between samples, the MgSt surface area was measured using BET adsorption analysis.

Figure 8-3 shows the % stearate for each commercial and lab-synthesized samples plotted against % dissolution at 15 minutes. Since the USP monograph for magnesium stearate specifies a range of acceptable fatty acid content for MgSt samples, chemical composition was evaluated as a potential important variable affecting functional properties such as dissolution. There does not appear to be an obvious correlation between fatty acid composition and dissolution, especially for the samples with stearate concentrations below 70%. In an attempt to control particle size, several lab-synthesized samples were sieved to a 75 – 125 μm sieve fraction, shown in Figure 8-4 and listed in Table 8-3. No correlation with fatty acid content was apparent for the commercial samples and unprocessed lab-synthesized samples.

The fatty acid content was measured for the commercial samples using GC-MS analysis, and the fatty acid ratio used in synthesis was used for the lab-synthesized samples. While fatty acid composition for the commercial samples was measured with a GC-MS extraction method using boron trifluoride, the composition of the lab-synthesized samples is defined from the acids used in synthesis, since the stearate and palmitate are chemically independent molecules and do not interconvert. That is, after the synthesized samples are prepared and dried, the fatty acid ratio is fixed for the samples. In a separate study (data not shown), some of the lab-synthesized MgSt samples were analyzed by GC-MS and found to have the same fatty acid ratio as used in preparation.
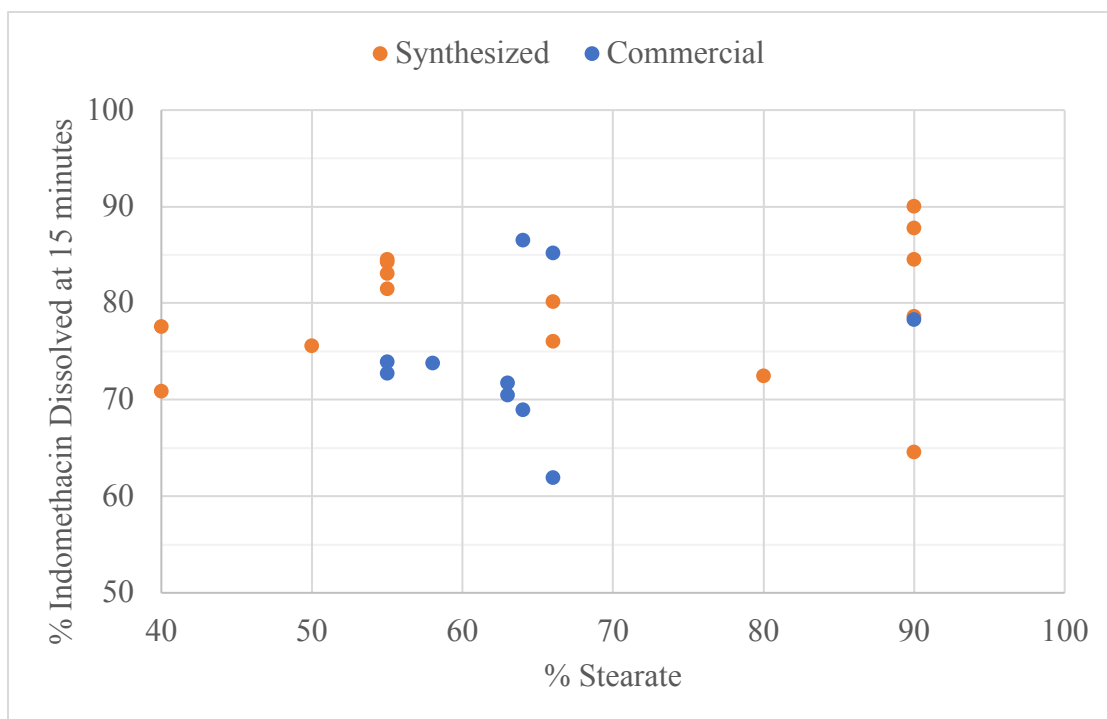
Figure 8-3. Dissolution of tablet formulations as a function of chemical composition (% stearate). Indomethacin tablet formulations were prepared containing different samples of MgSt from either commercial or lab synthesized sources.
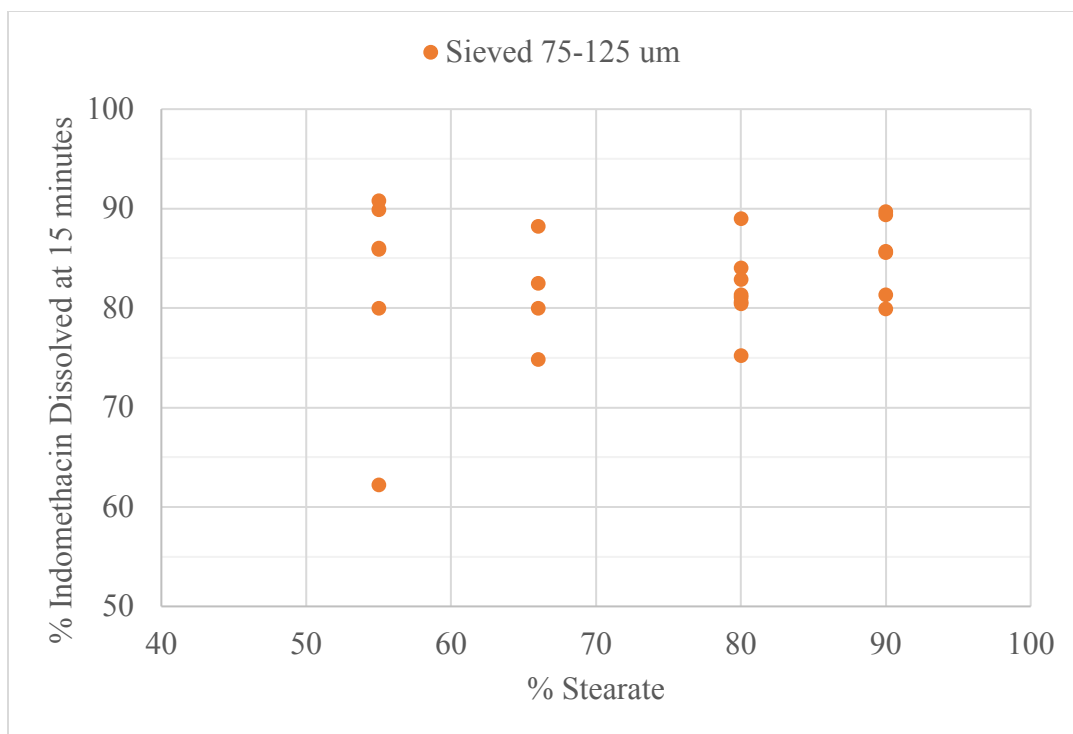
Figure 8-4. Dissolution of tablet formulations containing different samples of MgSt with 75-125 μm sieve fraction, as a function of chemical composition (% stearate)

8.5.4   Effect of Crystal Form on Indomethacin Tablet Dissolution

Figure 8-5 shows the effect of crystal form on dissolution for a few dozen commercial and lab-synthesized samples of MgSt, listed in Table 8-4. Monohydrate, dihydrate, trihydrate and disordered forms are compared. The dissolution observed for these lab-synthesized MgSt samples for each form is shown, ranging from 65 – 92% for monohydrate, 73 – 90% for dihydrate, 71 – 92% for trihydrate and 75 – 89% for disordered. Overall, it appears inconclusive that crystal form alone has a strong correlation with dissolution.
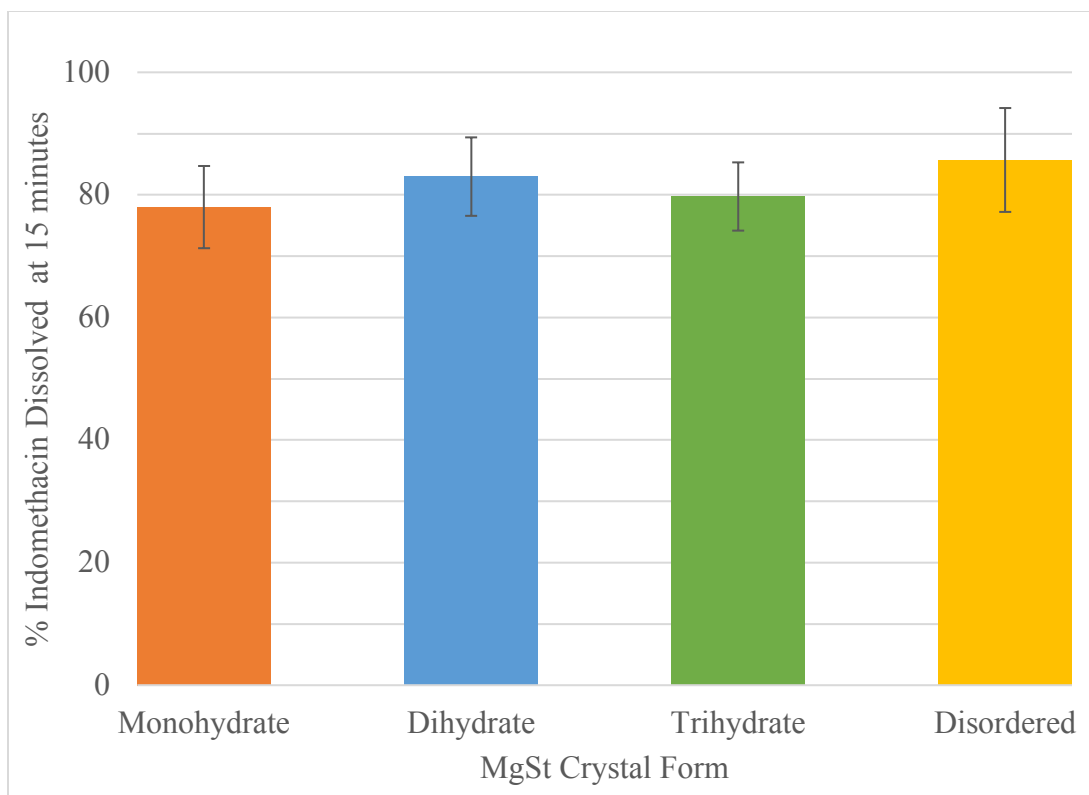
Figure 8-5. Comparison of tablet dissolution using different lab-synthesized crystal forms of MgSt

8.5.5 Effect of Particle Size and Surface Area on Indomethacin Tablet Dissolution

To investigate the effect of particle size on dissolution rate, a single sample of MgSt was sieved into different sieve fractions sizes and the dissolution rates were measured for formulations prepared using each sieve fraction. A pure monohydrate sample with 55:45 stearate: palmitate chemical composition, was used for this purpose. Figure 8-6 shows the dissolution rate of indomethacin tablets prepared using various sieve fractions. There is a clear effect of particle sieve size on dissolution rate when the crystalline form and fatty acid composition are controlled. For example, the particle size sieve fraction of 20-45 μm shows 67.8% dissolution at 15 minutes, where the 125-250 μm sieve fraction shows 86% dissolution at 15 minutes. As indicated by the error bars in

Figure 8-6, there is good reproducibility in the dissolution rates between formulation batches prepared from the same lot.
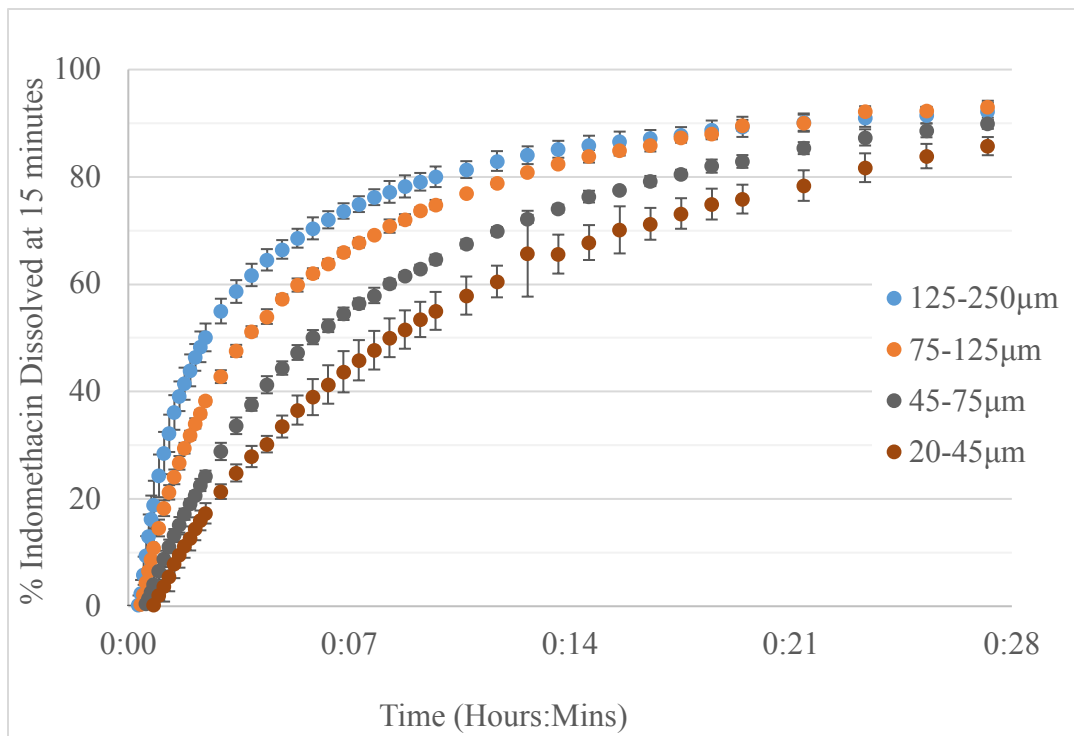
Figure 8-6. Effect of Particle Size for MgSt Monohydrate 55:45. Dissolution of indomethacin tablet formulations using MgSt of various particle size sieve fractions.

Figure 8-6 addresses the size of MgSt particles within a sample, and surface area was used to assess whether this trend holds between samples. Surface area was determined to be the most relevant measure of particle size for the purposes of dissolution, since it is the surface of the particles that is affected by the hydrophobic film coating of MgSt around the particles. Additionally, surface area eliminates differences based on agglomeration and particle morphology, which may differ significantly between the monohydrate and dihydrate forms.

Figure 8-7 showed a clear relationship between tablet dissolution and MgSt surface area for the commercial MgSt samples. A regression line drawn through the dissolution-surface area points shows a r^2 value of 0.74, as in Figure 8-8, indicating a

possible relationship with other factors, such as crystal form. In order to discern whether MgSt crystal form impacts dissolution rate, additional lines were drawn, separating the points corresponding to the different crystal forms. Interestingly, the surface area-dissolution relationship for the five monohydrate samples has a $r^2 = 0.97$. To confirm the relationships for all the forms, additional surface area-dissolution data for the different MgSt crystal forms is needed. While surface area is clearly the primary impact on dissolution between MgSt samples, additional studies separating out the effects of MgSt crystal forms will confirm (or deny) the secondary impact of MgSt crystal form on dissolution. Additional studies are needed to confirm the correlation of surface area and dissolution with crystal form.
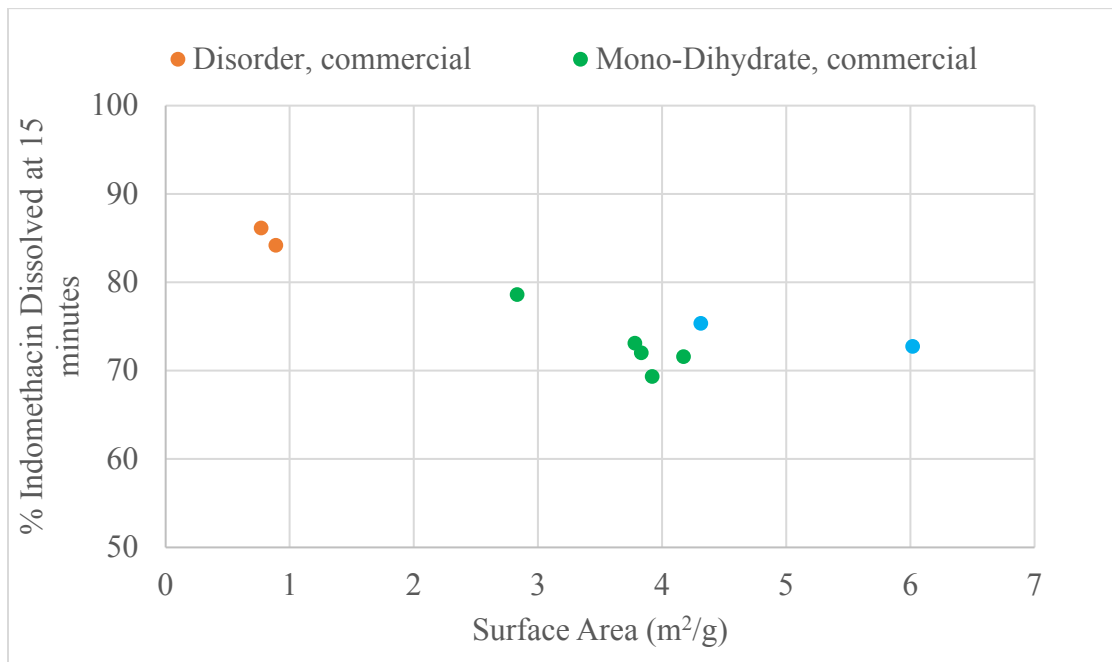
Figure 8-7. Correlation of surface area with dissolution for formulations containing commercial MgSt.
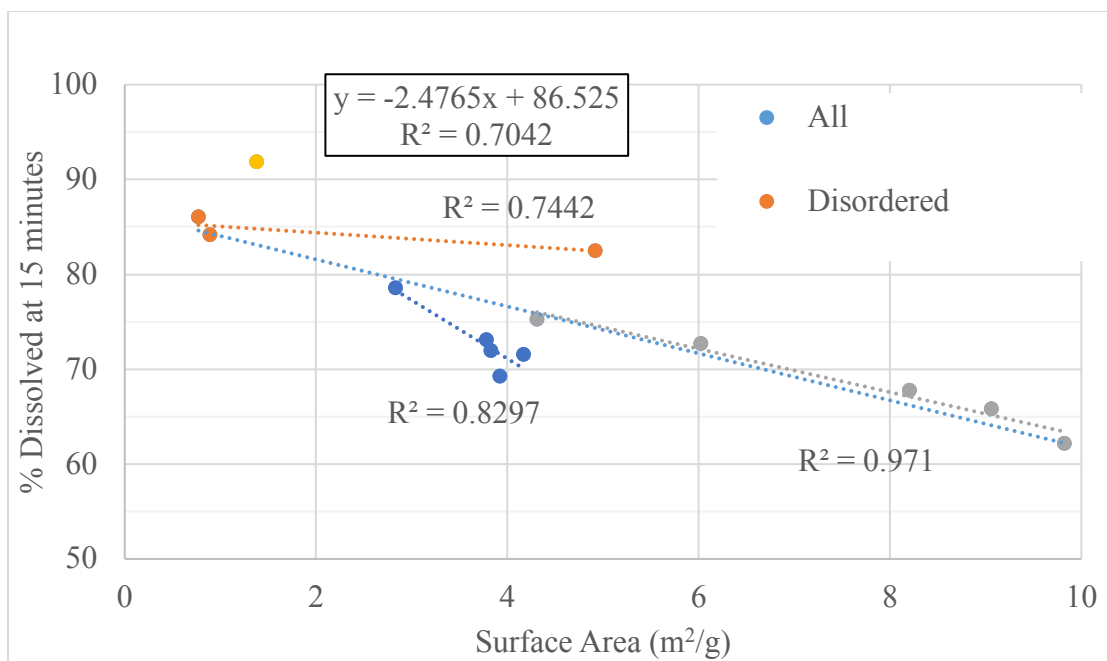
Figure 8-8. Correlation of surface area with dissolution for tablet formulations containing various samples of MgSt. Trend lines are added corresponding to the MgSt crystal forms present in the samples.

In summary, no relationship between fatty acid composition and dissolution is apparent. However, there does appear to be a correlation between surface area and dissolution, with a possible secondary effect of crystal form on dissolution rates. Additional studies are needed to confirm the correlation of surface area and dissolution with crystal form.

Table 8-2. List of lab-synthesized and commercial MgSt samples with physicochemical properties, used for Dissolution – Fatty Acid graph in Figure 8.3

Source	NB#/Lot#	Form by SSNMR	St	Pa	% Disso at 15min
Lab Synth	SD1-6	Trihydrate	40	60	70.9
Lab Synth	SD1-7	Di, tri	40	60	77.6
Lab Synth	CM1-71	Monohydrate	50	50	75.6
Lab Synth	BM1-20	Mono, di	55	45	83.1
Lab Synth	BM1-22	Mono, di	55	45	84.6
Lab Synth	JC3-52 melt	Mono, di	55	45	84.3
Lab Synth	JC3-58 bath	Di, tri	55	45	81.5
Lab Synth	CM1-14	Monohydrate	66	34	80.2
Lab Synth	CM1-95	Dihydrate	66	34	76.1
Lab Synth	MS1-07	Dihydrate	80	20	72.5
Lab Synth	JC3-51 melt	Di, tri	90	10	78.7
Lab Synth	JC3-56 melt	Mono, di	90	10	90.1
Lab Synth	JC4-49B	Monohydrate	90	10	64.6
Lab Synth	SD1-17	Dihydrate	90	10	87.8
Lab Synth	SD1-83 bath	Dihydrate	90	10	84.6
Commercial	ChemImpex	Mono, di	55	35	72.8
Commercial	Mallinckrodt 5712	Monohydrate	55	45	74.0
Commercial	MP Biomedicals	Di, mono	58	42	73.8
Commercial	Sigma Lot STBB0861V	Mono, di	63	37	70.5
Commercial	Acros Lot 781	Monohydrate	63	37	71.8
Commercial	Acros Lot 107	Mono, di	64	36	69.0
Commercial	Alfa Aesar 019	Disorder	64	36	86.6
Commercial	PG 315377	Mono, di	66	34	62.0
Commercial	Alfa Aesar 054	Disorder	66	34	85.2
Commercial	Mallinckrodt 1726	Mono, di	90	10	78.4

Table 8-3. List of lab-synthesized samples, sieved to 75 – 125 μm, with physicochemical properties used for Figure 8.4

Source	NB#/Lot#	Form by SSNMR	St	Pa	Disso % at 15min
Commercial	ChemImpex	Mono, di	55	35	72.8
Lab Synth	JC3-76 75-125 μm	Monohydrate	50	50	81.3
Lab Synth	JC4-45 75-125 μm	Mono, di	50	50	77.2
Lab Synth	JC4-47 75-125 μm	Mono, di, tri	50	50	77.2
Lab Synth	JC4-51 75-125 μm	Monohydrate	50	50	76.7
Lab Synth	JC4-53 75-125 μm	Monohydrate	50	50	77.5
Lab Synth	JC4-55 75-125 μm	Monohydrate	50	50	71.3
Lab Synth	SD1-9 75-125 μm	Trihydrate	50	50	76.6
Lab Synth	BM1-1 75-125 μm	Monohydrate	55	45	78.6
Lab Synth	BM1-10 75-125μm	Mono, di, tri	55	45	75.1
Lab Synth	BM1-19 75-125μm	Monohydrate	55	45	72.7
Lab Synth	BM1-21A 75-125μm	Monohydrate	55	45	72.0
Lab Synth	BM1-21 75-125 μm	Trihydrate	55	45	83.8
Lab Synth	BM1-24 75-125μm	Mono, di	55	45	70.2
Lab Synth	BM1-25 75-125μm	Mono, tri	55	45	70.2
Lab Synth	BM1-4 75-125 μm	Monohydrate	55	45	81.1
Lab Synth	BM1-6 75-125 μm	Monohydrate	55	45	91.4
Lab Synth	JC4-37 75-125 μm	Mono, di	66	34	82.5
Lab Synth	JC4-39A 75-125 μm	Dihydrate	66	34	78.7
Lab Synth	JC4-41 75-125 μm	Monohydrate	66	34	74.7
Lab Synth	JC4-43A 75-125 μm	Mono, di	66	34	63.8
Lab Synth	MS1-13 75-125μm	Dihydrate	80	20	77.2
Lab Synth	SD1-23 75-125μm	Dihydrate	80	20	81.2
Lab Synth	BM1-12 75-125μm	Dihydrate	90	10	77.9
Lab Synth	BM1-15 75-125μm	Mono, di	90	10	77.0

Table 8-4. List of Lab-synthesized MgSt samples with physicochemical properties, used for Dissolution – Crystal Form graph

Source	NB#/Lot#	SSNMR Form	% Disso at 15min
Lab synthesized mono	CM1-71	Monohydrate	75.6
Lab synthesized mono	CM1-14	Monohydrate	80.2
Lab synthesized mono	JC4-49B	Monohydrate	64.6
Lab synthesized mono	JC3-76 75-125μm	Monohydrate	81.3
Lab synthesized mono	JC4-53 75-125 μm	Monohydrate	77.5
Lab synthesized mono	JC4-51 75-125 μm	Monohydrate	76.7
Lab synthesized mono	JC4-55 75-125 μm	Monohydrate	71.3
Lab synthesized mono	BM1-19 75-125μm	Monohydrate	72.7
Lab synthesized mono	BM1-4 75-125 μm	Monohydrate	81.1
Lab synthesized mono	BM1-6 75-125 μm	Monohydrate	91.4
Lab synthesized mono	BM1-1 75-125 μm	Monohydrate	78.6
Lab synthesized mono	JC4-41 75-125 μm	Monohydrate	74.7
Lab synthesized mono	JC4-37 75-125 μm	Monohydrate	82.5
Lab synthesized mono	CM1-16 < 45 μm	Monohydrate	84.0
Lab synth dihydrate	JC3-1A > 45 μm	Dihydrate	86.9
Lab synth dihydrate	JC3-59 bath	Dihydrate	87.0
Lab synth dihydrate	JC3-37A 75-125 μm	Dihydrate	88.9
Lab synth dihydrate	CM1-95	Dihydrate	76.1
Lab synth dihydrate	MS1-07	Dihydrate	72.5
Lab synth dihydrate	SD1-17	Dihydrate	87.8
Lab synth dihydrate	SD1-83 bath	Dihydrate	84.6
Lab synth dihydrate	NW1-33 75-125 μm	Dihydrate	87.9
Lab synth dihydrate	JC4-39A 75-125 μm	Dihydrate	78.7
Lab synth dihydrate	MS1-13 75-125 μm	Dihydrate	77.2
Lab synth dihydrate	SD1-23 75-125 μm	Dihydrate	81.2
Lab synth dihydrate	BM1-12 75-125μm	Dihydrate	77.9
Lab synth dihydrate	BM1-17 125-250 μm	Dihydrate	89.4
Lab synth dihydrate	JC4-49A1 125-250	Dihydrate	85.6
Lab synth trihydrate	JC3-6B	Trihydrate	92.4
Lab synth trihydrate	JC3-53AA 75-125μm	Trihydrate	75.0
Lab synth trihydrate	SD1-6	Trihydrate	70.9
Lab synth trihydrate	SD1-9 75-125 μm	Trihydrate	76.6
Lab synth trihydrate	BM1-21 75-125 μm	Trihydrate	83.8

Table 8.4 continued

Lab synth Disordered	JC4-16A 75-125μm	Disordered	89.2
Lab synth Disordered	JC4-14A	Disordered	85.4
Lab synth Disordered	JC4-12A	Disordered	87.9
Lab synth Disordered	JC4-16B 75-125μm	Disordered	80.3

8.6   Discussion

8.6.1   Variability of Dissolution with Commercial MgSt Samples

The dissolution profiles of the commercial samples reported here vary from 69% to 86% at 15 minutes. The dissolution profiles show a consistent logarithmic trend, as opposed to a bi-exponential curve, suggesting that the samples are uniformly changed during the preparation. Fatty acid composition did not seem to directly correlate to any particular dissolution trend, for commercial or lab-synthesized samples. This exemplifies one of the problems with MgSt variability, as one variable that was expected to exhibit an influence showed no obvious trends with dissolution rate. However, MgSt particle size and surface area did show correlations with dissolution rate. The fastest dissolving commercial samples were the disordered samples, which have 84 - 86% dissolution at 15 minutes. The disordered samples also have a lower surface area, which is consistent with the fast dissolution, potentially resulting from a lack of lubrication. The commercial monohydrate lots have much slower dissolution and higher surface area. It is hypothesized that the monohydrate form consists of MgSt agglomerates of small fines and flakes surrounding the particles. These flakes and small fines are imagined to break off from the larger particles to provide a hydrophobic coating to other drug and excipient particles in the formulation and thereby slowing dissolution. The higher surface area of the monohydrate and slower dissolution are consistent with more effective lubrication coating of the other formulation particles by MgSt. Low surface area for the disordered samples is consistent with fast dissolution for formulations containing MgSt which does not coat the other formulation components as well. Similarly, the higher surface area observed for mixtures and pure monohydrate samples is consistent with fines and flakes

breaking off and coating the other formulation components. An implication of this is that switching MgSt suppliers could have a very large impact on dissolution profiles, especially if the existing supplier has MgSt that has properties that are closer to the fast-dissolving profile and was switched to a supplier with MgSt properties closer to the slow-dissolving profile.

The presence of significant dihydrate form in some of the commercial samples, such as the Chem-Impex and MP Biomedicals lots, did not seem to correlate with dissolution rates, as the MP Biomedicals sample had the greatest dihydrate concentration but also one of the slowest dissolution profiles. However, surface area data suggests not only a trend with dissolution, but also with hydrate form in general. It may be possible that monohydrate-dihydrate mixtures exhibit slightly slower dissolution due to crystal form inhomogeneity/defects which allow the particles to break apart easier, thus providing the lubricating coating characteristic of magnesium stearate.

8.6.2   Significant Variables Impacting MgSt Performance

Clearly one of the challenges that exists with MgSt is the fact that there are multiple variables that could impact dissolution rate, including the fatty acid composition, crystalline form, surface area, particle size, morphology and processing. Of these variables, surface area was clearly observed to trend with dissolution, with low surface area samples showing fast dissolution rate. Fatty acid composition showed no clear trend with the dissolution data for commercial or lab-synthesized samples.

In these studies, sieving was used to control particle size by selecting particle size fractions. The process of sieving can potentially cause changes in the structure of MgSt by reducing agglomerate size of the MgSt original particles. MgSt particles are often agglomerates of smaller particles with an "intrinsic" particle size of < 10 μm. Sieving may allow some of the more loosely bound particles on the surfaces of the agglomerates to come apart from the large agglomerates. These smaller particles may be described as

fines with < 1-2 μm size. It is believed that such small particles will more readily participate in lubrication by coating the other particles in the formulation.

Most of our data shows a clear correlation between surface area and dissolution, where samples prepared using smaller particle size sieved fractions of MgSt have a slower dissolution rate. One interpretation that can be drawn is that for samples sensitive to processing, such as the monohydrate form, smaller particles lead to slower dissolution. Surface area results for the samples discussed here indicate a correlation between surface area and hydrate form, as indicated in Figure 8-8. Surface area appears to be the primary factor in determining the impact of MgSt on dissolution rate. However, the surface area-dissolution curve is not perfectly linear, suggesting crystal form as a secondary variable impacting dissolution. The surface area-dissolution curves for the different crystal forms appear to differ and may account for the deviations from linearity in the surface area-dissolution curve.

8.7   Conclusions

Several conclusions could be made about the impact of MgSt variability on dissolution rate. First, no clear correlation could be made for the commercial samples or lab-synthesized samples based on fatty acid composition. Second, there is a clear impact of particle size on dissolution. Sieve fraction was used to show the particle size effect within a sample and surface area was used to assess the effect of size differences between samples on dissolution. Third, dissolution rate was found to trend with surface area for both commercial and lab-synthesized MgSt samples. Finally, the surface area-dissolution relationship may be impacted by crystal form as a secondary factor, where variation is observed in the slopes of the surface area-dissolution lines corresponding to different crystal forms.

8.8   Acknowledgements

CHAPTER 9.   AN EVALUATION OF THE SOLID-STATE FORM AND PARTICLE PROPERTIES OF MAGNESIUM STEARATE ON LUBRICATION EFFICIENCY, TABLETABILITY AND DISSOLUTION

9.1   Authors and Journal Information

Julie L. Calahan[1], Shubhajit Paul[3], Evelyn G. Yanez[4], Daniel DeNeve[1,2], Changquan Calvin Sun[3], Eric J. Munson[1,2*]

[1] *Department of Pharmaceutical Sciences, University of Kentucky, Lexington, KY, USA*
[2] *Current address: Department of Industrial and Physical Pharmacy, Purdue University, West Lafayette, IN, USA*
[3] *Department of Pharmaceutics, University of Minnesota, Minneapolis, MN, USA*
[4] *Small Molecule Pharmaceutical Sciences, Genentech, Inc., South San Francisco, CA, USA*

*Corresponding author:

Eric J. Munson
Purdue University
Robert E. Heine Pharmacy Bldg Rm 124D
575 Stadium Mall Drive
West Lafayette, IN 47907-2091
Phone: (765) 494-1450
Email: munsone@purdue.edu

9.2 Abstract

Magnesium stearate (MgSt) is a widely used pharmaceutical lubricant in tablet manufacturing. However, batch-to-batch variability in hydrate form and surface area can lead to inconsistency in tablet performance. In this work, the role of solid-state form and particle properties on lubrication efficiency, tabletability, and dissolution are studied using a model direct compression (DC) tablet formulation. It was found that the monohydrate and dihydrate forms had good lubrication efficiency compared to the disordered form, but also had poorer tabletability. The dissolution rate correlated with surface area, where monohydrate samples had high surface area and slower dissolution, and disordered samples had low surface area and faster dissolution. Of the dihydrate samples, a higher surface area sample had a slower dissolution rate, and a lower surface area sample had a faster dissolution rate. The choice of the best MgSt grade depends on the comprehensive evaluation of not only lubrication efficiency but also tabletability and dissolution. Overall, the lower surface area dihydrate MgSt had the best performance for this DC formulation.

9.3 Introduction

Magnesium stearate (MgSt) is the most commonly used excipient in solid oral dosage forms, with over half of the tablet formulations on the market using it as a lubricant. (1) The main function of MgSt is to reduce friction during the tableting process by forming a film between the tablet and the die wall,(2) reducing the tendency of a the active pharmaceutical ingredient (API) to stick to the tablet punch or die. However, because of its hydrophobicity, MgSt can also significantly impact the dissolution rate of API from tablets, especially if the amount of MgSt added is too high or the blending time is too long. Additionally, the weak bonding strength of MgSt can reduce tablet

mechanical strength, resulting in poor tabletability (tensile strength as a function of compaction pressure). Hence, the use of excessive MgSt may cause unacceptably slow API dissolution rate or poor tabletability.(16)

The popularity of MgSt as a lubricant in tablet formulation is linked to several distinct aspects of its lubricating mechanism: a) It is characterized as a "low shear strength laminar solid" that adheres to the lubricated surface with the polar head, with the long hydrophobic fatty acid chains pointing outward. (49) b) It can form a lubricant film one to two molecules thick. (2) c) It has a high melting point and is able to reduce static charges in the formulation powder. (49, 75) d) It can fill the particle cavities and spaces between the lubricated surfaces.(78)

The lubrication efficiency (ejection force as a function of compaction pressure) has been shown to be affected by several factors related to MgSt: a) amount in the formulation, (86) b) fatty acid composition, (30) c) particle size and surface area, (8, 85) d) mixing process, (80-82, 158) e) tableting speed, and f) crystal form. (85) It is generally accepted that higher surface area and/or smaller particle size corresponds to better lubrication. It has also been suggested that the hydration state likely affects lubrication properties,(84) with some sources suggesting the dihydrate form of MgSt was a better lubricant than other forms,(9, 28, 33, 87) but more work is needed to clarify the trends for the different crystal forms.

Because multiple factors can simultaneously affect lubrication efficiency of MgSt, it is hard to identify a single factor that accounts for different performance among commercial MgSt samples, (84) especially because there has been a general lack of form control when studying lubrication efficiency. A thorough investigation of lubrication efficiency of MgSt requires a technique capable of reliably identifying its crystal forms. (8, 39, 43, 84, 159)

Identifying the crystal form of MgSt is challenging with traditional analytical techniques. Thermal analyses are non-specific, which leaves room for error in assigning crystal hydration state, particularly for a mixture of forms. When XRPD is used to identify the crystal forms, the diffraction patterns can be hard to interpret due to the mixtures of fatty acid salts, as well as mixtures of hydrate forms in the sample.(30)

We have recently shown that SSNMR can reliably characterize MgSt crystal forms, regardless of particle size and fatty acid content.(38) SSNMR is particularly powerful for analyzing mixtures of crystal forms of MgSt, especially because it can be used to analyze the state of MgSt in a formulation.

In this paper, six samples of MgSt, two monohydrates, two dihydrates and two disordered samples of MgSt were studied with respect to lubrication efficiency, dissolution, and tabletability. In addition to crystal form, the samples also varied with respect to surface area, fatty acid content and water content. (160) It was found that the monohydrate and dihydrate samples had the best lubrication efficiency, but the disordered form had the best tabletability. The dissolution rate was fastest for the low surface area materials. The best performing MgSt sample was the dihydrate with low surface area.

9.4   Materials and Methods

9.4.1   Materials

Magnesium hydroxide was purchased from Fluka (St. Louis, MO). Stearic acid and palmitic acid were purchased from TCI (Tokyo, Japan). Magnesium chloride hexahydrate was purchased from EMD (Darmstadt, Germany). Phosphate buffer was prepared from sodium phosphate monobasic and sodium hydroxide, purchased from BDH Analytical (Radnor, PA). Tablet excipients Avicel PH102 (microcrystalline cellulose, MCC) and alpha-Lactose monohydrate were obtained as a complimentary sample from FMC Biopolymer (Philadelphia, MA) and Sigma Aldrich (St. Louis, MO), respectively. The commercial MgSt samples were ordered through VWR from Beantown (dihydrate) and Alfa Aesar (disordered), and the Peter Greven (monohydrate) sample was purchased in bulk by Genentech (South San Francisco, CA). The commercial and lab-synthesized MgSt samples are denoted "C" and "LS", respectively, throughout the

manuscript. Indomethacin (Sigma Aldrich, St. Louis, MO) was used as model drug for direct compression formulation.

9.4.2 MgSt Synthesis

Magnesium stearate lab-synthesized lots were prepared using stearate: palmitate ratios of 55:45 for the lab-synthesized disordered sample (LS-Disordered) and 90:10 for LS-Dihydrate and LS-Monohydrate.(38) The synthesis "melt" method for the LS-Disordered material combined magnesium hydroxide and water with melted stearic and palmitic acids at 70 - 90 °C, followed by heating/dehydrating the solid MgSt sample at 105 °C. To synthesize the 90:10 samples, a "bath method" was used, where the stearic and palmitic acids were dissolved in water, followed by addition of ammonium hydroxide at pH 9 to generate the ammonium soap. MgSt was then precipitated with the slow addition of $MgCl_2$ at 70 - 75 °C. Half of the reacted MgSt slurry was transferred to a filter before a reflux step to remove impurities and this material was recovered as the dihydrate form. The second half of the slurry was further heated up to 105 °C, then filtered and refluxed, producing the monohydrate form of MgSt. The only difference between LS-Monohydrate and LS-Dihydrate was the reaction temperature. The reflux step for all three LS samples involved washing the recovered solids using a reflux bath of 1:1 acetone: water for 24 hours to remove impurities and unreacted starting materials. The MgSt samples were dried in a vacuum oven at 25 °C overnight to remove surface water.

9.4.3 Mixing and Tableting

MgSt tablet formulations were prepared by adding the MgSt sample to a "Premix" containing 16.7% indomethacin, 50% alpha-lactose monohydrate and 33.3% Avicel

PH102. The lab-synthesized MgSt samples were sieved to 75–125 μm sieve fraction prior to mixing. Tablets for lubrication studies were prepared using 1% MgSt in the premix and blended for 15 minutes, then 300 mg tablets were compacted on Presster (Presster, Metropolitan Computing Corp., NJ) simulating Korsch XL100 press (10 stations) at a dwell time of 50 ms using 10 mm round flat-faced tooling. Necessary parameters such as in-die thickness, ejection force and take-off force were recorded as a function of pressure.

For dissolution studies, the powders were prepared using 2% MgSt in the premix, then mixed as 1 g batches in 40 mL glass vials for 60 minutes using a Turbula mixer (WAB, Basel, Switzerland) at ~ 100 rpm. Individual 150 mg tablets were made from each 1 g formulation batch and pressed using a single tablet press (Globe Pharma, North Brunswick, NJ) at 50 bar for 30 seconds. The tablet weights were recorded and the dissolution results were adjusted for tablet mass. A 2% level of MgSt was used for the dissolution studies to enhance the dissolution rate differences between samples.

9.4.4   Determination of Particle Density

The particle or true density (ρ_t) of formulated blends with different forms of MgSt was determined by helium pycnometry (Quantachrome Instruments, Ultrapycnometer 1000e, Byonton Beach, Florida). 1-2 g of powder was accurately weighed and placed into the sample cell. The measurement was allowed to repeat for a maximum of 100 iterations. The experiment was terminated when the coefficient of variation of five consecutive measurements was below 0.005%. The mean of the last five measurements was reported as the absolute density of the sample. The tablet porosity was obtained from Equation 9-1 where ρ is the tablet density:

$$\varepsilon = 1 - \frac{\rho}{\rho_t}$$ Equation 9-1

9.4.5 Compressibility Analysis

The powder deformability of different formulations under compressive stress was assessed by nonlinear fitting of the pressure (P) – porosity (ε) data using Kuentz – Leuenberger equation as follows:(161)

$$P = \frac{1}{C}\left[\varepsilon - \varepsilon_c - \varepsilon_c ln\left(\frac{\varepsilon}{\varepsilon_c}\right)\right]$$
<div align="right">Equation 9-2</div>

The parameter 1/C is related to yield stress of the material where a higher 1/C value corresponds to lower plasticity. ε_c denotes the porosity at which a powder bed just starts to approach a state with mechanical rigidity.(162)

9.4.6 Diametric Tablet Strength

Tablets were broken on a texture analyzer (Texture Technologies Corp., Surrey, UK) at 0.01 mm/s. Tablet tensile strength, σ, was calculated using Equation (3),

$$\sigma = \frac{2F}{\pi.D.h}$$
<div align="right">Equation 9-3</div>

where F, D, and h are the breaking force, tablet diameter, and thickness, respectively(163).

9.4.7   Compactibility Analysis

Compactibility profile (σ vs. ε) of each formulation was analyzed by non-linear regression of data using Equation (4) (84, 164).

$$\sigma = \sigma_0 e^{-b.\varepsilon} \qquad\qquad \text{Equation 9-4}$$

where σ_0 is the tensile strength of the tablet at zero porosity and b is an empirical constant that quantifies sensitivity of σ to changes in ε.

9.4.8   In Vitro Dissolution

Dissolution was performed by suspending each tablet in 900 mL of pH 7.2 phosphate buffer on a VanKel V7000 USP method 2 (paddle type) dissolution apparatus (Varian, Cary, NC) which was thermo-regulated at 37°C and equipped with 100 rpm stirring speed. The μDISS fiber optic UV probes (pION, Billerica, MA) were used to collect UV absorbance data at 320 nm over a 120-min period and the concentration of drug in solution was calculated based on an indomethacin standard curve. The μDISS probes were calibrated using indomethacin in phosphate buffer. The dissolution data was processed using the second derivative function to eliminate the effects of particles on the UV absorbance reading.

9.4.9   Solid-state NMR Spectroscopy (SSNMR)

^{13}C CP/MAS and ^{1}H T_1 relaxation data were collected using a home-built SSNMR system consisting of a Tecmag Redstone NMR Spectrometer (Houston, TX), Bruker 400 MHz magnet (Billerica, MA), and rebuilt Chemagnetics (Ft. Collins, CO) NMR probe with 7.5 mm rotors spinning at 4000 Hz. A relaxation delay of 12 seconds was used with 2K acquisition points and 1024 scans. TNMR software (Houston, TX) was used to process the data. 3-methylglutamic acid was used as a reference standard, with the methyl peak referenced to 18.84 ppm.

9.4.10 Thermogravimetric Analysis (TGA)

TGA percent weight loss was measured using TA Q50 (TA Instruments, Newcastle, DE) with a 10 °C/min ramp from 25 °C to 250 °C.

9.5   Results and Discussion

9.5.1   Characterization of MgSt Samples

Six MgSt samples, having a variety of physicochemical properties, were used to study lubrication and tableting properties, as listed in Table 9-1. To evaluate the impact of MgSt crystal form, samples of three forms (monohydrate, dihydrate and disordered) are compared from both commercial and lab-synthesized sources. The crystal form of MgSt is differentiated based on crystal packing differences in the carbonyl end of the molecules, observed in the 160 - 200 ppm region of the ^{13}C SSNMR spectrum (Figure 9-1). The monohydrate form has six signature peaks in the 177 - 183 ppm range, while the dihydrate has two peaks between 183 - 187 ppm and the disordered form is differentiated by a single broad peak centered around 182 ppm. Multiple peaks indicate different possible orientations of the carbon atoms in the crystal structure, arising from

the atoms being in different molecular environments. This is often an indication of having more than one molecule in the crystal unit cell.(165)
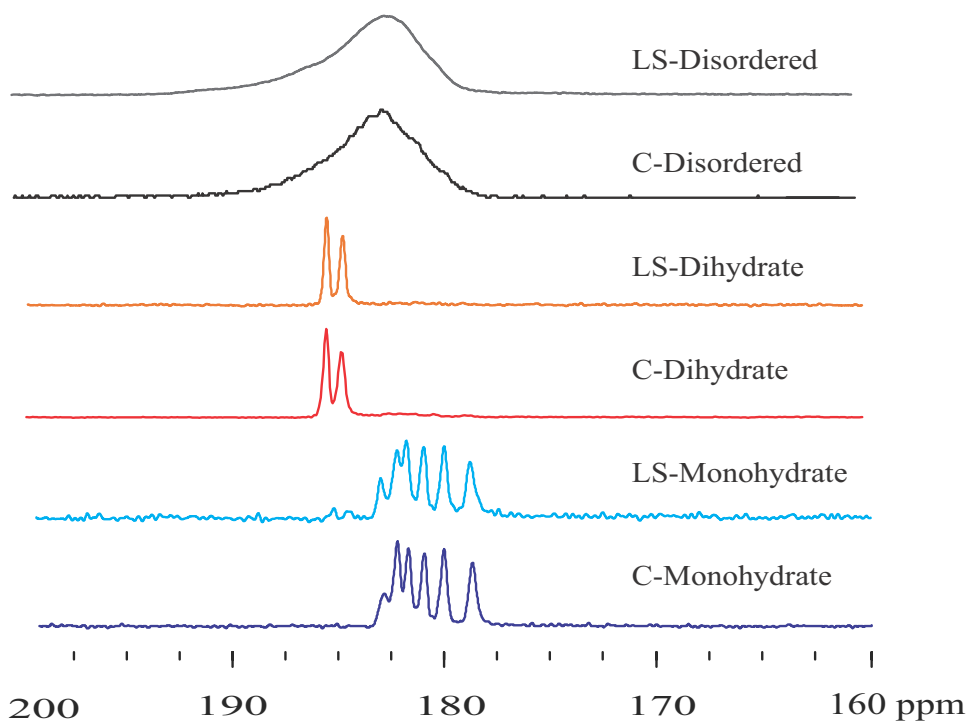
Figure 9-1. ^{13}C SSNMR spectra of the three lab-synthesized (LS) and three commercial (C) MgSt samples. Crystal form can be differentiated by the distinct peaks for monohydrate (177-183 ppm), dihydrate (183-187 ppm) and a single broad peak for disordered (around 182 ppm). SSNMR peaks indicate orientations of the carbon atoms in the crystal structure.

Table 9-1. Physicochemical characterization of lab-synthesized and commercial monohydrate, dihydrate and disordered forms of MgSt

Source	Crystal Form	Surface area m^2/g	TGA % weight loss
Lab-synthesized	Monohydrate	5.6	3.1
Commercial	Monohydrate	5.8	3.0
Lab-synthesized	Dihydrate	1.2	5.5
Commercial	Dihydrate	5.5	5.4
Lab-synthesized	Disordered	0.7	0.4
Commercial	Disordered	0.8	3.3

The two monohydrate samples had 3.1 or 3.0% weight loss when heated on TGA (Figure 9-2), consistent with the theoretical 3.0% water in the monohydrate. The 5.5 and 5.4% weight losses of the two dihydrate samples also reasonably agreed with the theoretical 5.7% of water for MgSt dihydrate. The disordered samples, on the other hand, showed broad weight loss from 25 - 100 °C, where the LS-Disordered and the C-Disordered materials showed 0.4% and ~3.3% weight loss, respectively.
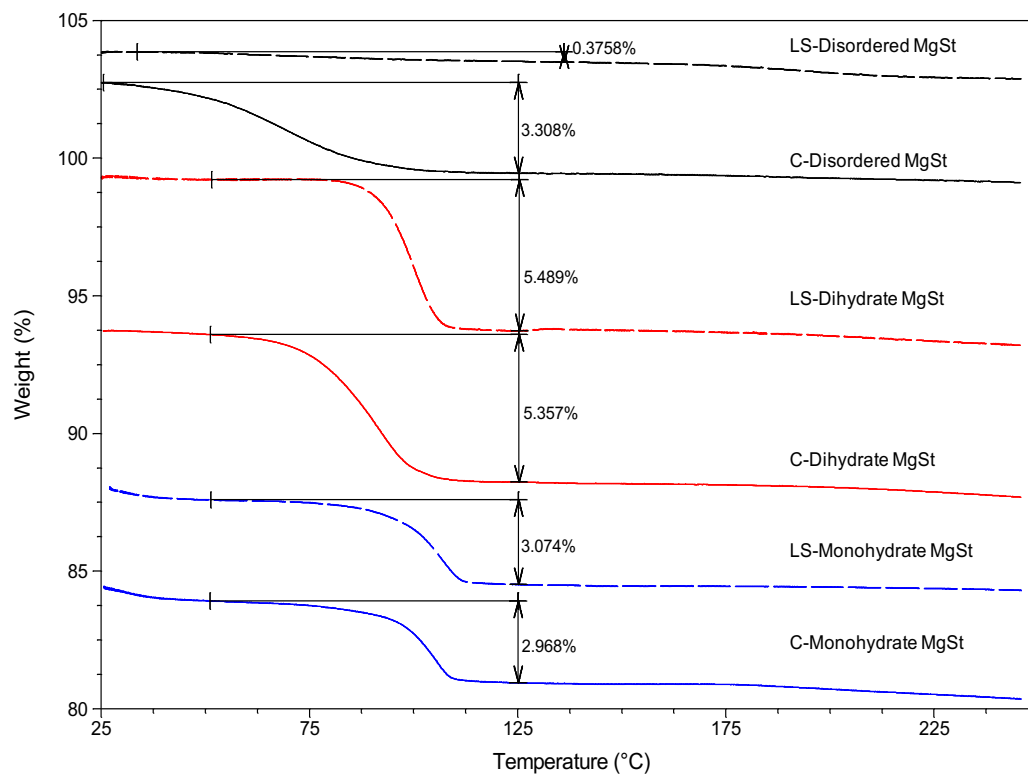
Figure 9-2. Thermogravimetric Analysis (TGA) for the three lab-synthesized (LS) and three commercial (C) MgSt samples. The monohydrate and dihydrate weight loss agreed with the theoretical water content.

9.5.2 Lubrication Properties

Lubrication efficiency of formulations containing various lots of MgSt in a lactose-MCC-indomethacin mixture was assessed in terms of the ejection force (EF) profile, i.e., EF vs. compaction pressure. EF is strongly associated with residual die-wall pressure.(158, 162, 166) Materials with greater rigidity tend to shrink less in the radial direction during decompression, resulting in greater residual die-wall pressure and higher EF than elastic or plastic materials. These forces could also be influenced by particle size and surface roughness, where EF could be higher as a result of greater friction caused by irregular small particles sliding against the die-wall. When the contact area between

tablet and die wall is controlled, EF is indicative of die-wall friction. In this study, EF increased with compaction pressure (Figure 9-3). The overall lubrication efficiency follows the order of Disordered > Monohydrate ≥ Dihydrate MgSt (Figure 9-3). The monohydrate and dihydrate forms, irrespective of their source, showed comparable EF profiles, hence, similar lubrication efficiency. The higher lubrication efficiency of the monohydrate and dihydrate is consistent with their particle structures that favor easy flaking off during mixing. Both disordered forms had higher EF, corresponding to poorer lubrication efficiency. The much lower lubrication efficiency of the LS-Disordered sample, indicated by the highest EF profile, corresponds to its much lower water content (0.4 %) compared to the C-Disordered form (3.3 %). Thus, water content in disordered MgSt may be critical for the lubrication efficiency of MgSt. The poor lubrication of the LS-Disordered sample (0.4 %) suggests that surface bound water (as opposed to hydrate water incorporated into the crystal lattice) could be an important factor in providing lubrication efficiency for the disordered samples.
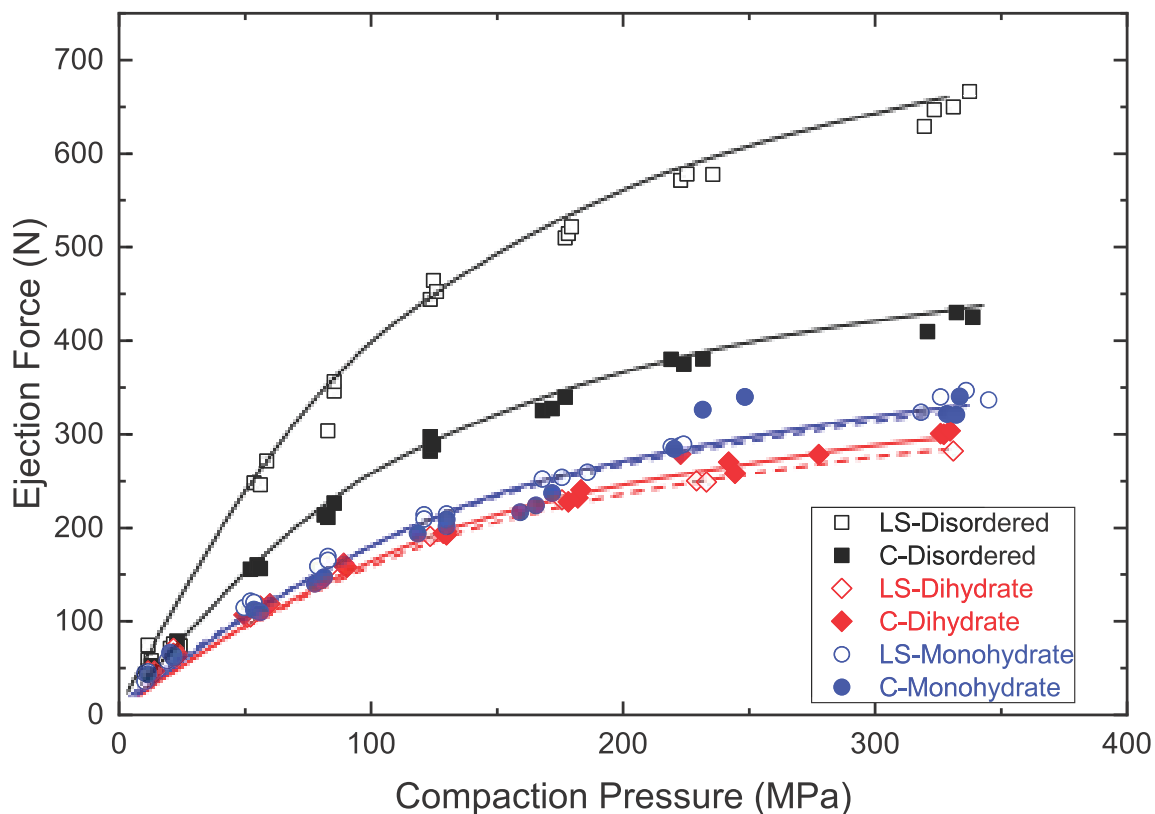
Figure 9-3. Lubrication efficiency (ejection force as a function of compaction pressure) of formulations containing different MgSt samples.

9.5.3 Effects on Tablet Compression Properties

At 1% MgSt level, the different solid-state forms of MgSt had a significant effect on the tabletability profiles. The tablet tensile strength (σ) increased with compaction pressure for all formulations. However, tabletability diverged with increasing pressure, leading to large variations in σ (4 - 6 MPa) at 330 MPa (Figure 9-4). The tabletability followed the order of LS-Disordered > C-Disordered > C-Dihydrate =LS-Dihydrate > LS-Monohydrate > C-Monohydrate (Figure 9-4). The reduced tabletability by MgSt was attributed to the coating of particles by the MgSt film, which leads to reduced inter-particulate bonding due to the low bonding strength of MgSt. Thus, a better lubrication efficiency is expected to be accompanied by greater reduction in tabletability for materials that do not undergo extensive brittle fragmentation during compaction. This

163

view is supported by the observation in this work, where bonding strength, σ_0, which indicates the inter-particulate bonding strength in a pore-free tablet, followed approximately the same order as that of tabletability (Table 9-2 and Figure 9-4). The tabletability of all the formulations was adequate despite the deteriorating effect by MgSt, since all the formulations could form tablets with tensile strength higher than the minimum proposed values of 2.0 MPa, and 1.7 MPa.(167-169)
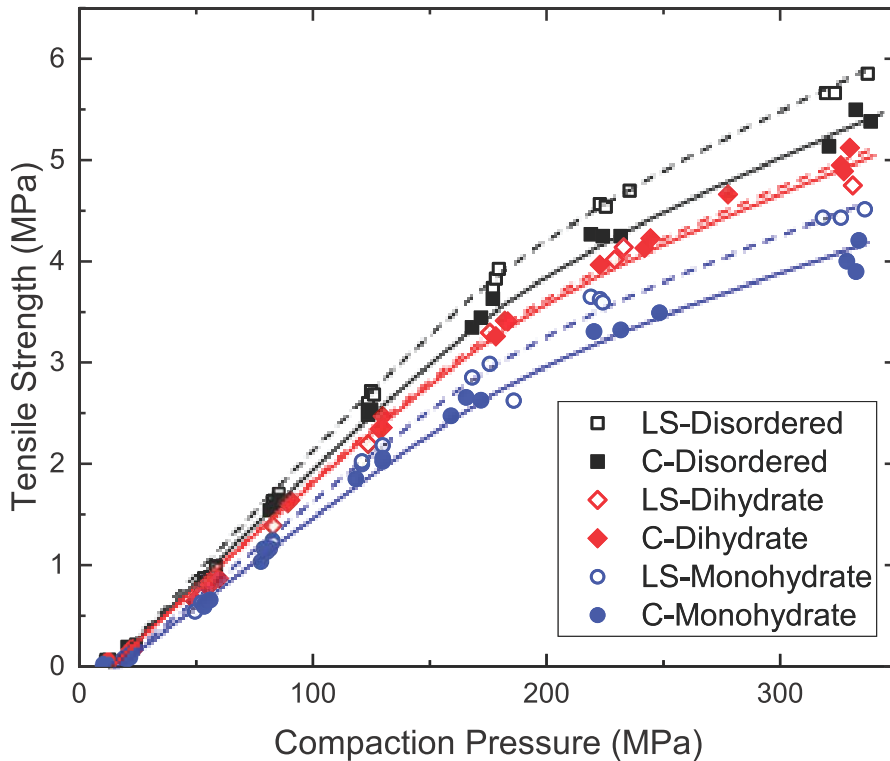
Figure 9-4. Tabletability (tensile strength as a function of compaction pressure) profiles of formulations containing different MgSt samples.

Table 9-2. Tensile strength at zero porosity (σ_0) and plasticity parameter (1/C) of tablet formulations containing different MgSt samples. Standard errors of fitting are shown in parenthesis.

MgSt source and form	σ_0 (MPa)[1]	1/C (MPa)[2]
LS-Disordered	12.4 (0.5)	635 (107)
C-Disordered	11.8 (0.7)	661 (102)
LS-Dihydrate	8.9 (0.8)	444 (56)
C-Dihydrate	11.4 (0.7)	672 (104)
LS-Monohydrate	9.5 (0.2)	624 (105)
C-Monohydrate	8.9 (0.3)	744 (106)

According to the bonding area - bonding strength (BABS) theory, (170, 171) another factor that controls tablet tensile strength is bonding area, which is assessed by compressibility (porosity as a function of compaction pressure). The compressibility plots did not visually differ among the different MgSt containing formulations (Figure 9-5), indicating that bonding area differences did not significantly contribute to the differences in tabletability among the formulations. The plasticity parameter, 1/C, obtained from quantitative analysis of compressibility data using the Kuentz –Leuenberger (K-L) method, shows the plasticity of the formulation containing LS-Dihydrate was significantly higher ($p < 0.05$) than all other five formulations (Table 9-2). The 1/C values of these five formulations were not significantly different. The K-L analysis was shown to be superior to the commonly used Heckel analysis in assessing deformability of diverse materials.(161) The significantly higher plasticity of the formulation containing LS-Dihydrate suggests the LS-Dihydrate had much higher plasticity than the other samples of MgSt.
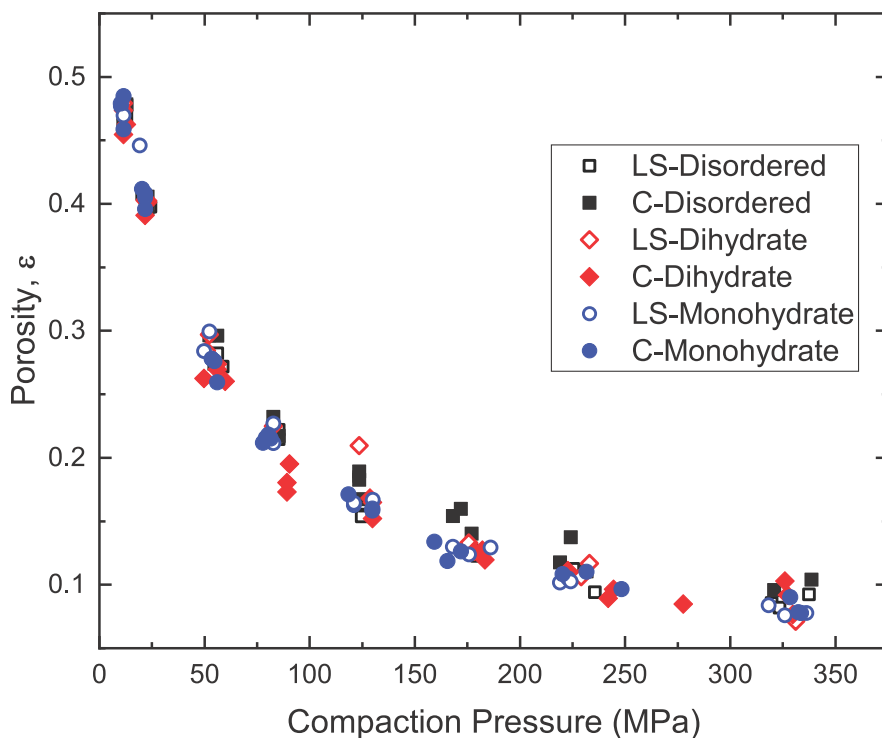
Figure 9-5. Compressibility profiles (porosity as a function of compaction pressure) of formulations containing each of the six different samples of MgSt.

9.5.4   In Vitro Dissolution

The tablet dissolution of the two monohydrate MgSt formulations was slowest, whereas dissolution from tablets using the two disordered MgSt formulations was fastest (Figure 9-6). To accentuate the differences in dissolution between the MgSt samples, the formulation mixtures were over-lubricated by using a 2% MgSt level and mixing the formulations for 60 minutes with a Turbula mixer. Minimal difference was observed between the lab-synthesized and commercial monohydrate samples, or between the lab-synthesized and commercial disordered MgSt samples. However, the lab-synthesized MgSt dihydrate had faster dissolution and the C-Dihydrate had slower dissolution (Figure 9-6). This may be attributed to the difference in their particle surface areas (Table 9-1), where the C-Dihydrate had surface area of 5.5 m^2/g, similar to surface area for the

monohydrate samples, and the LS-Dihydrate had surface area of 1.2 m²/g, slightly higher than surface area for the disordered samples. Dissolution showed a trend with surface area, where monohydrate samples with high surface area had slower dissolution and disordered samples with low surface area had faster dissolution. In terms of dissolution, the primary factor differentiating between MgSt samples appears to be surface area. The difference observed between the dissolution of tablets made from the two dihydrate samples is also likely due to MgSt surface area variability, which affected the extent of MgSt covering particle surfaces during the mixing process. MgSt with a much larger surface area can more efficiently coat drug particles, which slows down dissolution due to the hydrophobicity of MgSt.
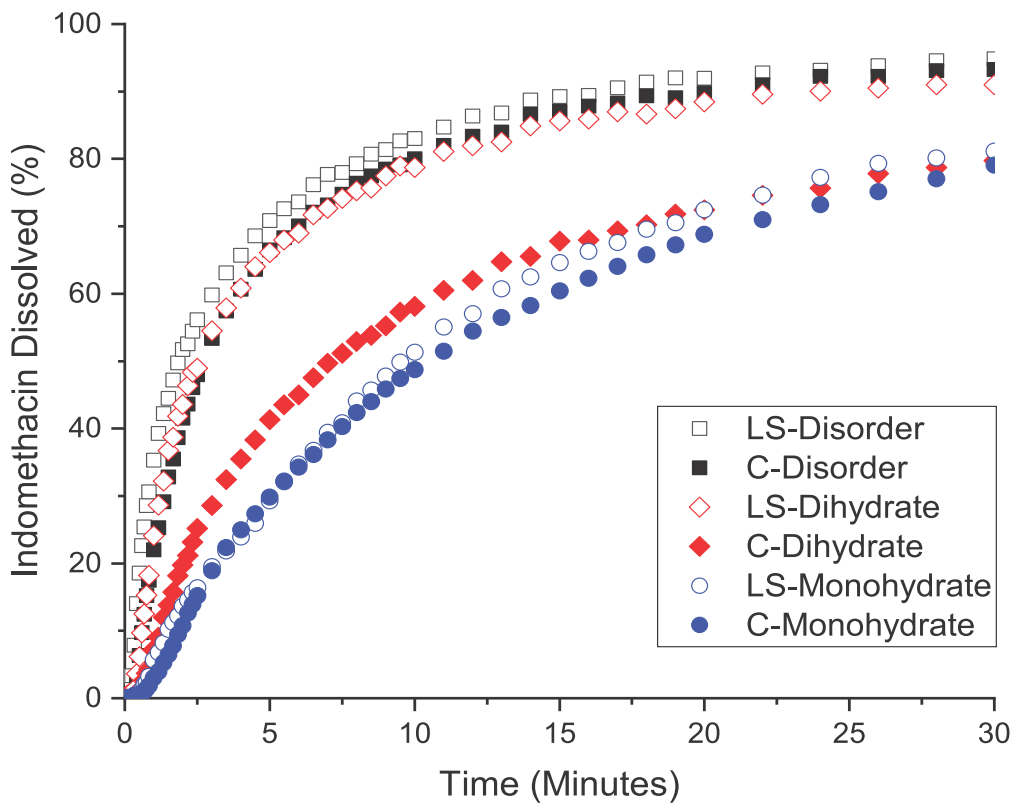
Figure 9-6. Dissolution of tablets containing different lots of MgSt

The comparable lubrication properties of the two sources of monohydrate and dihydrate MgSt (Figure 9-3), despite the very different specific surface area (Table 9-1),

suggests that the crystalline nature of MgSt is a more important variable in determining the lubrication efficiency than particle properties. Tabletability also suggests that the crystal form of MgSt impacts hardness more than specific surface area or water content (Figure 9-4). This may be explained from the mechanism of lubrication by MgSt, which is the shearing of lamellar layers of MgSt crystals during mixing to provide a hydrophobic coating of MgSt around the other particles in the formulation.

The formulation containing MgSt LS-Monohydrate had a lower EF profile than the formulation containing C-Disordered MgSt, despite similar water content. Here we note that the monohydrate has hydrated water incorporated into the crystal lattice, where the disordered water is not bound into the crystal. Thus, the lattice water in crystalline MgSt, rather than total water content, appears critical for good lubrication efficiency of MgSt. However, between the two disordered samples, the one with more water corresponded to much lower EF. This indicates the amount of non-lattice water also plays an important role in lubrication efficiency of disordered MgSt. Therefore, the role of water content on the lubrication efficiency of MgSt depends on the type of water in the sample. Total water content between disordered MgSt samples is critical, but the presence of hydrated water (i.e. crystalline MgSt hydrates) is even more important for lubrication efficiency.

While the main functionality of MgSt is to reduce EF to facilitate tablet manufacturing, the same mechanism of lubrication (i.e., covering of particle surfaces by MgSt) also tends to reduce tablet tensile strength and slow dissolution. Overall, the monohydrate form appears to be most effective in all these aspects of lubrication. However, low tensile strength and slow dissolution are not ideal for many formulations. The direct compression formulations in this work contained an appropriate proportion of plastic MCC and brittle lactose to attain a balanced mechanical property. This was to avoid the expected high sensitivity of tabletability to MgSt by a predominantly plastic powder, and insensitivity to MgSt by a brittle powder.(163, 172). Among the six MgSt samples evaluated in this study, LS-Dihydrate exhibited low EF, acceptable tabletability, and fast dissolution. Thus, the LS-Dihydrate MgSt is the best lubricant for this formulation. Although previous studies have suggested that the dihydrate performs better than the monohydrate, the choice of optimum MgSt depends on the nature of the

formulation that needs to be lubricated. For a formulation requiring stronger tablets and less effect on dissolution, the disordered form of MgSt may be a better choice. Instead of categorically claiming superiority for one type of MgSt, a comprehensive evaluation of lubrication efficiency, tabletability, and dissolution should be performed for the formulation, if possible.

9.6   Conclusions

Monohydrate and dihydrate forms of MgSt exhibited similar lubrication efficiency, while disordered MgSt was less effective, presumably due to differences in the extent of MgSt coating particle surfaces in the formulation. However, more efficient MgSt coating also tends to decrease the tabletability of the formulation. For tabletability, the lab-synthesized and commercial samples performed similarly for each form, with monohydrate MgSt leading to softer tablets (lower tensile strength), followed by the dihydrate and disordered forms. Disordered MgSt was least efficient in terms of lubrication efficiency, but also exhibited the least effect on dissolution, consistent with a low surface area and less effective particle coating by MgSt. These clear differences between monohydrate, dihydrate and disordered forms suggest that the crystal form of MgSt is an important variable in determining the lubrication properties, along with particle size which appears to be the primary factor affecting dissolution.

Given the different performance among these MgSt solid forms, the best choice of MgSt properties in a formulation depends on the desired formulation properties. To obtain lower ejection force, the monohydrate or dihydrate form is preferred. However, if the dissolution slowdown must be avoided, disordered MgSt with low surface area is preferred. For the six samples of MgSt evaluated in this work (monohydrate, dihydrate and disordered samples from lab-synthesized and commercial sources) with the model direct compression formulation, the lab-synthesized dihydrate MgSt was the best lubricant, with good lubrication efficiency and acceptable dissolution.

9.7   Acknowledgements

CHAPTER 10.   CONCLUSIONS

10.1 Physicochemical Properties of MgSt and their Relationships

10.1.1 Characterization of Magnesium Stearate Solid-state Properties

The solid-state characterization for eight commercial MgSt samples and five lab-synthesized samples identified five different pure forms of MgSt and that ^{13}C SSNMR was the best technique to distinguish between the forms, particularly for mixtures of forms. The TGA water loss dehydration peaks were used to assign the proposed hydration states for monohydrate, dihydrate and trihydrate samples. DSC and XRPD data were consistent with SSNMR form trends and it was possible to identify the forms for the pure form samples. However, it is much more challenging to distinguish and/or quantify for mixtures of MgSt forms with traditional techniques, compared with ^{13}C SSNMR. The additional correlation of ^{1}H T_1 relaxation values with TGA weight loss, and potentially fatty acid composition, may provide insight into structural aspects of the various forms.

10.1.2 Fatty Acid Composition – Synthesis and Fatty Acid Effects on Crystal Form

The investigation of magnesium stearate synthesis revealed an important role of fatty acid composition for MgSt, particularly in the relationship between fatty acid composition and crystal form. First, the chemical composition (stearate: palmitate ratio) and the synthesis reaction method both affect the crystal form of magnesium stearate that is produced from synthesis reactions. Pure fatty acid compositions (i.e. stearate only or palmitate only) showed a preference to produce the dihydrate form and mixtures of fatty acids tended to yield more of the monohydrate form. The melt method, a spontaneous reaction of fatty acids with magnesium hydroxide, preferentially produced the monohydrate form, with increasing amounts of dihydrate yielded from higher stearate content samples. The bath method, a two-step reaction precipitating MgSt from soap and

magnesium chloride, also yielded higher amounts of dihydrate form at higher stearate content samples. Combining the observed trends with fatty acid composition and synthesis method, it was concluded that the monohydrate form could be most easily produced from the melt method with a 50:50 St:Pa composition and the dihydrate form could most easily be produced from the bath method at 90:10 St:Pa composition.

Second, synthesis reaction conditions, such as reaction water and reaction temperature, affect the form of MgSt produced. Addition of a small amount of excess water during the melt method reaction appeared to aid formation of the monohydrate form. The reaction temperature in the bath method was also found to affect the crystal form produced. For a 90:10 St:Pa composition, dihydrate was yielded at 70 °C, but monohydrate was yielded when the temperature was increased to 100 °C.

Additionally, drying magnesium stearate was found to affect the physical form of the material, with more significant effects seen for the dihydrate and form mixtures. On a practical level, air drying for a few days was found to be the most gentle and effective drying method for lab-scale synthesis of MgSt. The dihydrate appears to be more sensitive to drying than the monohydrate form, but both forms can dehydrate in harsh drying conditions such as nitrogen drying or desiccation.

10.1.3 Crystal Form – Conditions for Form Conversions

An increased understanding of the form conversions of MgSt, both in bulk and in tablet formulations was gained by investigating the crystal form at various storage conditions. Thermal data was used as a guide to choose likely conversion conditions based on the dehydration temperatures of the MgSt hydrate forms. It was shown that at 80 °C, 100 %RH, the trihydrate converts into the dihydrate and/or monohydrate form, indicating that in the presence of excess water, the crystal form depends on temperature. A form conversion schematic for MgSt is presented, proposing conditions for direct conversions between MgSt crystal hydrate forms, as well as form conversions through an intermediate disordered or anhydrous form. Tablet formulations also showed MgSt form

conversions at 40 °C/ 75%RH, with an increase in dihydrate form, and a loss of dihydrate form at 40 °C/ 0%RH due to likely dehydration. Overall, it is shown that the crystal form of MgSt can change under varying temperature and humidity conditions, both in bulk and in tablet formulations.

10.1.4 Surface Area – Effect of Drying on Crystal Form

Several conclusions can be drawn from the study of surface area and the effects of drying on MgSt samples. First, there appeared to be a correlation between MgSt crystal form and surface area, where the disordered form showed low surface area and the monohydrate form showed higher surface area. Second, drying MgSt at 40 °C led to dehydration of the material, with a decrease in surface area being accompanied by an increase in the amount of disordered form in the sample. In dry conditions, the dihydrate appeared to dehydrate into the disordered form and the monohydrate also changed form. In addition to the form change with drying, dissolution showed that drying MgSt can also have an impact on tablet performance.

10.2 Effects on Functional Properties

10.2.1 Dissolution

A discriminating dissolution method was developed to study the over-lubrication of indomethacin tablets using various samples of MgSt. Several different factors were explored in the method development, including mixing method, sampling technique, the effect of MgSt concentration, compaction pressure, formulation mixing speed, formulation mixing time, reproducibility of the overall method and differentiation

between samples. Using this method, differences between variations in properties of MgSt samples were addressed in Chapter 8.

Several conclusions could be made about the impact of MgSt variability on dissolution rate. First, no clear correlation could be made for the commercial samples or lab-synthesized samples based on fatty acid composition. Second, there is a clear impact of particle size on dissolution, in terms of sieve fraction within a sample and surface area between samples. Sieve fraction was used to show a clear effect particle size on dissolution rate within a sample and surface area was used to assess the effect of size differences between samples on dissolution. Third, a correlation between surface area and dissolution rate was found for both commercial and lab-synthesized MgSt samples. Additionally, the surface area-dissolution relationship may also be impacted by crystal form as a secondary factor, where variation was observed in the slopes of the surface area-dissolution lines corresponding to different crystal forms.

10.2.2 Lubrication

In terms of lubrication, several conclusions were made. Monohydrate and dihydrate forms of MgSt exhibited similar lubrication efficiency, while disordered MgSt was less effective, presumably due to differences in the extent of MgSt coating particle surfaces in the formulation. However, more efficient MgSt coating also tended to decrease the tabletability of the formulation. For tabletability, the lab-synthesized and commercial samples performed similarly for each form, with monohydrate MgSt leading to softer tablets (lower tensile strength), followed by the dihydrate and disordered forms. Disordered MgSt was least efficient in terms of lubrication efficiency, but also exhibited the least effect on dissolution, consistent with a low surface area and less effective particle coating by MgSt. These clear differences between monohydrate, dihydrate and disordered forms suggest that the crystal form of MgSt is an important variable in determining the lubrication properties, along with particle size which appears to be the primary factor affecting dissolution.

Given the different performance among these MgSt solid forms, the best choice of MgSt properties in a formulation depends on the desired formulation properties. To obtain lower ejection force, the monohydrate or dihydrate form is preferred. However, if the dissolution slowdown must be avoided, disordered MgSt with low surface area is preferred. For the six samples of MgSt evaluated in this work (monohydrate, dihydrate and disordered samples from lab-synthesized and commercial sources) with the model direct compression formulation, the lab-synthesized dihydrate MgSt was the best lubricant, with good lubrication efficiency and acceptable dissolution.

10.3 Overall Conclusions

Overall, this work showed that the variability in the physicochemical properties of magnesium stearate samples can affect the dissolution and lubrication performance of tablet formulations. A major factor in understanding this variability is the ability to identify and track the crystal forms of MgSt. This is most easily done using ^{13}C SSNMR, an important analytical technique used throughout the project. The synthesis process showed the effect of fatty acid composition and other reaction conditions on crystal form. It was then shown that the crystal forms can interconvert based on temperature and humidity conditions, both in bulk and in tablet formulations. A dissolution method was developed to distinguish between MgSt samples and this method showed that the primary property of MgSt affecting dissolution was particle size and surface area, with a possible secondary effect of crystal form. Specifically, lower surface area correlated with faster dissolution rates, while higher surface area correlated with slower dissolution rates. In terms of lubrication, MgSt crystal form was found to impact lubrication efficiency and tabletability. An overall trend with crystal form was observed, with disordered < dihydrate ~ monohydrate in terms of lubrication efficiency but monohydrate < dihydrate < disordered for tabletability. It has been shown that the physicochemical properties of MgSt, particularly crystal form and surface area, show trends with functional properties of MgSt dissolution and lubrication. This highlights the importance of choosing a MgSt

material with the desired form and surface area properties to match the lubrication and dissolution requirements for the formulation.

REFERENCES

1.   Dave R. Overview of Pharmaceutical Excipients Used in Tablets and Capsules. Drug Topics - Modern Medicine. 2008;October 24, 2008.
2.   Moody G, Rubinstein MH, FitzSimmons RA. Tablet lubricants I. Theory and modes of action. International Journal of Pharmaceutics. 1981;9(2):75-80.
3.   Hanssen D, Fuehrer C, Schaefer B. Evaluation of magnesium stearate as tablet lubricating agent by electronic pressure measurements. Pharm Ind. 1970;32(2):97-101.
4.   Butcher AE, Jones TM. Some physical characteristics of Magnesium Stearate. J Pharm Pharmac 1972;24(Supp):1P-9P.
5.   Hoelzer AW. Batch to batch variations of commercial magnesium stearates. Chemical, physical and lubricant properties. Labo-Pharma - Probl Tech. 1984;338:28-36.
6.   Dansereau R. The Effect of the Variability in the Physical and Chemical Properties of Magnesium Stearate on the Preparation of Compressed Tablets. University Microfilms International. 1984;Purdue University(1984).
7.   Dansereau R, Peck GE. The effect of the variability in the physical and chemical properties of magnesium stearate on the properties of compressed tablets. Drug Dev Ind Pharm. 1987;13(6):975-99.
8.   Barra J, Somma R. Influence of the Physicochemical Variability of Magnesium Stearate on Its Lubricant Properties: Possible Solutions. Drug Development and Industrial Pharmacy. 1996;22(11):1105-20.
9.   Lugge D, editor The Story of Magnesium Stearate as a Powder and a Tablet Lubricant. ExcipientFest Americas 2013; 2013 2013: Covidient/Mallinckrodt; 2013.
10.   Kushner JIV, Langdon BA, Hiller JI, Carlson GT. Examining the impact of excipient material property variation on drug product quality attributes: A quality-by-design study for a roller compacted, immediate release tablet. J Pharm Sci. 2011;100(6):2222-39.
11.   Haware RV, Vivek S. Dave; Bhavyasri Kakarala, Sean Delaney, Scott Staton, Eric Munson, Mali Ram Gupta, William C. Stagner. Vegetable-derived magnesium stearate functionality evaluation by DM3 approach. European Journal of Pharmaceutical Sciences. 2016;89:115-24.
12.   Haware RV, Shivagari R, Johnson PR, Staton S, Stagner WC, Gupta MR. Application of Multivariate Methods to Evaluate the Functionality of Bovine- and Vegetable-Derived Magnesium Stearate. J Pharm Sci. 2014;103(5):1466-77.
13.   Wang T, Potts AR, Hoag SW. Elucidating the Variability of Magnesium Stearate and the Correlations with Their Spectroscopic Features. J Pharm Sci. 2018.
14.   Wang T, Ibrahim A, Hoag SW. Understanding the impact of magnesium stearate variability on tableting performance using a multivariate modeling approach. Pharmaceutical Development and Technology. 2020;25(1):76-88.
15.   Wang J, Wen H, Desai D. Lubrication in tablet formulations. Eur J Pharm Biopharm. 2010;75(1):1-15.
16.   Li JW, Yongmei. Lubricants in Pharmaceutical Solid Dosage Forms. Lubricants. 2014;2:21-43.

17.	Kanher PR, Bakhle SS, Upadhye KP, Dixit GR, Dakhole A. Lubricants in pharmaceutical solid dosage forms with special emphasis on magnesium stearate. World J Pharm Res. 2017;6(9Spec.Iss.):131-46.

18.	Anon. USP Quality Standards for Compounding. In: usp.org, editor.: USP.

19.	Anon. Magnesium Stearate Monograph. In: USP, editor. USP-NF Stage 6 Harmonization. Rockville, MD, USA: The United States Pharmacopeial Convention; 2016.

20.	Anon. Relative content of stearic acid and palmitic acid. USP-NF.

21.	La Nasa J, Modugno F, Aloisi M, Lluveras-Tenorio A, Bonaduce I. Development of a GC/MS method for the qualitative and quantitative analysis of mixtures of free fatty acids and metal soaps in paint samples. Anal Chim Acta. 2018;1001:51-8.

22.	Metcalfe LD. Gas chromatographic analysis of the derivatives of fatty acids. J Chromatogr Sci. 1975;13(11):516-19.

23.	Rajala R, Laine E. The effect of moisture on the structure of magnesium stearate. Thermochim Acta. 1995;248:177-88.

24.	Ertel KD, Carstensen JT. An examination of the physical properties of pure magnesium stearate. Int J Pharm. 1988;42(1-3):171-80.

25.	Miller TA, York P. Physical and chemical characteristics of some high purity magnesium stearate and palmitate powders. International Journal of Pharmaceutics. 1985;23:55-67.

26.	Heider TP, Wolfgang SM, Randle SR, inventors; Mallinckrodt Inc., USA . assignee. Neutralization process for the preparation of an alkaline earth metal stearate composition patent US20060281937A1. 2006.

27.	Wolfgang SM, Helder TP. Stearate Composition and Method of Production Thereof. United States Patent. 2008;US 7,456,306 B2.

28.	Wu SH. Magnesium Stearate Dihydrate - A New High Performance Pharmaceutical Lubricant for Lubricating Powder and Making Tablets. Mallinckrodt Pharmaceuticals.

29.	Wu SH, Cheng BK, Nichols GA, Park JH, inventors; Mallinckrodt Inc., USA . assignee. Use of magnesium stearate dihydrate for lubrication of solid pharmaceutical compositions patent WO2009114226A1. 2009.

30.	Marwaha SB, Rubinstein MH. Structure-lubricity evaluation of magnesium stearate. Int J Pharm. 1988;43(3):249-55.

31.	Muller BW. Pseudopolymorphism of magnesium salts of higher fatty acids. Arch Pharm (Weinheim). 1977;310(9):693-704.

32.	Ertel KD. The Chemical, Physical and Lubricative Propertis of Magnesium Stearate. University Microfilms International. 1987;The University of Wisconsin - Madison(1987).

33.	Ertel KD, Carstensen JT. Chemical, physical, and lubricant properties of magnesium stearate. J Pharm Sci. 1988;77(7):625-9.

34.	Wada Y, Matsubara T. Pseudopolymorphism and lubricating properties of magnesium stearate. Powder Technol. 1994;78(2):109-14.

35.	Sharpe SA, Celik M, Newman AW, Brittain HG. Physical characterization of the polymorphic variations of magnesium stearate and magnesium palmitate hydrate species. Structural Chemistry. 1997;8(1).

36.   Bracconi P, Andres C, Ndiaye A. Structural properties of magnesium stearate pseudopolymorphs: effect of temperature. Int J Pharm. 2003;262(1-2):109-24.

37.   Bracconi PCA, A. N'diaye, Y. Pourcelot. Thermal analyses of commercial magnesium stearate pseudopolymorphs. Thermochimica Acta. 2005;429:43.

38.   Delaney SP, Nethercott MJ, Mays CJ, Winquist NT, Arthur D, Calahan JL, et al. Characterization of Synthesized and Commercial Forms of Magnesium Stearate Using Differential Scanning Calorimetry, Thermogravimetric Analysis, Powder X-Ray Diffraction, and Solid-State NMR Spectroscopy. J Pharm Sci. 2017;106(1):338-47.

39.   Swaminathan V, Kildsig DO. An examination of the moisture sorption characteristics of commercial magnesium stearate. PharmSciTech. 2001;2(4):28.

40.   Frattini C, Simioni L. Should magnesium stearate be assessed in the formulation of solid dosage forms by weight or by surface area? Drug Dev Ind Pharm. 1984;10(7):1117-30.

41.   Phadke DS, Collier JL. Effect of degassing temperature on the specific surface area and other physical properties of magnesium stearate. Drug Dev Ind Pharm. 1994;20(5):853-8.

42.   Phadke DS, Eichorst JL. Evaluation of particle size distribution and specific surface area of magnesium stearate. Drug Dev Ind Pharm. 1991;17(6):901-6.

43.   Andres C, Bracconi P, Pourcelot Y. On the difficulty of assessing the specific surface area of magnesium stearate. Int J Pharm. 2001;218(1-2):153-63.

44.   Koivisto M, Jalonen H, Lehto V-P. Effect of temperature and humidity on vegetable grade magnesium stearate. Powder Technol. 2004;147(1-3):79-85.

45.   Lapham DP. Magnesium Stearate: The Effects of Hydration State and Degassing on Isotherms and BET Surface Area. The Microreport from Micromeritics. 2018;26(1):3-5.

46.   Lapham DP, Lapham JL. Gas adsorption on commercial magnesium stearate: Effects of degassing conditions on nitrogen BET surface area and isotherm characteristics. Int J Pharm (Amsterdam, Neth). 2017;530(1-2):364-76.

47.   Lapham DP, Lapham JL. Gas adsorption on commercial magnesium stearate: The origin of atypical isotherms and BET transform data. Powder Technol. 2019;342:676-89.

48.   Delaney SP, Nethercott MJ, Mays CJ, Winquist NT, Arthur D, Calahan JL, et al. Characterization of Synthesized and Commercial Forms of Magnesium Stearate Using Differential Scanning Calorimetry, Thermogravimetric Analysis, Powder X-Ray Diffraction, and Solid-State NMR Spectroscopy. Journal of Pharmaceutical Sciences. 2017;106(1):338-47.

49.   Ragnarsson G, Hoelzer AW, Sjoegren J. The influence of mixing time and colloidal silica on the lubricating properties of magnesium stearate. Int J Pharm. 1979;3(2-3):127-31.

50.   Ong JTH, Chowhan ZT, Samuels GJ. Drug-excipient interactions resulting from powder mixing. VI. Role of various surfactants. Int J Pharm. 1993;96(1-3):231-42.

51.   Chaudhuri B, Mehrotra A, Muzzio FJ, Tomassone MS. Cohesive effects in powder mixing in a tumbling blender. Powder Technol. 2006;165(2):105-14.

52.   Virtanen SHS, J. Yliruusi. The Effect of Mixing Time of the Magnesium Stearate on Crushing Strengths of Tablets. European Journal of Pharmaceutical Sciences. 2008;34S(07):S25-S9.

53.   Perrault M, Bertrand F, Chaouki J. An investigation of magnesium stearate mixing in a V-blender through gamma-ray detection. Powder Technol. 2010;200(3):234-45.

54.   Kushner JI. Incorporating Turbula mixers into a blending scale-up model for evaluating the effect of magnesium stearate on tablet tensile strength and bulk specific volume. International Journal of Pharmaceutics. 2012;429:1-11.

55.   Jojart I, Sovany T, Pintye-Hodi K, Kasa P. Study of the behaviour of magnesium stearate with different specific surface areas on the surface of particles during mixing. J Adhes Sci Technol. 2012;26(24):2737-44.

56.   Nakamura S, Yamaguchi S, Hiraide R, Iga K, Sakamoto T, Yuasa H. Setting Ideal Lubricant Mixing Time for Manufacturing Tablets by Evaluating Powder Flowability. AAPS PharmSciTech. 2017;18(7):2832-40.

57.   Horibe M, Sonoda R, Watano S. Scale-Up of lubricant mixing process by using V-Type blender based on discrete element method. Chem Pharm Bull. 2018;66(5):548-53.

58.   Zannou EA, Ji Q, Joshi YM, Serajuddin ATM. Stabilization of the maleate salt of a basic drug by adjustment of microenvironmental pH in solid dosage form. Int J Pharm. 2007;337(1-2):210-8.

59.   Serajuddin ATM. Salt formation to improve drug solubility. Adv Drug Delivery Rev. 2007;59(7):603-16.

60.   Guerrieri P, Taylor LS. Role of salt and excipient properties on disproportionation in the solid-state. Pharm Res. 2009;26(8):2015-26.

61.   Stephenson GA, Aburub A, Woods TA. Physical stability of salts of weak bases in the solid-state. J Pharm Sci. 2010.

62.   Hsieh Y-L, Merritt JM, Yu W, Taylor LS. Salt Stability - The Effect of pHmax on Salt to Free Base Conversion. Pharm Res. 2015;32(9):3110-8.

63.   Hsieh Y-L, Taylor LS. Salt Stability - Effect of Particle Size, Relative Humidity, Temperature and Composition on Salt to Free Base Conversion. Pharm Res. 2015;32(2):549-61.

64.   Nie H, Xu W, Ren J, Taylor LS, Marsac PJ, John CT, et al. Impact of Metallic Stearates on Disproportionation of Hydrochloride Salts of Weak Bases in Solid-State Formulations. Molecular Pharmaceutics. 2016;13(10):3541-52.

65.   John CT, Xu W, Lupton LK, Harmon PA. Formulating Weakly Basic HCl Salts: Relative Ability of Common Excipients to Induce Disproportionation and the Unique Deleterious Effects of Magnesium Stearate. Pharm Res. 2013;30(6):1628-41.

66.   Merritt JM, Viswanath SK, Stephenson GA. Implementing Quality by Design in Pharmaceutical Salt Selection: A Modeling Approach to Understanding Disproportionation. Pharm Res. 2013;30(1):203-17.

67.   Wray PS, Sinclair WE, Jones JW, Clarke GS, Both D. The use of in situ near infrared imaging and Raman mapping to study the disproportionation of a drug HCl salt during dissolution. Int J Pharm (Amsterdam, Neth). 2015;493(1-2):198-207.

68.   Ewing AV, Wray PS, Clarke GS, Kazarian SG. Evaluating drug delivery with salt formation: Drug disproportionation studied in situ by ATR-FTIR imaging and Raman mapping. J Pharm Biomed Anal. 2015;111:248-56.

69.   Nie H, Xu W, Taylor LS, Marsac PJ, Byrn SR. Crystalline solid dispersion-a strategy to slowdown salt disproportionation in solid state formulations during storage and wet granulation. Int J Pharm (Amsterdam, Neth). 2017;517(1-2):203-15.

70.   Thakral NK, Behme RJ, Aburub A, Peterson JA, Woods TA, Diseroad BA, et al. Salt Disproportionation in the Solid State: Role of Solubility and Counterion Volatility. Mol Pharmaceutics. 2016;13(12):4141-51.

71.   Thakral NK, Kelly RC. Salt disproportionation: A material science perspective. Int J Pharm (Amsterdam, Neth). 2017;520(1-2):228-40.

72.   Koranne S, Govindarajan R, Suryanarayanan R. Investigation of Spatial Heterogeneity of Salt Disproportionation in Tablets by Synchrotron X-ray Diffractometry. Mol Pharmaceutics. 2017;14(4):1133-44.

73.   Patel MA, Luthra S, Shamblin SL, Arora KK, Krzyzaniak JF, Taylor LS. Assessing the Risk of Salt Disproportionation Using Crystal Structure and Surface Topography Analysis. Cryst Growth Des. 2018;18(11):7027-40.

74.   Hirsh DA, Su Y, Nie H, Xu W, Stueber D, Variankaval N, et al. Quantifying Disproportionation in Pharmaceutical Formulations with 35Cl Solid-State NMR. Mol Pharmaceutics. 2018;15(9):4038-48.

75.   Gold G, Palermo BT. Hopper flow electrostatics of tableting material. II. Tablet lubricants. J Pharm Sci. 1965;54(10):1517-19.

76.   Train D, Hersey JA. The use of laminar lubricants in compaction processes. J Pharm Pharmacol. 1960;12(Suppl):97-104.

77.   Lewis CJ, Train D. The compaction of some solid lubricant materials. J Pharm Pharmacol. 1965;17(9):577-83.

78.   Roblot-Treupel L, Puisieux F. Distribution of magnesium stearate on the surface of lubricated particles. Int J Pharm. 1986;31(1-2):131-6.

79.   Johansson ME. Granular magnesium stearate as a lubricant in tablet formulations. Int J Pharm. 1984;21(3):307-15.

80.   Vromans H, Bolhuis GK, Lerk CF. Magnesium stearate susceptibility of directly compressible materials as an indication of fragmentation properties. Powder Technology. 1988;54(1):39-44.

81.   Lakio S, Vajna B, Farkas I, Salokangas H, Marosi G, Yliruusi J. Challenges in Detecting Magnesium Stearate Distribution in Tablets. AAPS PharmSciTech. 2013;14(1):435-44.

82.   Paul S, Sun CC. Lubrication with magnesium stearate increases tablet brittleness. Powder Technology. 2017;309:126-32.

83.   Hussain MSH, York P, Timmins P. Effect of commercial and high purity magnesium stearates on in vitro dissolution of paracetamol DC tablets. Int J Pharm. 1992;78(2-3):203-7.

84.   Leinonen UI, Jalonen HU, Vihervaara PA, Laine ESU. Physical and lubrication properties of magnesium stearate. J Pharm Sci. 1992;81(12):1194-8.

85.   Rao KP, Chawla G, Kaushal AM, Bansal AK. Impact of solid-state properties on lubrication efficacy of magnesium stearate. Pharm Dev Technol. 2005;10(3):423-37.

86.   Hamad ML, Gupta A, Shah RB, Lyon RC, Sayeed VA, Khan MA. Functionality of magnesium stearate derived from bovine and vegetable sources: dry granulated tablets. J Pharm Sci. 2008;97(12):5328-40.

87.   Okoye P. To systemically characterize magnesium stearate polymorphs and practically evaluate their effect on physicochemical properties of naproxen (BCS Class II) and acetaminophen (BCS Class III) as model drugs. In: Dave R, editor.: ProQuest Dissertations Publishing; 2013.

88.   Wu SH. Effect of Magnesium Stearate Lubricant Attributes on Product Processibility and Quality. Mallinckrodt Pharmaceuticals. 2009;Land O'Lake Industrial Pharmacy Conference.

89.   Levy G, Gumtow RH. Effect of certain tablet formulation factors on dissolution rate of the active ingredient. III. Tablet lubricants. J Pharm Sci. 1963;52(12):1139-44.

90.   Chowhan ZT, Chi LH. Drug-excipient interactions resulting from powder mixing. IV: Role of lubricants and their effect on in vitro dissolution. J Pharm Sci. 1986;75(6):542-5.

91.   Lerk CF, Bolhuis GK, Smallenbroek AJ, Zuurman K. Interaction of tablet disintegrants and magnesium stearate during mixing. II. Effect on dissolution rate. Pharm Acta Helv. 1982;57(10-11):282-6.

92.   Uzunovic A, Vranic E. Effect of magnesium stearate concentration on dissolution properties of ranitidine hydrochloride coated tablets. Bosnian journal of basic medical sciences. 2007;7(3):279-83.

93.   Patra S, Pattnaik S, Barik BB. Effect of lubricant concentration and granule size on dissolution rate of ciprofloxacin HCl tablets. J Teach Res Chem. 2008;15(1):43-6.

94.   Johansson ME, Nicklasson M. Investigation of the film formation of magnesium stearate by applying a flow-through dissolution technique. J Pharm Pharmacol. 1986;38(1):51-4.

95.   Demuth B, Galata DL, Balogh A, Szabo E, Nagy B, Farkas A, et al. Application of hydroxypropyl methylcellulose as a protective agent against magnesium stearate induced crystallization of amorphous itraconazole. Eur J Pharm Sci. 2018;121:301-8.

96.   Demuth B, Galata DL, Szabo E, Nagy B, Farkas A, Balogh A, et al. Investigation of Deteriorated Dissolution of Amorphous Itraconazole: Description of Incompatibility with Magnesium Stearate and Possible Solutions. Mol Pharmaceutics. 2017;14(11):3927-34.

97.   Ariyasu A, Hattori Y, Otsuka M. Delay effect of magnesium stearate on tablet dissolution in acidic medium. International Journal of Pharmaceutics. 2016;511(2):757-64.

98.   Fukui E, Miyamura N, Kobayashi M. Effect of magnesium stearate or calcium stearate as additives on dissolution profiles of diltiazem hydrochloride from press-coated tablets with hydroxypropyl methyl cellulose acetate succinate in the outer shell. Int J Pharm. 2001;216(1-2):137-46.

99.   Uchimoto T, Iwao Y, Ikegami Y, Murata T, Sonobe T, Miyagishima A, et al. Lubrication properties of potential alternative lubricants, glycerin fatty acid esters, to magnesium stearate. Int J Pharm. 2010;386(1-2):91-8.

100.   Uchimoto T, Iwao Y, Takahashi K, Tanaka S, Agata Y, Iwamura T, et al. A comparative study of glycerin fatty acid ester and magnesium stearate on the dissolution of acetaminophen tablets using the analysis of available surface area. Eur J Pharm Biopharm. 2011;78(3):492-8.

101.   Pudio RPE. Wettable Magnesium Stearate. Mallinckrodt Pharmaceuticals. 2015;April 29, 2015.

102.   Perveen S, Hamid S, Hassan S, Usman S. In vitro dissolution of metronidazole (400 Mg) tablets: effects of lubricants on the dissolution of tablets. Am J PharmTech Res. 2018;8(1):232-43.

103.   Harris RK, Roderick E. Wasylishen, Melinda J. Duer. NMR Crystallography. Chichester, West Sussex: John Wiley & Sons; 2009.

104.   Keeler J. Understanding NMR Spectroscopy - Second Editioin. Chichester, West Sussex: John Wiley & Sons, Ltd; 2010.

105.   Levitt MH. Spin Dynamics - Basics of Nuclear Magnetic Resonance. 2nd Edition ed. Chichester, WEst Sussex: John Wiley & Sons Ltd; 2008.

106.   Apperley DC, Robin K. Harris, Paul Hodgkinson. Solid-State NMR: Basic Principles and Practice. New York, NY: Momentum Press LLC; 2012.

107.   Byrn SR, Pfeiffer RR, Stowell JG. Solid-State Chemistry of Drugs. 2nd ed. West Lafayette, IN: SSCI, Inc.; 1999.

108.   Lowe IJ. Free Induction Decays of Rotating Solids. Phys Rev Lett. 1959;2(7):285-7.

109.   Arnold JT, S.S. Dharmatti, M.E. Packard. Variations in Absolute Chemical Shift of Nuclear Induction Signals of Hydroxyl Groups of Methyl and Ethyl Alcohol. Journal of Chemical Physics. 1951;19(12).

110.   Stejskal EO, Schaefer J. Magic-Angle Spinning and Polarization Transfer in Proton-Enhanced NMR. J Magn Reson. 1977;28:105-12.

111.   Andrew AR, Bradbury A, Fades RG. Removal of dipolar broadening of nuclear magnetic resonance spectra of solids by specimen rotation. Nature. 1958;183:1802-3.

112.   Dixon WT, Schaeffer J, Sefcik MD. Total suppression of sidebands in CPMAS carbon-13 NMR. J Magn Reson. 1982;49(2):341-5.

113.   Pines A, Gibby MG, Waugh JS. Proton-enhanced NMR of Dilute Spins. Journal of Chemical Physics. 1973;59:569-90.

114.   Lubach JW, Xu D, Segmuller BE, Munson EJ. Investigation of the Effects of Pharmaceutical Processing upon Solid-state NMR Relaxation Times and Implications to Solid-state Formulation Stability. J Pharm Sci. 2007;96(4):777-87.

115.   Berendt RT, Sperger DM, Munson EJ, Isbester PK. Solid-state NMR spectroscopy in pharmaceutical research and analysis. TrAC. 2006;25(10):977-84.

116.   Geppi M, Mollica G, Borsacchi S, Veracini CA. Solid-state NMR Studies of Pharmaceutical Systems. Appl Spectrosc. 2008;43:202-302.

117.   Offerdahl TJ, Munson EJ. Solid-state NMR spectroscopy of pharmaceutical materials. Amer Pharm Rev. 2004;7(1):109-12.

118.   Saindon PJ, Cauchon NS, Sutton PA, Chang C, Peck GE, Byrn SR. Solid-state Nuclear Magnetic Resonance (NMR) Spectra of Pharmaceutical Dosage Forms. Pharm Res. 1993;10(2):197-203.

119.   Tishmack PA, D. E. Bugay, S. R. Byrn. Solid-state nuclear magnetic resonance spectroscopy - pharmaceutical applications. J Pharm Sci. 2003;92(3):441-74.

120.   Nagapudi K. Applications of Multinuclear Solid-State NMR Spectroscopy in Characterizing Drug Substances and Drug Product. unpublished. [Presentation]. In press 2010.

121.   Wu SH, editor Effect of Magnesium StearateLubricant Attributes on Product Processibility and Quality. Land O'Lake Industrial Pharmacy Conference; 2009: Covidien/Mallinckrodt.

122.   Dave RH. Overview of pharmaceutical excipients used in tablets and capsules. Drug Topics [Internet]. 2008.

123.   Hymavathi G, Adilakshmi J, Dwarathi K, Kavya M, Pravallika G. Review article on inprocess problems and evaluation tests of tablet manufacturing. Int J Res Pharm Nano Sci. 2015;4(3):175-9.

124.   Shipar MAH, Wadhwa A, Varughese C. Affect of granule sizes, types and concentrations of lubricants and compression forces on tablet properties. Int J Pharm Sci Res. 2014;5(11):4893-901, 9 pp.

125.   Ager B, Mills AJ, Bentham AC. Investigation into tablet picking and sticking using an instrumented adhesion punch. J Pharm Pharmacol. 2010;62(10):1445-6.

126.   Okoye P, Wu SH, Dave RH. To evaluate the effect of various magnesium stearate polymorphs using powder rheology and thermal analysis. Drug Dev Ind Pharm. 2012;38(12):1470-8.

127.   Demuth B, Farkas A, Balogh A, Bartosiewicz K, Kallai-Szabo B, Bertels J, et al. Lubricant-Induced Crystallization of Itraconazole From Tablets Made of Electrospun Amorphous Solid Dispersion. J Pharm Sci. 2016.

128.   Billany MR, Richards JH. Batch variation of magnesium stearate and its effect on the dissolution rate of salicylic acid from solid dosage forms. Drug Dev Ind Pharm. 1982;8(4):497-511.

129.   Wada Y, Matsubara T. Pseudo-polymorphism and crystalline transition of magnesium stearate. Thermochim Acta. 1992;196(1):63-84.

130.   York P. Application of Powder Failure Testing Equipment in Assessing Effect of Glidants on Flowability of Cohesive Pharmaceutical Powders. J Pharm Sci. 1975;64:1216-21.

131.   Sharpe SA, Celik M, Newman AW, Brittain HG. Physical characterization of the polymorphic variations of magnesium stearate and magnesium palmitate hydrate species. Struct Chem. 1997;8(1):73-84.

132.   Pintye-Hodi K, Toth I, Kata M. Investigation of the formation of magnesium stearate film by energy dispersive x-ray microanalysis. Pharm Acta Helv. 1981;56(11):320-4.

133.   Abe H, Otsuka M. Effects of lubricant-mixing time on prolongation of dissolution time and its prediction by measuring near infrared spectra from tablets. Drug Dev Ind Pharm. 2012;38(4):412-9.

134.   Duong N-H, Arratia P, Muzzio F, Lange A, Timmermans J, Reynolds S. A homogeneity study using NIR spectroscopy: Tracking magnesium stearate in bohle bin-blender. Drug Dev Ind Pharm. 2003;29(6):679-87.

135.   Okoye P, Wu SH. Lubrication of direct-compressible blends with magnesium strearate monohydrate and dihydrate. Pharm Technol. 2007;31(9):116, 8, 20, 22-29.

136.   Miller TA, York P. Physical and chemical characteristics of some high purity magnesium stearate and palmitate powders. Int J Pharm. 1985;23(1):55-67.

137.   Miller TA, York P. Frictional assessment of magnesium stearate and palmitate lubricant powders. Powder Technol. 1985;44(3):219-26.

138.   Hussain MSH, York P, Timmins P. A study of the formation of magnesium stearate film on sodium chloride using energy-dispersive x-ray analysis. Int J Pharm. 1988;42(1-3):89-95.

139.   Hussain MSH, York P, Timmins P, Humphrey P. Secondary ion mass spectrometry (SIMS) evaluation of magnesium stearate distribution and its effects on the physico-technical properties of sodium chloride tablets. Powder Technol. 1990;60(1):39-45.

140.   Hussain MSH, York P, Timmins P. Influence of commercial and high purity magnesium stearates on sodium chloride and paracetamol DC granules during tabletting. Int J Pharm. 1991;70(1-2):103-9.

141.   Mueller BW, Steffens KJ, List PH. Tribological laws and experimental results in tablet technology. 6. Effect of physical properties of chemically pure magnesium stearates on tablet lubrication. Pharm Ind. 1982;44(7):729-34.

142.   Haware RV, Dave VS, Kakarala B, Delaney S, Staton S, Munson E, et al. Vegetable-derived magnesium stearate functionality evaluation by DM3 approach. Eur J Pharm Sci. 2016;89:115-24.

143.   Andrew ER, Bradbury A, Eades RG. Removal of dipolar broadening of nuclear magnetic resonance spectra of solids by specimen rotation. Nature. 1959;183(4678):1802-3.

144.   Pines A, Gibby MG, Waugh JS. Proton-enhanced NMR of dilute spins in solids. The Journal of Chemical Physics. 1973;59(2):569-90.

145.   Dixon WT, Schaefer J, Sefcik MD, Stejskal EO, McKay RA. Total suppression of sidebands in CPMAS C-13 NMR. Journal of Magnetic Resonance. 1982;49(2):341-5.

146.   Fung BM, Khitrin AK, Ermolaev K. An improved broadband decoupling sequence for liquid crystals and solids. Journal of Magnetic Resonance. 2000;142(1):97-101.

147.   Barich DH, Gorman EM, Zell MT, Munson EJ. 3-Methylglutaric acid as a ^{13}C solid-state NMR standard. Solid State Nuclear Magnetic Resonance. 2006;30(3–4):125-9.

148.   Yuan X, Sperger D, Munson EJ. Investigating Miscibility and Molecular Mobility of Nifedipine-PVP Amorphous Solid Dispersions Using Solid-State NMR Spectroscopy. Mol Pharmaceutics. 2014;11(1):329-37.

149.   Wada YTM. Pseudo-polymorphism and crystalline transition of magnesium stearate. Thermochimica Acta. 1992;196:63-84.

150.   Moody G, M. H. Rubinstein, R. A. FitzSimmons. Lubricity measurements of magnesium stearate [proceedings]. Journal of Pharmacy and Pharmacology. 1979;31(S1):71pp.

151.   Barra JRS. The influence of the physicochemical variability of magnesium stearate on its lubricant properties: possible solutions. Drug Dev Ind Pharm. 1996;22:1105.

152.   Leinonen UIHUJ, P. A. Vihervaara, E. S. U. Laine. Physical and lubrication properties of magnesium stearate. Journal of Pharmaceutical Sciences. 1992;81(12):1194.

153.   Yalkowsky S, Dannenfelser R. Aquasol Database of Aqueous Solubility. In: College of Pharmacy UoA-T, editor. 5 ed1992.

154.   Fukui ENM, M. Kobayashi. International Journal of Pharmaceutics. 2007;216.

155.   Muller BW. 1st Int Conf Pharm Tech. 1977;IV(Paris):134.

156.   Cyrille Andres PB, Yvette Pourcelot. On the difficulty of assessing the specific surface area of magnesium stearate. International Journal of Pharmaceutics. 2001;218:153-63.

157.   Wu SH. Effect of Magnesium Stearate Lubricant Attributes on Product Processibility and Quality. Land O' Lake Industrial Pharmacy Conference: Covidient/ Mallinckrodt; 2009.

158.   Sun CC. Dependence of ejection force on tableting speed-A compaction simulation study. Powder Technol. 2015;279:123-6.

159.   Bracconi P, Andres C, N'Diaye A, Pourcelot Y. Thermal analyses of commercial magnesium stearate pseudopolymorphs. Thermochim Acta. 2005;429(1):43-51.

160.   Dun J, Osei-Yeboah F, Boulas P, Lin Y, Sun CC. A systematic evaluation of dual functionality of sodium lauryl sulfate as a tablet lubricant and wetting enhancer. Int J Pharm (Amsterdam, Neth). 2018;552(1-2):139-47.

161.   Kuentz M, Leuenberger H. Pressure Susceptibility of Polymer Tablets as a Critical Property: A Modified Heckel Equation. J Pharm Sci. 1999;88(2):174-9.
162.   Paul S, Sun CC. Systematic evaluation of common lubricants for optimal use in tablet formulation. Eur J Pharm Sci. 2018;117:118-27.
163.   Fell JT, Newton JM. Determination of tablet strength by the diametral-compression test. J Pharm Sci. 1970;59(5):688-91.
164.   Ryshkewitch E. Compression strength of porous sintered alumina and zirconia: 9th communication to ceramography. J Am Ceram Soc. 1953;36:65-8.
165.   Taylor MG, Robert H. Marchessault, Serge Perez, Peter J. Stephenson, Colin A. Fyfe. 13C CP/MAS nuclear magnetic resonance of crystalline methylxylopyranosides. Can J Chem 1984:270.
166.   Abdel-Hamid S, Koziolek M, Betz G. Study of radial die-wall pressure during high speed tableting: effect of formulation variables. Drug Dev Ind Pharm. 2012;38(5):623-34.
167.   Pitt KG, Heasley MG. Determination of the tensile strength of elongated tablets. Powder Technology. 2013;238:169-75.
168.   Sun CC, Hou H, Gao P, Ma C, Medina C, Alvarez FJ. Development of a high drug load tablet formulation based on assessment of powder manufacturability: moving towards quality by design. J Pharm Sci. 2009;98(1):239-47.
169.   Osei-Yeboah F, Sun CC. Validation and applications of an expedited tablet friability method. Int J Pharm (Amsterdam, Neth). 2015;484(1-2):146-55.
170.   Osei-Yeboah F, Chang S-Y, Sun CC. A critical Examination of the Phenomenon of Bonding Area - Bonding Strength Interplay in Powder Tableting. Pharm Res. 2016;33(5):1126-32.
171.   Sun CC, Kleinebudde P. Mini review: Mechanisms to the loss of tabletability by dry granulation. Eur J Pharm Biopharm. 2016;106:9-14.
172.   Zuurman K, Van der Voort Maarschalk K, Bolhuis GK. Effect of magnesium stearate on bonding and porosity expansion of tablets produced from materials with different consolidation properties. Int J Pharm. 1999;179(1):107-15.

VITA

1. Education
   - University of Kansas   M.S. Pharmaceutical Chemistry, 2011
   - California State University, Fresno   B.S. Chemistry, 1997

2. Professional Experience
   - Associate Scientist, Pharmaceutics, Preformulation at Amgen, Inc. 2003-2015
   - Analyst II, Inorganic Dept, Columbia Analytical Services, 2000-2003
   - Chemist, QA/QC Laboratory, Ag Formulators, 1997-1999

3. Scholastic and professional honors
   - USP Global Fellowship 2015-2016
   - PhRMA Foundation Pre-Doctoral Fellowship 2018, 2019
   - Dennis Casey Pharmaceutical Chemistry Travel Award 2017

4. Professional publications
   - Julie L. Calahan, Shubhajit Paul, Evelyn G. Yanez, Daniel DeNeve, Changquan (Calvin) Sun, Eric J. Munson. "An Evaluation of the Solid-State Form and Particle Properties of Magnesium Stearate on Lubrication Efficiency, Tabletability, and Dissolution", manuscript in review
   - Delaney, Sean P., Matthew J. Nethercott, Christopher J. Mays, Nickolas T. Winquist, Donia Arthur, Julie L. Calahan, Manish Sethi, Gregory Amidon, and Eric J. Munson. "Characterization of Synthesized and Commercial Forms of Magnesium Stearate using DSC, TGA, PXRD, and Solid-State NMR Spectroscopy." Journal of Pharmaceutical Science, Vol. 106, Issue 1, p. 338-347, **2017**.
   - Hanrahan, Michael P.; Amrit Venkatesh, Scott L. Carnahan, Julie L. Calahan, Joe Lubach, Eric J. Munson, Aaron J. Rossini. "Enhancing the Resolution of 1H and 13C Solid-State NMR Spectra by Reduction of Anisotropic Bulk

Magnetic Susceptibility Broadening." *Physical Chemistry Chemical Physics*, 2017, **19**, 28153 - 28162.

- Jennings, John A., Sean Parkin, Eric Munson, Sean P. Delaney, Julie L. Calahan, Mark Isaacs, Kunlun Hong, Mark Crocker. "Regioselective Baeyer-Villiger Oxidation of Lignin Model Compounds with Tin Beta Zeolite Catalyst and Hydrogen Peroxide." RSC Advances **2017**, 7, 25987-25997.

- Calahan, J. L., Azali, S. C., Munson, E. J., Nagapudi, K. "Investigation of Phase Mixing in Amorphous Solid Dispersions of AMG 517 in HPMC-AS using DSC, Solid State NMR and Solution Calorimetry." Molecular Pharmaceutics, October 12, **2015**.

- Calahan, J. L., Zanon, R. L., Alvarez-Nunez, F., Munson, E. J. "Isothermal Microcalorimetry to Investigate the Phase Separation for Amorphous Solid Dispersions of AMG 517 with HPMC-AS." Molecular Pharmaceutics, Vol. 10. p.1949-1957, **2013**.

5. Julie L. Calahan